AUGUST 28, 2023

NUMERICAL MODELING OF ASPIRATION THROMBECTOMY

UTILIZING NUMERICAL METHODS FOR IMPROVING THE CURRENT ASPIRATION CATHETER

CHUNGHSU LING
TU DELFT

Numerical modeling of aspiration thrombectomy: Utilizing numerical methods for improving the current aspiration catheter

MSC Thesis

by

Chunghsu Ling

Student number :	5456479	
Defense time:	August 28, 2023, at 12:00 PM	
Thesis committee:	Dr. Ir. F.J.H. Gijsen	TU Delft & Erasmus MC, Supervisor
	Dr. B. Fereidoonnezhad	TU Delft, Supervisor
	Dr. Ir. N. Tümer	TU Delft

TU Delft

Preface

My journey into the field of biomedical engineering began with my first course, 'Cardiovascular Biomechanics,' during my college days. Ever since then, the intricacies of clot removal procedures have captivated my interest. It is with gratitude that I conduct research and contribute to this fascinating domain.

Prior to enrolling in the biomedical engineering program at TU Delft, I had not received formal education in this field. Thus, I extend my appreciation to my mentors, Frank Gijsen and Behrooz Fereidoonnezhad, for generously sharing their knowledge of the cardiovascular system and aiding me in learning finite element analysis. I also wish to acknowledge Olaf van der Sluis, whose constructive feedback have consistently pushed me to dive deeper into the foundations of my work. Without their guidance and support, the successful completion of this thesis is not possible.

Furthermore, I am deeply grateful for the substantial emotional and financial backing provided by my parents, Hao Chen, and Hsiaolien Ling. Their unwavering support has enabled me to pursue my master's degree in the Netherlands, and for this, I extend my heartfelt appreciation.

Eventually, I want to extend my thanks to my girlfriend, Chiapei, for her unwavering support throughout my journey. I would also like to express my appreciation to my friends for being there for me through good times and bad, whether it is by having a drink or playing video games together.

Chunghsu Ling
Capelle aan den IJssel, August 2023

Abstract

Acute ischemic stroke (AIS) is a medical emergency which happens when a thrombotic or embolic blood clot blocks a brain artery, leading to brain damage or tissue death. AIS is the second leading cause of death worldwide and affects approximately 700,000 people in the United States alone. Since 2015, endovascular treatment (EVT) has become the standard of care for stroke patients. However, it is important to note that the current treatment options for AIS still have significant room for improvement. The aim of this thesis is to acquire a deeper understanding of how thrombi, the vessel wall, and thrombectomy devices interact through numerical modeling of aspiration thrombectomy. This can help explain the limitations in the effectiveness of the procedure and possibly pave the way for designing new devices that yield better results.

The thesis starts with reviewing relevant literature and identifying research gaps. The initial phase of the research involves identifying and validating an appropriate clot material model. Additionally, cohesive zone modeling (CZM) is integrated to simulate the interaction between the clot and vessel wall. A validation study is conducted to confirm the accurate implementation of CZM within the finite element analysis software, Abaqus. Subsequently, a parameter study is undertaken to explore how clot dimensions impact aspiration performance. This study aims to gather insights that can contribute to the enhancement of catheter design. Finally, an approach involving the combination of an expandable stent and an aspiration catheter is proposed. A parameter study is conducted to optimize the design geometry to achieve the first-pass recanalization (FPR). The findings of the research demonstrate that achieving a specific threshold of suction area in direct contact with the clot is crucial for the clinical outcome.

Regarding the content covered in each chapter, Chapter 2 outlines the methodologies employed for material parameter analysis, validation of the material model, cohesive zone modeling (CZM), clot dimension investigation, and catheter design examination. Chapter 3 presents the outcomes of these studies, while Chapter 4 offers an in-depth discussion of the findings. Finally, Chapter 5 provides the conclusion. Supplementary scripts and input files utilized in this thesis are available in the Appendix.

In conclusion, this thesis establishes a groundwork for future research. Furthermore, enhancing the present models requires the incorporation of factors like authentic aspiration pressure, clot fragmentation mechanisms, and accurate damage criteria for the clot-vessel interface. These enhancements would bring the simulation closer to real-world medical scenarios, providing valuable and insightful insights.

Table of Contents

Chapter 1. Introduction

1.1. Acute ischemic stroke (AIS)

Acute ischemic stroke (AIS) is a medical emergency which happens when a thrombotic or embolic blood clot blocks a brain artery, leading to a reduction of blood flow and oxygen supply to the brain and can cause brain damage or tissue death (Walter, 2022) (illustrated in *Figure 1*).

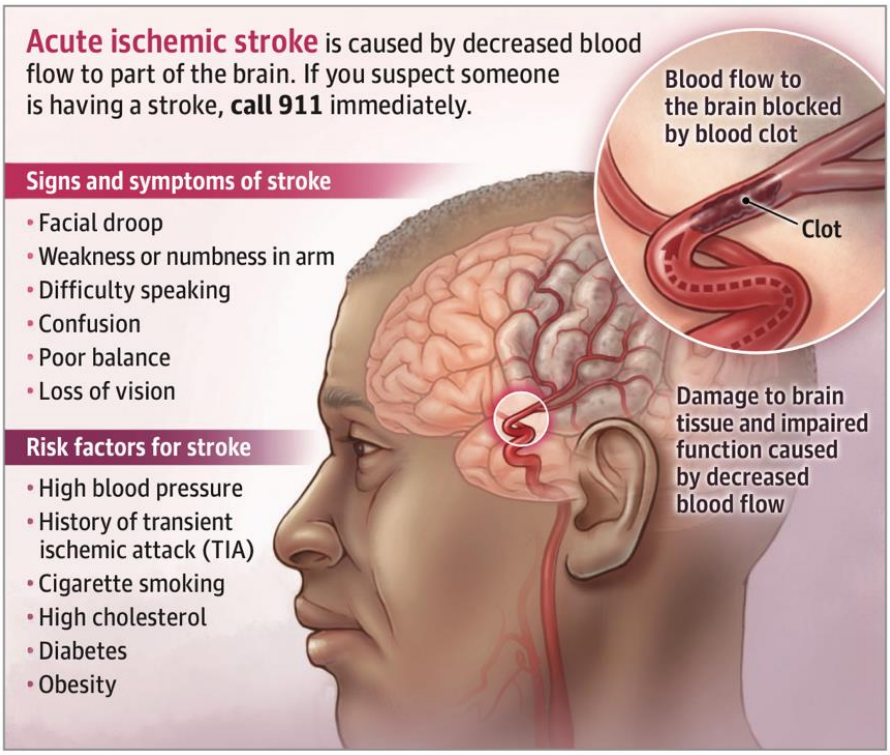

Figure 1. An illustration of AIS (Walter, 2022)

The symptoms of AIS include various types of disabilities, such as partially paralysis, difficulty speaking or understanding speech, trouble with balance and loss of vision (Walter, 2022). To elaborate the severity, AIS is responsible for almost 90% of all strokes and affects approximately 700,000 people in the United States alone (Walter, 2022). Moreover, it is the second leading cause of death worldwide (WHO, 2020). Therefore, the diagnosis and treatment of AIS is definitely an important issue and should be executed immediately since early treatment could lead to improved clinical outcomes (Walter, 2022).

1.2. The current treatments

Initially, the only available treatment for stroke patients was intravenous thrombolysis. Nevertheless, studies have shown that only 7-30% of patients with large vessel occlusion were able to achieve recanalization with intravenous thrombolysis (Menon et al., 2018). Hence, the treatment cannot be considered as effective.

Since 2015, endovascular treatment (EVT) has become the new standard of care for stroke patients (Goyal et al., 2016; Powers et al., 2018). EVT relies on mechanical thrombus retrieval, which can be helpful in restoring blood flow to the brain (Ospel et al., 2021). Furthermore, EVT can be divided into three categories: stent retriever thrombectomy, aspiration thrombectomy, and a combination of the two (Fanous & Siddiqui, 2016; Ospel et al., 2021).

Stent retriever thrombectomy involves the use of a self-expanding stent retriever, which is compressed and inserted into a microcatheter (Ospel et al., 2021). Once the microcatheter is placed in the target site, the stent retriever will be deployed and expands within the clot, allowing it to be captured and removed from the blood vessel, the process is demonstrated in *Figure 2*. (Ospel et al., 2021).

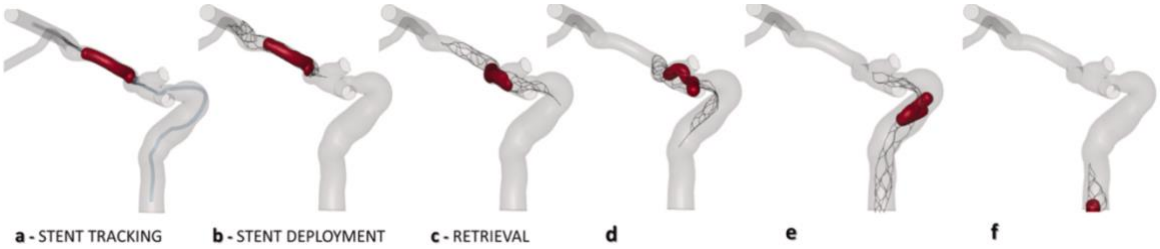

Figure 2. The illustration of stent retriever thrombectomy procedure (Luraghi, Bridio, et al., 2021).

Aspiration thrombectomy uses an aspiration catheter connected to a vacuum pump or syringe. The catheter is firstly guided to the proximal thrombus face, then negative pressure is applied, causing the thrombus to be sucked up into the catheter (Ospel et al., 2021). In the end, the blood flow can be restored due to the removal of the thrombus in the affected area. An illustration is provided in *Figure 3*.

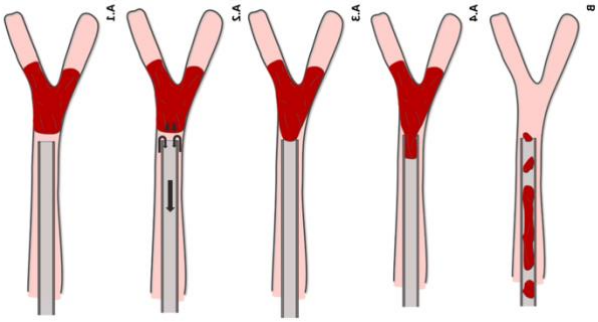

Figure 3. The illustration of aspiration thrombectomy procedure (McCarthy et al., 2022).

Combined approaches involve the simultaneous use of both stent retriever thrombectomy and thrombus aspiration to extract the clots (*Figure 4*.) (Ospel et al., 2021). Clinical trials have demonstrated the effectiveness of combined approaches in treating stroke patients (Deshaies, 2013; Humphries et al., 2015).

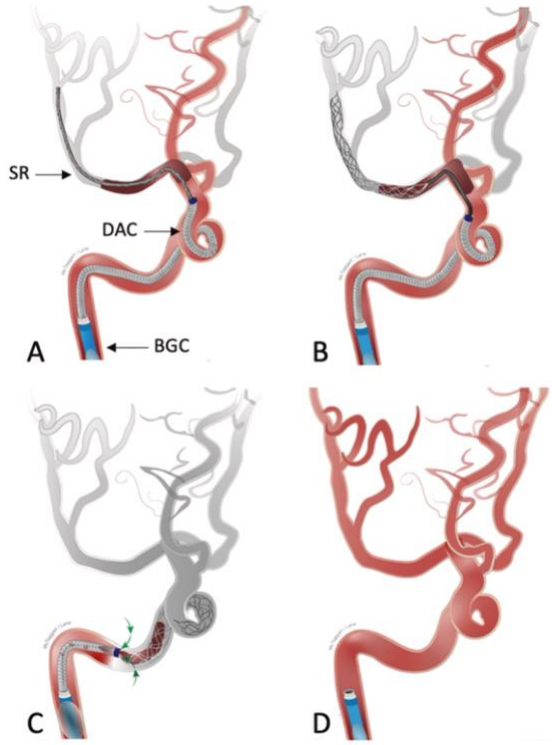

Figure 4. The procedure of the combined thrombectomy approach using a stent retriever (SR), a distal access catheter (DAC) and a balloon guide catheter (BGC) (Ospel et al., 2021).

Furthermore, these methods can be performed with a balloon guide catheter (*Figure 5.*), which includes a balloon that can be inserted into the internal carotid artery (ICA) to halt blood flow and prevent distal embolization (Baek et al., 2019; Nguyen et al., 2014).

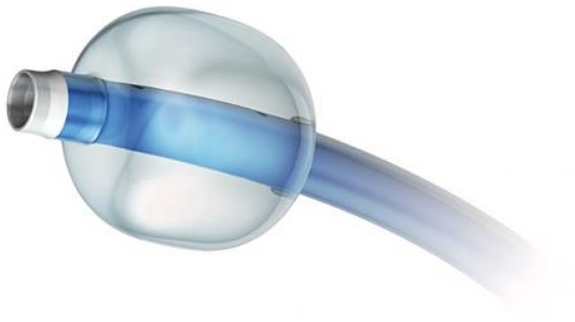

Figure 5. A balloon guide catheter (Ospel et al., 2021).

While EVT has increased the rate of successful recanalization to 85% (Grech et al., 2015), there is still a noticeable risk of mortality and major disability associated with this procedure. In fact, 17% of patients treated with EVT die within 90 days (Grech et al., 2015) and approximately 80% of patients either die or suffer from significant disability following the procedure (Oyekole et al., 2021). Possible explanations for this phenomenon include blood vascular trauma caused by mechanical thrombectomy (Oyekole et al., 2021) and the low probability of achieving first-pass recanalization, which is associated with better clinical

outcomes (Fereidoonnezhad & McGarry, 2022) since multiple passes at revascularization tend to cause clot fracture, which can lead to distal embolization (Fereidoonnezhad, Dwivedi, et al., 2021; Gralla et al., 2006; Kaesmacher et al., 2017; "The Penumbra Pivotal Stroke Trial," 2009). Therefore, it is important to note that the current treatment options for AIS still have significant room for improvement, and more research is needed to develop more effective and safer approaches that increase the likelihood of successful recanalization while minimizing complications.

1.3. In-silico modeling

Numerous studies have been undertaken to gain a better understanding of the processes required to improve current treatments (Gralla et al., 2006; Pearce et al., 2010). However, in vivo studies and experiments pose ethical issues due to the critical nature of this topic (Oyekole et al., 2021). Additionally, it can be challenging to control experiment parameters, such as the distance between catheters and clots, thrombus size, and clot properties (Soleimani et al., 2016). As a result, computational analysis using in-silico models has emerged as an alternative technique. This method has become increasingly popular not only for testing new devices virtually and investigating their efficacy in endovascular treatments (Colombo et al., 2020; Kusner et al., 2021; Luraghi, Matas, et al., 2021; Migliori et al., 2020; Zaccaria et al., 2020) but also for building the first patient-specific thrombectomy procedure (Luraghi, Bridio, et al., 2021). Thus, with advances in medical imaging and computer simulation techniques, in-silico models have become a robust method to evaluate the performance of different devices in clinical scenarios, even in a patient-specific manner (Luraghi, Bridio, et al., 2021). In conclusion, it is evident that in-silico models offer significant potential to gain valuable insights into the treatment of AIS. This thesis specifically focuses on the numerical modeling of the aspiration clot removal procedure.

1.4. State-of-the-art

The aspiration thrombectomy is a complex procedure with several factors that can affect the success rate and potential complications and these factors must be carefully considered and optimized to ensure optimal patient outcomes. First of all, the applied aspiration pressure and pattern are important factors in the success of the aspiration thrombectomy procedure because they determine the suction force applied to the clots (Simon et al., 2014). Additionally, the properties of the thrombus, such as the size, shape, composition, and the interaction between the clot and vessel, can also affect the outcomes (Dutra et al., 2019; Good et al., 2020; Oyekole et al., 2021; Santos et al., 2016). Thus, the factors should be considered when performing the procedure. Furthermore, the design of the catheters used for aspiration thrombectomy can also influence the suction force and the difficulty of clot removal (Talayero et al., 2020).

To investigate the impacts of these factors, several indicators need to be adopted. The first-pass recanalization (FPR) will be used to determine the efficacy and speed of recanalization (Ospel et al., 2019; Zaidat et al., 2018). Another important aspect in EVT is avoiding distal embolization caused by clot rupture (Gralla et al., 2006; Kaesmacher et al., 2017), thus, clot fracture (CF) will also be monitored as it is equally important to avoid complications.

Hence, research that emphasize these aspects using numerical analysis or can offer valuable insights into these areas will be thoroughly examined.

1.4.1. Aspiration design

Several articles have proposed different types of catheter designs for aspiration thrombectomy. Some suggest that catheters that can deliver the suction force close to the clot-vessel interface have a better first-pass recanalization rate (Talayero et al., 2019; Talayero et al., 2020), while others argue that catheters with larger diameters can achieve better outcomes (Chitsaz et al., 2018; Hu & Stiefel, 2016). However, these arguments are not conflicting since catheters with larger diameters can induce suction forces to the clot-vessel interface. Nevertheless, using catheters with larger diameters may pose navigational difficulties, so a trade-off between suction force and feasibility must be made to optimize the design. (Talayero et al., 2020) proposed a catheter design with peripheral pores (the last row in *Figure 6*.) that has the potential to improve the current treatment by producing higher suction force (*Figure 7*.) while minimizing the risk of clot fracture. This design could achieve better clinical outcomes in a relatively small size.

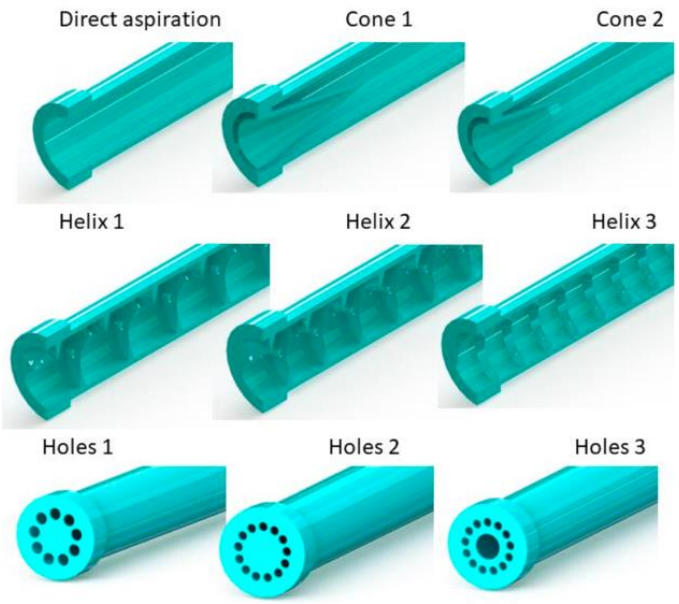

Figure 6. The catheter designs studied by (Talayero et al., 2020) to investigate the optimal catheter geometry.

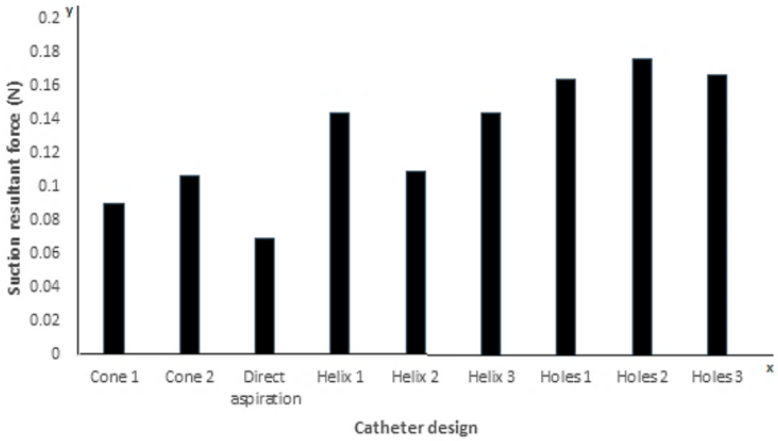

Figure 7. The suction forces created by aspiration catheters with different designs, according to (Talayero et al., 2020)

Other proposals, such as lateral holes on the catheter tip (Soleimani et al., 2014) and helical geometry (Romero et al., 2020), are not recommended. Lateral holes only work better in circumstances where the viscosity of the blood clot is low (Soleimani et al., 2014), while the helical geometry was outperformed by the catheters with peripheral pores (Talayero et al., 2018; Talayero et al., 2020).

1.4.2. Aspiration pressure and pattern

Studies usually apply suction pressures ranging from -10 to -100 kPa in the computational models. These studies have generally concluded that higher suction pressures tend to result in better outcomes, particularly in terms of the amount of clot mass that is aspirated. (Chitsaz et al., 2018; Soleimani et al., 2014; Talayero et al., 2020).

In previous studies, the hypothesis that a cyclic aspiration pattern may be more effective than a static pattern for thrombus removal seems plausible, as cyclic loading can facilitate material failure through fatigue mechanisms (Bathias & Pineau, 2013; Withey, 1997). However, only (Simon et al., 2014) has directly compared the two patterns using a glass artery model, synthetic clots, and air and water as the medium *(Figure 8. & Figure 9.)*. Although the authors concluded that the cyclic pattern achieved better outcomes, the conclusion may not be definitive due to the limited similarity between the experimental setup and the clinical scenario.

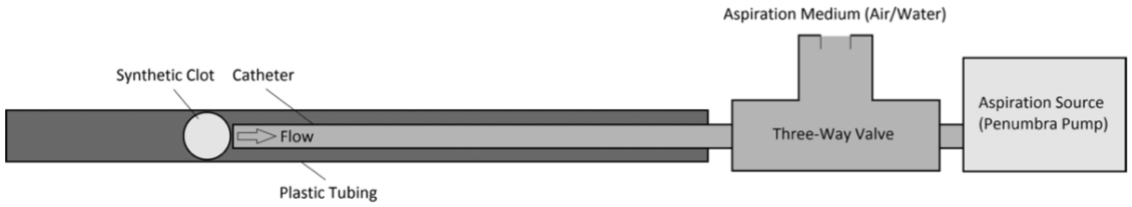

Figure 8. The experimental setup of (Simon et al., 2014) to conduct in-vitro aspiration experiments to compare static and cyclic aspiration pattern

Regarding in-silico studies, (Good et al., 2020) tried to optimize the waveform of the cyclic suction and concluded that lower frequency (0.5 Hz vs. 1 Hz) could achieve higher cohesive zone (the interface of the clot and artery) opening. In addition, (Oyekole et al., 2021) investigated the mechanism of clot removal with the cyclic aspiration. Nevertheless, both studies applied low suction pressure (less than 10 mmHg) due to the limitations of the model they employed (Good et al., 2020; Oyekole et al., 2021). Therefore, both models must be improved to better resemble real-world scenarios.

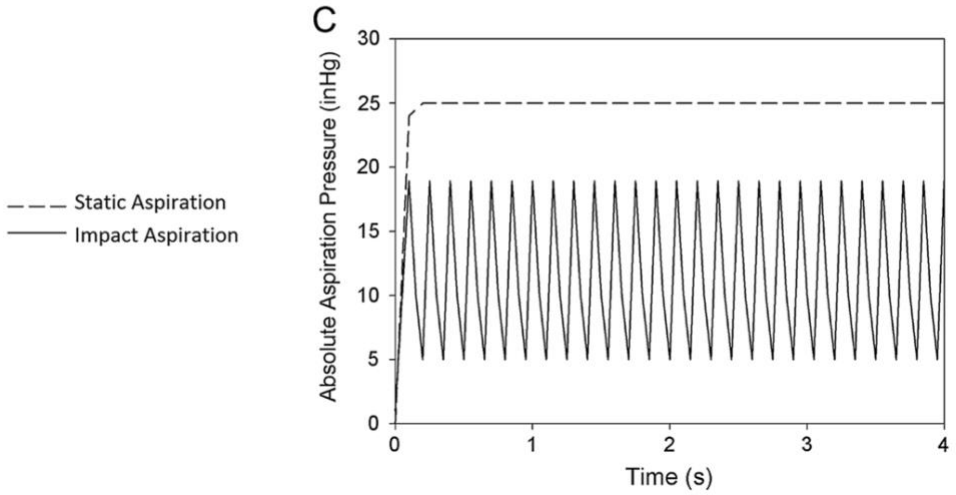

Figure 9. An illustration of the waveform of a cyclic suction loading, the cyclic pattern was applied to compare with the static aspiration which also shown in the figure (Simon et al., 2014).

1.4.3. Thrombus models

The composition of thrombi is highly heterogeneous (Chueh et al., 2011; Staessens & De Meyer, 2021) and can significantly impact various aspects of aspiration thrombectomy, including mechanical properties, recanalization rate, clinical outcomes, and risk of clot fragmentation (Brouwer et al., 2018; Cahalane et al.,

2021; Chueh et al., 2011; Simons et al., 2015; Yuki et al., 2012). Thus, it is essential to use appropriate material models in numerical simulations to accurately represent the behaviour of thrombi. Several material models have been used in previous studies, including the fluid model (Soleimani et al., 2014, 2016), hyper-elastic model (Fereidoonnezhad, Moerman, et al., 2021; Liu et al., 2022; Luraghi, Rodriguez Matas, et al., 2021; Rausch & Humphrey, 2016; Rausch et al., 2021; Romero et al., 2020; Sugerman et al., 2021; Talayero et al., 2018; Talayero et al., 2020), which appears to be the most relevant constitutive model, and visco-elastic model (Fereidoonnezhad, Moerman, et al., 2021; Good et al., 2020; Johnson et al., 2021; Oyekole et al., 2021; Tashiro et al., 2021). Furthermore, few studies have considered additional properties such as porosity (Chitsaz et al., 2018; He et al., 2022) and plasticity (Fereidoonnezhad & McGarry, 2022; Sugerman et al., 2020).

1.4.4. Clot fracture mechanism

The majority of the studies have come to a consensus that fibrin plays a significant role in determining the fracture mechanism and toughness (Brown et al., 2009; Fereidoonnezhad, Dwivedi, et al., 2021; Liang et al., 2017; Litvinov & Weisel, 2017; Münster et al., 2013; Rausch & Humphrey, 2016; Tutwiler et al., 2021; Tutwiler et al., 2020). A recent study conducted by (Tutwiler et al., 2021) has provided further insight into the fracture process, which can be divided into three regimes: (1) alignment of the fibrins, (2) further alignment leading to extensions of 10-30%, and (3) irreversible fibrin breakage. (*Figure 10.*)

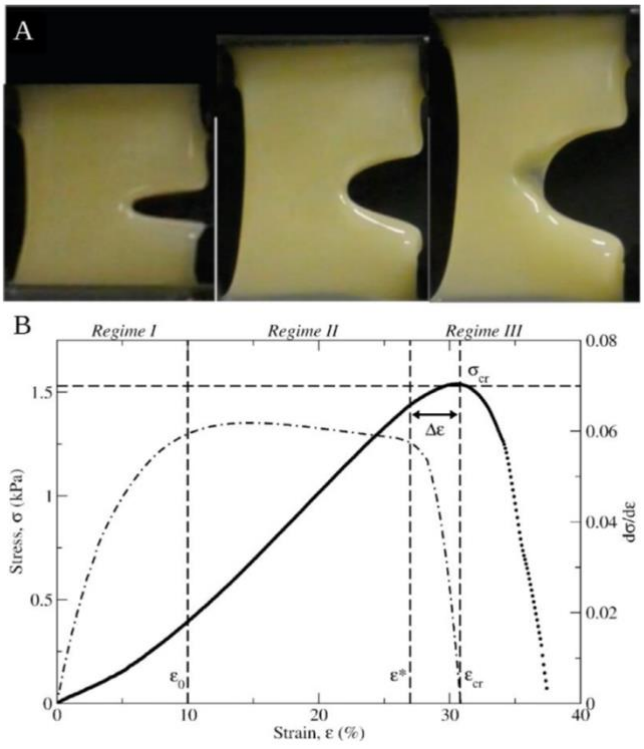

Figure 10. Stress strain analysis of the deformation and rupture process of a fibrin clot. The three regimes of fibrin rupture process are included. (Tutwiler et al., 2021)

Certainly, incorporating the risk of clot fracture into computational models is essential to better understand and predict the behaviour of thrombi during endovascular treatment. An example of a study that effectively modeled the fibrin networks in thrombi can be found in (Chitsaz et al., 2018). In this study, the researchers

employed a 3D network of branch points interconnected by fibrins and utilized the Kelvin-Voigt model for fibrin bonds. By setting the breakage point to be 100% of strain, they were able to successfully capture the fracture behaviour of the clot. Other studies suggest that hyper-elastic models (Fereidoonnezhad, Dwivedi, et al., 2021; Rausch & Humphrey, 2016; Tutwiler et al., 2020) or visco-hyper-elastic models (Rausch et al., 2021) can be used for the fibrins.

1.4.5. Clot-vessel interaction

The numerical modeling of the clot removal procedure involves another important aspect, which is defining the contact property between the thrombi and artery walls. Different approaches have been employed in the literature. For example, (Liu et al., 2022) applied different friction coefficients at the thrombus-artery interface and modeled the vessels as linear elastic materials. On the other hand, (Good et al., 2020) assumed the vessel walls to be rigid and employed a cohesive zone (CZ) model for the interface. The scholars investigated the separation of the clot by incorporating a damage model, where damage accumulation occurred when the CZ opening displacement reached a specific criterion. Moreover, (Oyekole et al., 2021) took the deformability of the artery into consideration and model it as a hyper-elastic material, however, the artery still behaved as it were rigid eventually. Similar to (Good et al., 2020), a cohesive zone was implemented for the interface, and damage accumulation was initiated when the CZ opening displacement surpassed a predefined threshold.

1.5. Research aim

Considering the potential for significant improvement in current EVT procedures and the emergence of computational modeling, this project aims to leverage the potential of *in-silico* modeling techniques to improve the current EVT by focusing on the simulation of aspiration thrombectomy.

Despite the extensive research conducted on thrombi, gaps in knowledge still exist. For example, the hyper-elastic model is the most commonly used constitutive model for thrombi, researchers have mainly relied on fitting experimental compression and tension test data of clots or analogues to reproduce clot behaviours. Nonetheless, no current literature has demonstrated the ability of their model to predict the mechanical behaviours of other clots or analogues. As a result, validating clot material models is a fascinating area of research.

Furthermore, only (Good et al., 2020; Oyekole et al., 2021) explicitly considered the clot-vessel interaction by incorporating a sticky, cohesive zone model to investigate the damage accumulation in the interface when subjected to cyclic aspiration patterns. Moreover, except for the work by (Chitsaz et al., 2018), the current studies on *in-silico* modeling of aspiration clot removal procedure have not incorporated the clot fragmentation, which relates to distal embolization and is a crucial factor in evaluating the clinical outcomes (Fereidoonnezhad, Dwivedi, et al., 2021; Gralla et al., 2006; Kaesmacher et al., 2017; "The Penumbra Pivotal Stroke Trial," 2009).

Hence, to address the research gaps mentioned earlier, the initial phase of this thesis aims to validate a hyper-elastic model by predicting experimental data of a different clot analogue. In addition, an *in-silico* model of the occlusion in the brain, including the clot and vessel walls, is constructed. The interaction properties of the interface between these components are also implemented. By incorporating the aspiration pressure, the numerical simulations could better resemble medical practice, and this allows for the study of clot separation from the artery. Eventually, the simulations incorporate several catheter designs (Chitsaz et al., 2018; Hu & Stiefel, 2016; Romero et al., 2020; Soleimani et al., 2014; Talayero et al., 2018, 2019; Talayero et al., 2020) to optimize the aspiration catheter to achieve the first-pass recanalization.

Regarding the clot fragmentation, modeling the feature is highly challenging and time-consuming, besides, validating the results can present difficulties. Finally, incorporating the fracture mechanism into the constitutive model can be the research aim for future studies and this thesis could serve as a foundation.

1.6. Thesis outline

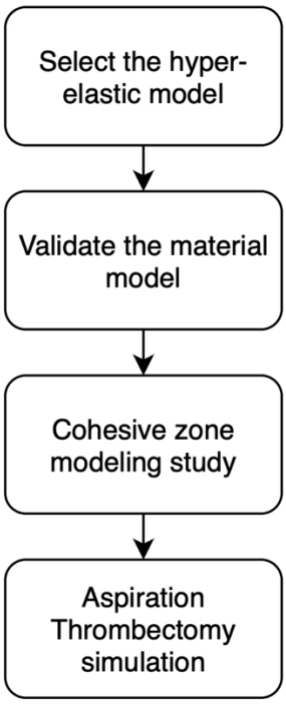

Figure 11. The workflow of this thesis

The thesis can be divided into four stages according to *Figure 11*:

1) **Select the hyper-elastic model and parameters:**
To acquire the ideal constitutive model, the stress-strain curve of a mechanical test of whole blood analogues, which were conducted by other students in the same laboratory, was used as a target. By adjusting the coefficients, the output stress-strain curve of the hyper-elastic model can be manipulated to match the target curve. Additionally, a parameter study of the coefficients is conducted to better replicate the behaviour of the target clot analogue.

2) **Validate the material model:**
The following step is demonstrating the model is capable of predicting the behaviours of other unseen clots. To accomplish this goal, an attempt is made to predict the behaviour of a different whole blood clot analogue during a tensile experiment using computational simulation with a commercial finite element analysis (FEA) software, Abaqus/Standard (2020). The actual sample and experiment, as shown in *Section 2.2.*, were conducted and prepared by other students in the same laboratory. The objective is to replicate the force-displacement and deformation characteristics observed during the experiment.

3) **Cohesive zone modeling (CZM) study**
Since the previous studies (Good et al., 2020; Oyekole et al., 2021) modeled the clot-vessel interface using the cohesive zone (CZ) modeling, the method is implemented in the project as well. However, there is a lack of literature investigating the initiation and evolution of damage in the interface, making it unclear what level of separation or stress triggers the detachment between thrombi and arteries. Additionally, the

fracture energy is unknown. Therefore, a parameter study focusing on the damage behavior within the cohesive zone is conducted to provide some insights into these aspects.

4) **Aspiration Thrombectomy simulation:**

Once the desired clot and interface model have been established, a comprehensive simulation of aspiration thrombectomy can be created. Moreover, a study focusing on the influence of clot dimensions is undertaken, aiming to determine the optimal catheter size. Subsequently, the final simulation incorporates important factors such as clot-vessel interaction and clot-catheter interaction. Furthermore, by implementing various catheter designs, the simulations can provide valuable insights into optimizing the aspiration device to achieve better clinical outcomes.

Chapter 2. Method

2.1. Material model and parameter identification

The nonlinear mechanical behaviour of blood clot is described by hyper-elastic models (Fereidoonnezhad, Moerman, et al., 2021; Liu et al., 2022; Luraghi, Rodriguez Matas, et al., 2021; Rausch & Humphrey, 2016; Rausch et al., 2021; Romero et al., 2020; Sugerman et al., 2021; Talayero et al., 2018; Talayero et al., 2020). Regarding the selection of hyper-elastic model, based on my previous work, neither the Neo Hookean, Ogden, nor Hyper Foam material models were able to accurately replicate the behavior of the clot analogue (Ling, 2023).Therefore, to precisely replicate the mechanical behaviour of thrombi, the clot material is simulated as an anisotropic hyperplastic fibrous soft tissue using a recently introduced formulation (Fereidoonnezhad et al., 2020). This formulation has been proven to effectively predict the isochoric and volumetric characteristics of blood clots across various compositions (Fereidoonnezhad, Moerman, et al., 2021).

The isochoric strain energy density function is given as:

$$\psi_{iso}(\bar{\lambda}_1, \bar{\lambda}_2, \bar{\lambda}_3) = \sum_{i=1}^{3} \bar{\psi}(\bar{\lambda}_i),$$

$$\bar{\psi}(\bar{\lambda}_i) = \begin{cases} E_{1m}(\bar{\lambda}_i - ln\bar{\lambda}_i - 1), & |\bar{\lambda}_i - 1| \le D_{1m} \\ p_m\left(\frac{\bar{\lambda}_i^{\,2}}{2} - 2\bar{\lambda}_i + ln\bar{\lambda}_i\right) + q_m(\bar{\lambda}_i - ln\bar{\lambda}_i) + r_m ln\bar{\lambda}_i + \psi_{01m}, & D_{1m} < |\bar{\lambda}_i - 1| < D_{2m} \\ E_{2m}(\bar{\lambda}_i - (1 + D_{2m})ln\bar{\lambda}_i) + (p_m D_{2m}^2 + q_m D_{2m} + r_m)ln\bar{\lambda}_i + \psi_{02m}, & |\bar{\lambda}_i - 1| \ge D_{2m} \end{cases} \quad (1)$$

D_{1m}, D_{2m}, E_{1m} and E_{2m}: material coefficients
$\bar{\lambda}_i (i = 1, 2, 3)$: isochoric principal stretches, $J = \lambda_1\lambda_2\lambda_3$ is the Jacobian
ψ_{01m} and ψ_{02m}: two constants which ensure the continuity of strain energy
p_m, q_m, and r_m satisfy *Eq. (2)* to maintain C^0 and C^1 continuity

$$p_m = \frac{E_{1m} - E_{2m}}{2(D_{1m} - D_{2m})}, q_m = E_{1m} - 2D_{1m}p_m, r_m = (E_{1m} - q_m)D_{1m} - p_m D_{1m}^2 \quad (2)$$

Moreover, the volumetric strain energy density function is given as:

$$\psi_{vol}(J) = \begin{cases} \kappa_1(J - lnJ - 1), & |J - 1| \le D_{1v} \\ p_v\left(\frac{J^2}{2} - 2J + lnJ\right) + q_v(J - lnJ) + r_v lnJ + \psi_{01v}, & D_{1v} < |J - 1| < D_{2v} \\ \kappa_2(J - (1 + D_{2v})lnJ) + (p_v D_{2v}^2 + q_v D_{2v} + r_v)lnJ + \psi_{02v}, & |J - 1| \ge D_{2v} \end{cases} \quad (3)$$

κ_1, κ_2: initial small-strain and large-strain bulk modulus
D_{1v}, D_{2v} control the transition volumetric strains

p_v, q_v, and r_v are acquired in a similar way as shown in *Eq. (2)*, utilizing the corresponding volumetric parameters

Furthermore, the anisotropic strain energy density function related to the influence of fibrin fibers in a blood clot is presented:

$$\psi_{aniso} = \sum_{i=1}^{2} \psi_{fi},$$

$$\psi_{fi} = \begin{cases} E_{1f}\left(\frac{2}{3}\lambda_{fi}^3 - \lambda_{fi}^2 + \frac{1}{3}\right), & \lambda_{fi} - 1 \le D_{1f} \\ \frac{2}{3}\lambda_{fi}^3\left(q_f - 2p_f\right) + \frac{p_f}{2}\lambda_{fi}^4 + \lambda_{fi}^2(p_f - q_f + r_f) + \psi_{01f}, & D_{1f} < \lambda_{fi} - 1 < D_{2f} \\ \frac{2E_{2f}}{3}\lambda_{fi}^3 + \lambda_{fi}^2\left(p_f D_{2f}^2 + q_f D_{2f} + r_f - E_{2f}(1 + D_{2f})\right) + \psi_{02m}, & \lambda_{fi} - 1 \ge D_{2f} \end{cases} \quad (4)$$

p_f, q_f, and r_f are acquired in a similar way as shown in *Eq. (2)*, utilizing the corresponding volumetric parameters.

In the end, the total strain energy density of the clot material is given as $\psi_f(\lambda_{fi}) + \psi_{iso}(\bar{\lambda}_1, \bar{\lambda}_2, \bar{\lambda}_3) + \psi_{vol}(J)$. Thus, the anisotropic bilinear model, which adopts *Eq. (1)-(4)* to describe the clot behaviours, is utilized in this study. The model was developed by Fereidoonnezhad et al. (2022) (Fereidoonnezhad, Dwivedi, et al., 2021; Fereidoonnezhad, Moerman, et al., 2021; Fereidoonnezhad et al., 2020) (In Abaqus, the material model can be implemented through utilizing a user subroutine, UMAT (ABAQUS User Subroutines Reference Manual, Dassault Systèmes Simulia Corp.)) Moreover, the material parameters are presented in *Table 1.*

Table 1. The associate parameters of the anisotropic bilinear model

D_{1m}	The value of the first transitional strain for the matrix.
D_{2m}	The value of the second transitional strain for the matrix.
E_{1m}	Stiffness of the matrix when the strain is lower than D_{1m}.
E_{2m}	Stiffness of the matrix when the strain is higher than D_{2m}.
D_{1v}	The value of the first transitional strain for the volumetric part.
D_{2v}	The value of the second transitional strain for the volumetric part,
κ_1	The bulk modulus when the strain is lower than D_{1v}.
κ_2	The bulk modulus when the strain is higher than D_{2v}.
D_{1f}	The value of the first transitional strain for the fibrin.
D_{2f}	The value of the second transitional strain for the fibrin.
E_{1f}	Stiffness of the fibrin when the strain is lower than D_{1f}.
E_{2f}	Stiffness of the fibrin when the strain is higher than D_{2f}.

Additionally, stress-strain curve obtained from unconfined compression and uniaxial tests of a whole blood clot analogue was used as the target experimental data (the analogue, made from human blood, and the experiments were conducted by other students in the same laboratory), and the goal of this phase is to

modify the coefficients of the anisotropic bilinear model in order to make the output stress-strain curve as similar as possible to the experimental data.

To obtain the stress-strain curves of the proposed hyper-elastic model, a computational simulation is built in Abaqus, involving a unit cube representing the clot material. In this simulation, a compression and tensile test will be performed on the unit cube, with strain values ranging from -0.8 to 1. To simplify this process, a MATLAB script developed by Fereidoonnezhad et al. (2022) (Fereidoonnezhad, Dwivedi, et al., 2021; Fereidoonnezhad, Moerman, et al., 2021; Fereidoonnezhad et al., 2020) is utilized. This script automates the simulation, data collection, and stress-strain curve plotting, additionally, the experimental data is plotted in the same figure to compare with the proposed model.

Furthermore, a parameter study using the same MATLAB script is conducted to facilitate this process. Specifically, an arbitrary parameter set is selected, and the stress-strain curve is plotted based on this set. Subsequently, each parameter is individually modified, both by increasing and decreasing its value, and the resulting curve is plotted on the same figure for comparison with the original curve. By performing this study for the parameters, the influence of each coefficient can be determined.

Eventually, by modifying the coefficients according to the conducted parameter study, the optimal parameter set which captures the target curve is identified.

2.2. Validation of the material model

Once the desirable constitutive model that accurately represents the behavior of clots is found, it is important to validate its capability of predicting unseen experimental data that were not used in the fitting procedure. For this purpose, we use the results of tensile test on a rectangular sample with a circular inclusion (*Figure 12.*), made from the same blood sample that used for tensile and compression tests.

In order to achieve the objective, a clot model is created in Abaqus based on the geometry of the experimental sample (described in *Table 2.* and illustrated in *Figure 13.).* Subsequently, the proposed constitutive model is assigned to the virtual analogue. Regarding the boundary conditions, to simulate the actual tensile test, the bottom is fixed, and the x-symmetric condition is applied to the right side. As for the top side, a displacement of 3.1 mm is applied, and the movement in the x-direction is constrained.

A mesh sensitivity study is conducted to visualize the relationship between the mesh density and maximum principal stress. Thus, the model with proper mesh density and element number is identified. In the next step, the primary comparisons between the physical and numerical tests are the force-displacement curves and the shape-changing processes. Hence, the relative resulting data is collected.

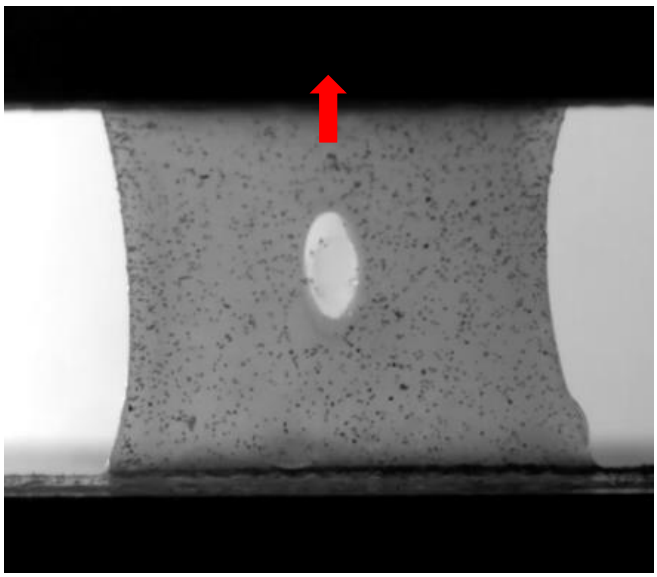

Figure 12. Tensile test of the clot analogue (the red arrow indicates the tensile direction). The experiment is utilized for the validation study of the anisotropic bilinear material model

Table 2. The dimensions of the clot analogue and experimental setup of the thrombus tensile test. The numerical model for the validation study of the anisotropic bilinear model is built according to these values.

Initial length	3.1 mm
Strain rate (tensile rate)	10%/s
Width (Bottom)	3.11 mm
Thickness of the clot analogue	1.171 mm
Hole length	0.9 mm
Hole width	0.35 mm

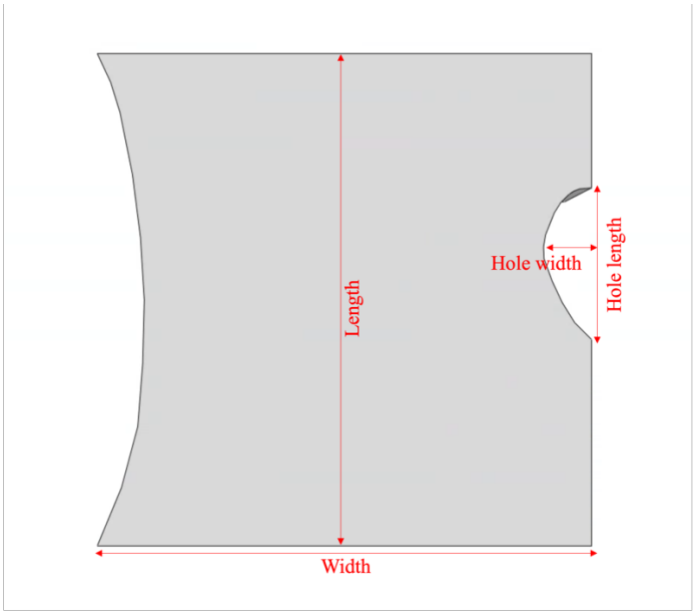

Figure 13. Clot analogue built in Abaqus (Due to symmetry, half of the model is simulated.)

Another important aspect is to avoid permanent damage since the damage model is not implemented. According to the findings from a tensile-failure test conducted on a clot analogue by the colleagues in the same laboratory, the total strain over 65% could lead to permanent damage. Thus, only the total deformation below 65% was considered. Since the strain rate is set at 10% per second, specific time points at 0, 2.5, 4.5, and 6.5 seconds (representing 0%, 25%, 45%, and 65% of strain) were selected for analysis.

Subsequently, the shapes of both the computational and physical samples at those specific time points are captured and digitized using a graphic digitizer software, xyExtract. This process allows for the acquisition of coordinate data for the outlines, which can then be plotted using MATLAB. Furthermore, the resulting force-displacement curve from the simulation is collected. Finally, the validation process involves comparing the shapes and force-displacement curves of the *in-vitro* and *in-silico* experiments at the corresponding time points.

2.3. Investigation of the traction-separation behavior in the cohesive zone

In Abaqus, users can define the traction-separation curve to model the cohesive behaviour as well as the initiation and evolution of cohesive zone damage (*Figure 14*). Regarding the cohesive behaviour, the stiffness of the linear elastic region, K, can be assigned. For damage initiation, users can define the criterion using either stress or separation values. Which means they can specify the point at which damage starts to occur based on a certain stress or separation threshold. Moreover, to capture the progression of damage, two options are available: (i) fracture energy, which represents the total area under the traction-separation curve, and (ii) final separation, which indicates the extent of separation at complete failure. In terms of softening, choice between linear and exponential modes is made. The linear mode provides a simple reduction in stiffness as separation increases, while the exponential mode allows for a more rapid decrease in stiffness.

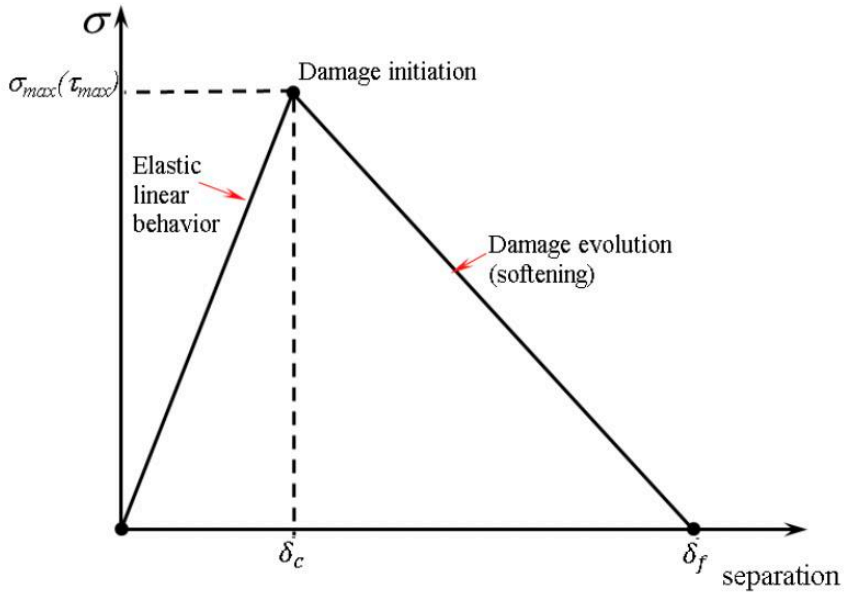

Figure 14. A typical traction-separation curve (Bustamante-Góez et al., 2019)

σ_{max},τ_{max}: Maximum (shear) stress, stress at damage initiation
δ_c: Critical separation, separation at damage initiation
δ_f: Final separation, separation at failure

Hence, before implementing the cohesive and damage behaviour into the simulation, it is necessary to verify that the resulting traction-separation curve satisfies all the predetermined criteria. To achieve this, a simple two-dimensional computational model which consists of a rigid surface and a single-element, rigid, unit square connected by a cohesive interface is built and shown in *Figure 15.* Nonetheless, due to the limitations of Abaqus, the square is modeled as an incompressible linear elastic material with a high Young's modulus, 10^{12} MPa, instead of being treated as a true rigid body. This is because Abaqus does not allow defining contact interactions between actual rigid bodies. In addition, the square is assigned the element type of plane stress.

(a) (b)

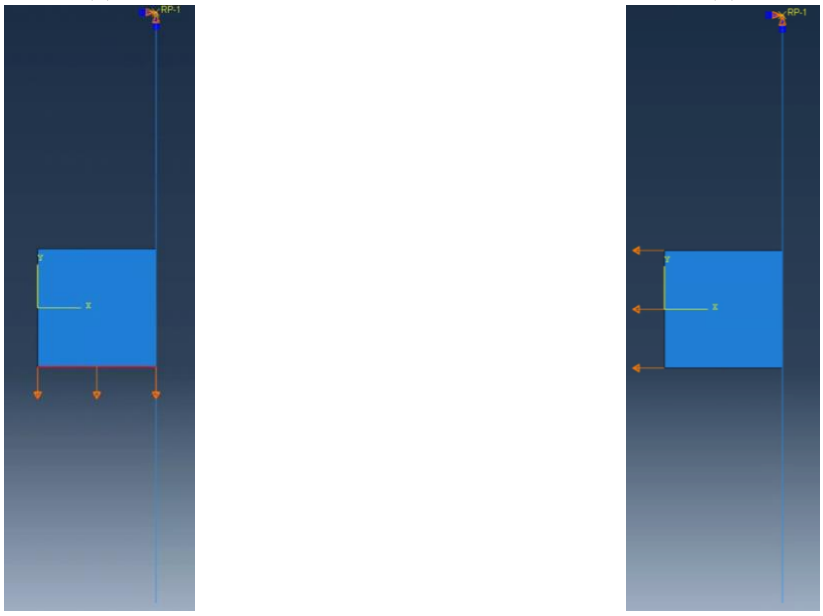

Figure 15. Simple model which consists of a rigid surface (the blue line in the right) and a single-element unit square. (a) Applying a shear displacement (b) Applying a normal displacement

Furthermore, to investigate the traction-separation behavior in different scenarios, a displacement is applied to the bottom side of the square to study its behaviour in the shear direction. On the other hand, a displacement is imparted to the left surface of the square to investigate its behavior in the normal direction. Additionally, the rigid surface is fixed. The other simulation configuration details can be found in *Table 3*, providing an overview of the specific parameters and settings used in the simulation. In addition, the stiffness of the linear elastic region is set to be 4000 MPa/mm in the normal, first shear and second shear direction to demonstrate the curves.

Table 3. The predefined settings for examining the traction-separation curves in the simulations using Abaqus

Case no.	**Displacement direction**	**Damage initiation**	**Damage evolution**	**Softening**
Case 1	normal	Maximum stress = 1 (MPa)	Fracture energy = 3.5e-4 (MPa/mm)	Linear
Case 2	shear	Maximum stress = 1 (MPa)	Fracture energy = 3.5e-4 (MPa/mm)	Linear
Case 3	normal	Maximum stress = 1 (MPa)	Fracture energy = 3.5e-4 (MPa/mm)	Exponential
Case 4	shear	Maximum stress = 1 (MPa)	Fracture energy = 3.5e-4 (MPa/mm)	Exponential
Case 5	normal	Maximum separation = 5e-4 (mm)	Fracture energy = 1e-3 (MPa/mm)	Linear
Case 6	shear	Maximum separation = 5e-4 (mm)	Fracture energy = 1e-3 (MPa/mm)	Linear

Case 7	normal	Maximum separation = 5e-4 (mm)	Fracture energy = 1e-3 (MPa/mm)	Exponential
Case 8	shear	Maximum separation = 5e-4 (mm)	Fracture energy = 1e-3 (MPa/mm)	Exponential

After the completion of the simulations, the reaction force value can be obtained, which is equivalent to the value of nominal stress since the dimensions of the square as 1×1 (mm). Thus, the relationship between traction and separation can be acquired and plotted to verify if the resulting curves match the predefined settings.

Once the traction-separation curves are verified, the rigidity of the clot is replaced with a deformable material property to observe the interaction between the realistic clots and vessel wall. This is accomplished by utilizing the hyper foam model, which has been found to resemble the characteristics of the whole blood clot analogue in my previous work *(Table 4.)*(Ling, 2023).

Table 4. The parameter coefficients of the hyper foam model which mimics the behaviour of a whole blood clot analogue (Ling, 2023)

Coefficient	**Value**
μ_1	0.0043 (MPa)
α_1	6.9409
ν_1	0.1778
μ_2	0.0002 (MPa)
α_2	-0.2094
ν_2	0.35

In terms of the simulation settings, unit square clots are adopted, while the vessel wall is assumed to be rigid. The element type of plane stress is adopted once again. Moreover, the rigid vessel wall remains fixed while a displacement is applied to the entire bottom or the entire left side (as shown in *Figure 15.*). The purpose is to examine the traction-separation behaviour in both the shear and normal directions. As for the cohesive behaviour, it is assumed that the stiffness of the cohesive zone, K, is 0.02 MPa/mm, which is approximately ten times higher than the stiffness of the underlying elements. Regarding the damage initiation and evolution criteria, as specific values are not available in current literature, the simulations adopt the damage initiation criteria based on the assumptions made in (Fereidoonnezhad, Dwivedi, et al., 2021) as a starting point. Furthermore, due to the unknown value of the fracture energy of the clot-vessel interface, the fracture energy of the clot itself, as shown in *Table 5.* (Fereidoonnezhad, Dwivedi, et al., 2021),is utilized instead.

Table 5. The damage criteria of the whole blood clot analogue (Fereidoonnezhad, Dwivedi, et al., 2021)

Clot composition	**40% H (hematocrit)**
Damage initiation	Maximum stress = 0.01 MPa
Damage evolution	Fracture energy = 0.00744 N/mm

CZ stiffness	0.02 MPa/mm

Subsequently, the mesh sensitivity is executed firstly and following simulations are conducted. To avoid interference from stresses in other directions, we collect the traction stress and displacement data at the right-bottom node for the shear displacement case, and at the node in the middle of the right side for the normal displacement case. The relationship between traction-separation curves and elements is presented to identify the desirable mesh density.

For the next step, parameter studies of damage initiation and evolution are executed to determine the impact. To be more specific, each parameter is individually modified according to *Table 6.*, and the resulting reaction force-displacement curve is compared with the original curve. By performing these studies, the influence of maximum stress, CZ stiffness, and fracture energy are identified.

Table 6. Parameter study plan for the cohesive and damage behaviours in the cohesive zone. The coefficients are adopted when modeling the interaction between deformable clots and rigid vessel walls to examine the influence of each parameter.

Damage initiation	**Fracture energy**	**CZ stiffness, K**
Maxs = 0.01 MPa (default)	0.00744 N/mm (default)	0.02 MPa/mm (default)
Maxs = 0.012 MPa	0.008 N/mm	0.043 MPa/mm
Maxs = 0.008 MPa	0.005 N/mm	0.015 MPa /mm

To take the analysis one step further, the material model is replaced with the anisotropic bilinear model *(Table 7.)*, which is suitable for three-dimensional elements with anisotropic properties, such as fibers. In this case, the element type is set to axisymmetric. Also, an additional boundary condition, symmetry in the X direction, is added to simulate real-world scenarios. Furthermore, the displacement is applied only to the bottom side of the clot due to the nature of axisymmetric models. The model is demonstrated in *Figure 16*.

Table 7. The material parameters of 40%H clot analogues in the anisotropic bilinear model (Fereidoonnezhad, Dwivedi, et al., 2021)

Clot composition	**40% H (hematocrit)**
D_{1m}	0.55
D_{2m}	0.65
E_{1m}	2e-5
E_{2m}	0.008
D_{1f}	0.001
D_{2f}	0.003
E_{1f}	0.03
E_{2f}	0.032
D_{1v}	0.014
D_{2v}	0.022
κ_1	0.002
κ_2	0.006

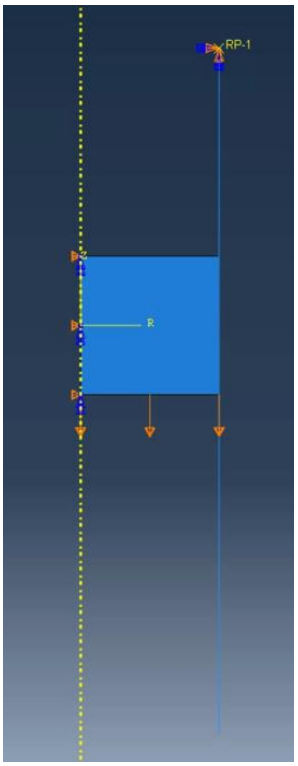

Figure 16. Illustration of the simple axis-symmetric simulation consisting of a unit square clot (the blue square) with anisotropic bilinear *material model and a rigid vessel wall (the blue line in the right). An x-symmetric boundary condition is applied to the left side of the clot and a displacement is applied to the clot bottom. The vessel wall is fixed.*

In terms of the cohesive and damage behavior of the cohesive zone, the parameters listed in *Table 5.* are utilized once again. Moreover, a mesh sensitivity analysis is conducted to determine the relationship between traction-displacement curves and the number of elements, in order to identify the optimal mesh density. Subsequently, parameter studies are conducted to investigate the impact of damage initiation and evolution coefficients, as specified in *Table 6.* By comparing the resulting traction-separation curves with the original curve, the impact of maximum stress, cohesive zone stiffness, and fracture energy can be evaluated.

2.4. Numerical modeling of aspiration thrombectomy

Once the appropriate constitutive model for clot with varying compositions and CZM method are identified and validated, the *in-silico* aspiration thrombectomy model can be created accordingly to investigate the performance of different suction catheter designs.

First of all, a parameter study is conducted to investigate the impact of clot size on the procedure using typical diameters of internal carotid artery (ICA) and middle cerebral artery (MCA) (Rai et al., 2013). The study focuses on modifying the ratio of the clot dimensions (diameter and length) to the catheter diameter while applying a suction pressure of 0.02 MPa to the clot bottom. The resulting deformation at the center of the clot bottom are collected to evaluate how the clot size influences the aspiration process.

In terms of the geometry, only the clot and the catheter are incorporated into the model to simplify the calculation, and the clot is assumed to be a cylinder. As for the catheter specifications, the dimensions of Penumbra 5MAX (*Table 8.*)(Penumbra Inc., Alameda, CA, USA) is utilized. Thus, an axisymmetric model is utilized, and a x-symmetric boundary condition is applied. Besides, the element type of axis-symmetric element is adopted for the clot. In addition, the catheter tip is in direct contact with the clot and the contact property between the clot and the catheter is defined as frictionless, hard contact to simplify the simulation. The model is demonstrated in *Figure 17.*

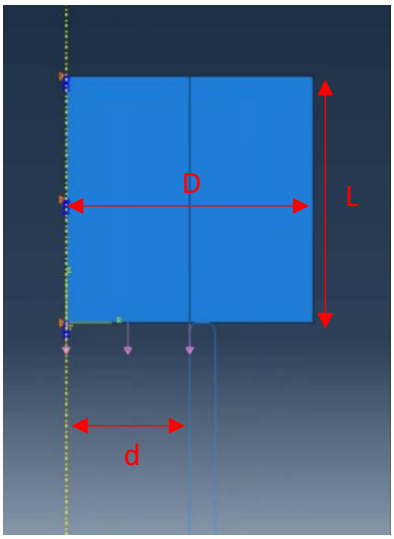

Figure 17. The model for the parameter study of in the aspiration thrombectomy simulation. The blue square represents the clot and the frame consisting of blue line represents the catheter. A boundary condition of x-symmetricity is applied to the left side of the clot and a suction pressure of 0.02 MPa is applied to the clot bottom (area equals to the inner part of the catheter). The catheter is assumed to be rigid and fixed. The values of D/d and L/d are modified and the impact on deformation at the center of the clot bottom are recorded.

D: clot diameter (mm)
L: clot length (mm)
d: catheter diameter (mm)

Table 8. The dimensions of the catheter used for simulation in this thesis

Distal outer diameter	1.67 mm
Distal inner diameter	1.37 mm
Length	8 mm

In relation to the material parameters, the anisotropic bilinear model is adopted to model different types of clots with different compositions ranging from low fibrin/high red blood cell (RBC) to high fibrin/low RBC. The material coefficients for these clots are obtained from the work of (Fereidoonnezhad, Dwivedi, et al., 2021) and the details are presented in *Table 9.* In the simulation, the softest (40%H) and the toughest (5%H) clot are examined.

Table 9. Material parameters of anisotropic bilinear model for three different clot analogues (Fereidoonnezhad, Dwivedi, et al., 2021). %H stands for the percentage of Hematocrit.

Clot composition	**40% H (hematocrit)**	**20% H**	**5% H**
D_{1m}	0.55	0.35	0.4
D_{2m}	0.65	0.45	0.55
E_{1m}	2e-5	2e-5	5e-5
E_{2m}	0.008	0.006	0.02
D_{1f}	0.001	0.01	0.01
D_{2f}	0.003	0.015	0.02
E_{1f}	0.03	0.085	0.065
E_{2f}	0.032	0.095	0.15
D_{1v}	0.014	0.015	0.015
D_{2v}	0.022	0.025	0.025
κ_1	0.002	0.004	0.004
κ_2	0.006	0.006	0.006

Subsequently, the vessel wall is included into the model to mimic the medical practice. The artery is assumed to have a rigid behavior (Good et al., 2020). Subsequently, the clot-vessel interface is modeled as a cohesive zone with implemented criteria for damage initiation and evolution. As specific cohesive and damage parameters are not available in current literature, the objective is to investigate the impact of damage initiation criterion, fracture energy, and cohesive stiffness. Similar to *section 2.3*, the damage criteria in *(Table 10.)* (Fereidoonnezhad, Dwivedi, et al., 2021) serve as a starting point.

Table 10. The damage initiation and evolution criteria for clots with different compositions (Fereidoonnezhad, Dwivedi, et al., 2021)

Clot composition	**40% H**	**20% H**	**5% H**
Damage initiation	Maximum stress = 0.01 MPa	Maximum stress = 0.025 MPa	Maximum stress = 0.045 MPa
Damage evolution	Fracture energy = 0.00744 N/mm	Fracture energy = 0.0170 N/mm	Fracture energy = 0.0219 N/mm
CZ stiffness	0.3 MPa/mm	0.85 MPa/mm	0.65 MPa/mm

The geometries of the clot and artery are simplified as cylindrical shapes, with the clot resembling a cylinder and the artery resembling a hollow tube. Thus, an axis-symmetric model is selected the element type of axis-symmetric element is adopted for the clot. For clot diameter, a value of 2.74 mm is chosen since it is approximately the typical diameter of the M1 segment of the middle cerebral artery (MCA) (Oyekole et al., 2021) and precisely twice of the inner diameter of the Penumbra 5MAX reperfusion catheter. In terms of clot length, a value according to result of the last parameter study (*Figure 17.*) is utilized.

In addition to the Penumbra 5MAX catheter, a catheter with a larger inner diameter (as determined by the parameter study shown in *Figure 17.*) is used to assess the potential improvement in performance. That is because, larger suction diameter can deliver suction forces close to the clot-vessel interface and has been recommended in multiple studies (Chitsaz et al., 2018; Hu & Stiefel, 2016; Talayero et al., 2019; Talayero et al., 2020). Therefore, it may have the potential to improve clinical outcomes. The resulting deformation at the center of the clot bottom are collected to evaluate how the CZM coefficients influence the aspiration process. Different scenarios, including adopting clot damage criteria, reduced maximum nominal stress, and decreased fracture energy are examined. The values in (Fereidoonnezhad, Dwivedi, et al., 2021) once again provides a starting point.

Regarding the rest settings and boundary conditions, the catheter tip is in direct contact with the clot and the interaction between the clot and catheter is defined as frictionless and hard contact. Moreover, an aspiration pressure of 0.02 MPa is applied to the clot bottom and the suction area is equal to the inner area of the catheter. The model is demonstrated in *Figure 18.* Finally, both the softest (40%H) and the toughest (5%H) clot are examined (*Table 9.*).

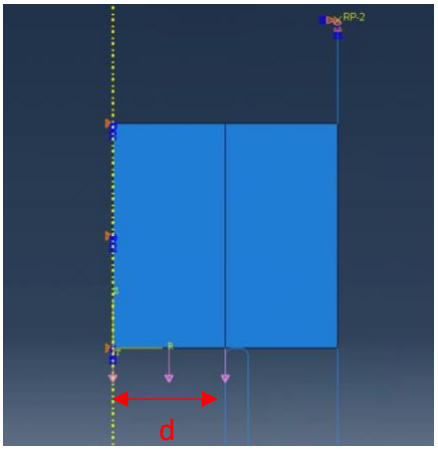

Figure 18. The model for parameter study of CZM coefficients in the aspiration thrombectomy simulation. The blue square represents the clot and the frame consisting of blue line represents the catheter. The vessel wall (the blue line in the right) is included and both the vessel wall and the catheter are assumed to be rigid and fixed. A boundary condition of x-symmetricity is applied to the left side of the clot and a suction pressure of 0.02 MPa is applied to the clot bottom (area equals to the inner part of the catheter). The values of CZM coefficients and d are changed to observe the impact of the parameters. d: catheter diameter (mm)

2.5. Proposing a new catheter design

A larger catheter tip can be achieved by incorporating an expendable stent with a cover, extending over the catheter tip. This approach allows for enlarging the diameter of the catheter tip while mitigating navigation difficulties. Therefore, a final parameter study is conducted to identify the optimal design of the catheter and the stent.

Specifically, the distances between the location where the stent starts to extend and the clot (L_1), as well as the distance between the clot and the location where the stent turns straight (L_2), are modified to optimize the dimensions of the catheter and stent. To elaborate, the simulations involve varying L_1 values of 4, 5, and 6 mm, while keeping L_2 at 3 mm. Additionally, scenarios with L_2 values of 2, 3, and 4 mm, while maintaining L_1 at 5 mm, will also be executed. The CZM parameters are chosen based on the results of the last parameter study (*Figure 18.*). The remaining settings and boundary conditions adopt the same values as shown in *Figure 18. The model for this catheter design study is presented in Figure 19.* Once again, the resulting deformation at the center of the clot bottom are collected to evaluate how the CZM coefficients influence the aspiration process.

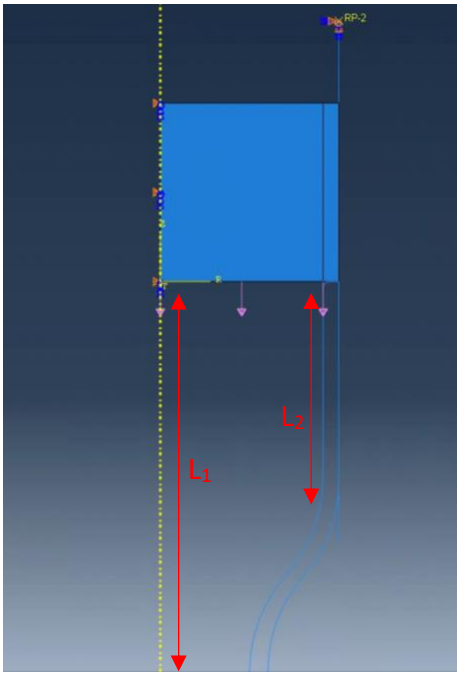

Figure 19. The model for parameter study of catheter and stent design in the aspiration thrombectomy simulation. The blue square represents the clot and the frame consisting of blue line represents the catheter. The vessel wall (the blue line in the right) is included and both the vessel wall and the catheter are assumed to be rigid and fixed. A boundary condition of x-symmetricity is applied to the left side of the clot and a suction pressure of 0.02 MPa is applied to the clot bottom (area equals to the inner part of the catheter). The values of L_1 and L_2 are changed to observe the impact of the parameters.

L_1: the distance between the location where the stent starts to extend and the clot
L_2: the distance between the clot and the location where the stent turns straight

Chapter 3. Results

3.1. Parameter study of the material model and the fitting result

In this section, the results of parameter study and parameter identification for the anisotropic bilinear model are presented. Some typical parameters are chosen as baseline parameters (*Table 11.*) Next, each parameter is modified by both increasing and decreasing its value, and then assigned as the material model for the deformation test simulation of the unit cube in Abaqus. Subsequently, the according stress-strain curves are plotted and compared to the curve obtained from the original parameter set. The resulting plots are shown in *Figure 20.*

Table 11. Baseline parameters for the parameter study and parameter identification for the anisotropic bilinear model

D_{1m}	0.1
D_{2m}	0.4
E_{1m}	5e-5
E_{2m}	0.003
D_{1v}	0.27
D_{2v}	0.8
κ_1	0.0015
κ_2	0.06
D_{1f}	0.08
D_{2f}	0.016
E_{1f}	0.2
E_{2f}	0.4

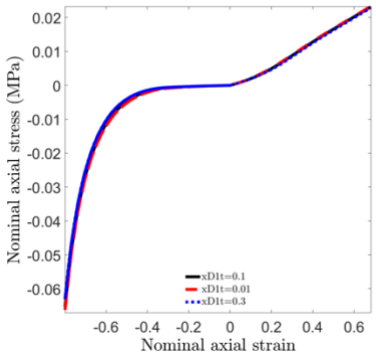

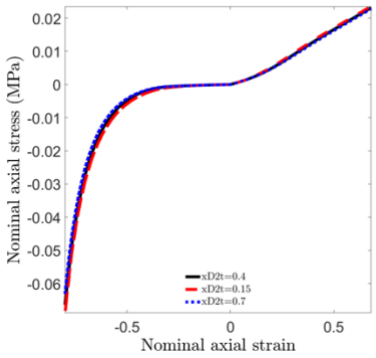

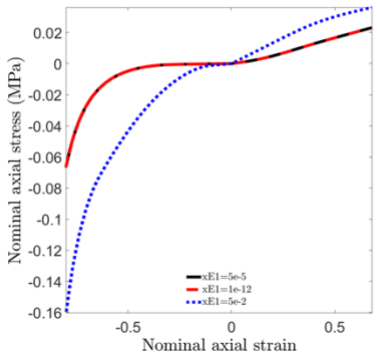
Nominal axial stress (MPa)
Nominal axial strain
xE1=5e-5
xE1=1e-12
xE1=5e-2

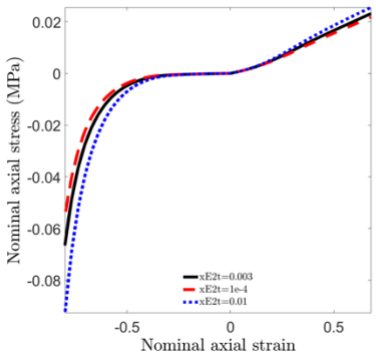
Nominal axial stress (MPa)
Nominal axial strain
xE2t=0.003
xE2t=1e-4
xE2t=0.01

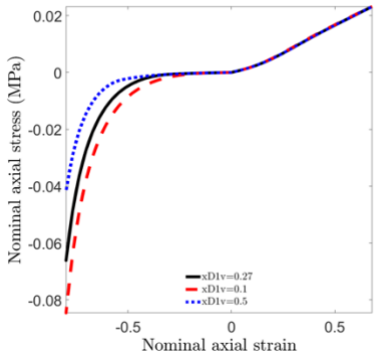
Nominal axial stress (MPa)
Nominal axial strain
xD1v=0.27
xD1v=0.1
xD1v=0.5

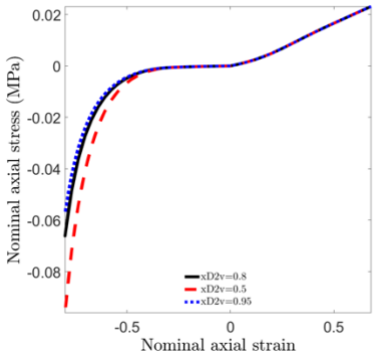
Nominal axial stress (MPa)
Nominal axial strain
xD2v=0.8
xD2v=0.5
xD2v=0.95

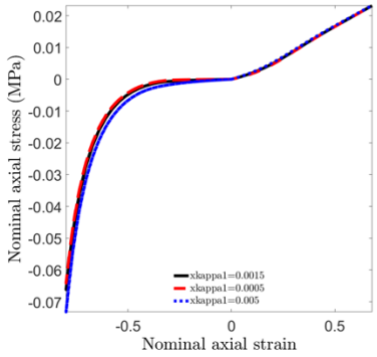
Nominal axial stress (MPa)
Nominal axial strain
xkappa1=0.0015
xkappa1=0.0005
xkappa1=0.005

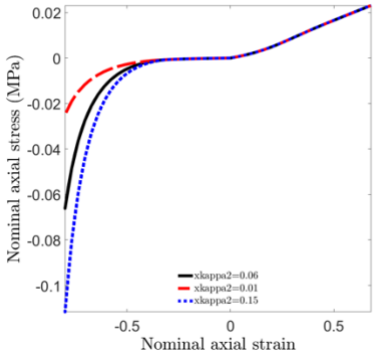
Nominal axial stress (MPa)
Nominal axial strain
xkappa2=0.06
xkappa2=0.01
xkappa2=0.15

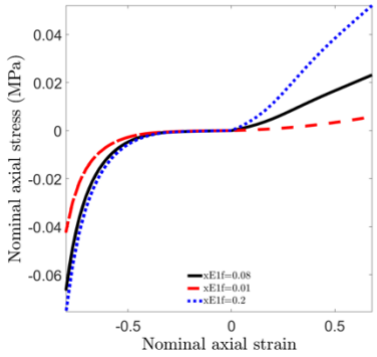
Nominal axial stress (MPa)
Nominal axial strain
xE1f=0.08
xE1f=0.01
xE1f=0.2

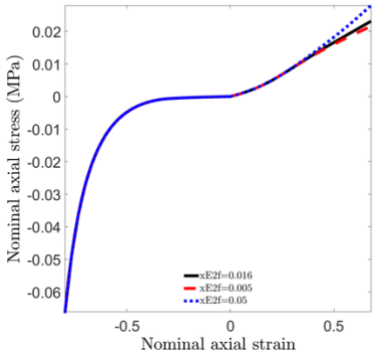
Nominal axial stress (MPa)
Nominal axial strain
xE2f=0.016
xE2f=0.005
xE2f=0.05

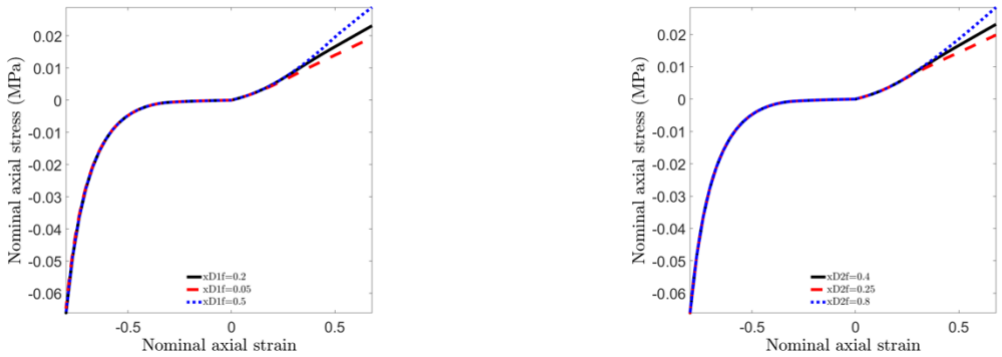

Figure 20. The influence of each parameter to the stress-strain curve in the anisotropic bilinear model

Thus, the influence of ethe coefficients are determined. For instance, E_{2f}, D_{1f}, and D_{2f} have a significant effect on the tension regime, while D_{1v}, D_{2v}, κ_1, and κ_2 have a greater impact on the compression regime. Moreover, E_{1m}, E_{2m}, and E_{1f} have a substantial influence on both the tension and compression regimes largely. On the other hand, the influence of D_{1m} and D_{2m} are relatively insignificant.

With the information, the output stress-strain curve is predicted and controlled when adjusting the parameters. Consequently, the optimized parameter set which matches the experimental data is obtained and shown in *Figure 21 and Table 12.*

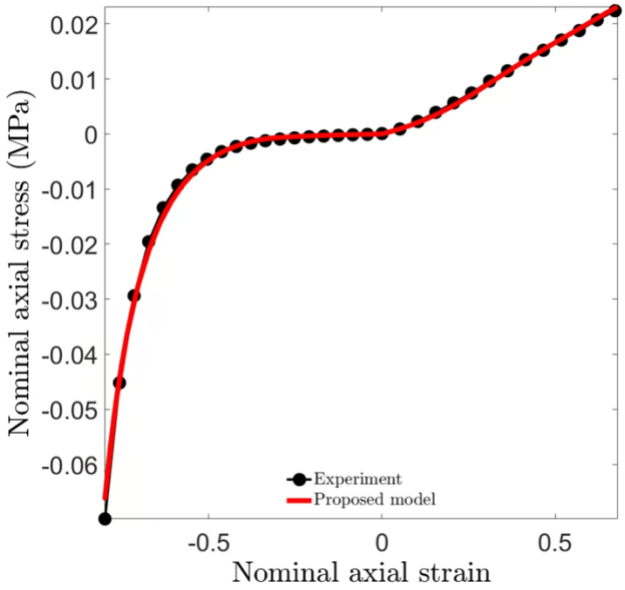

Figure 21. Capability of the anisotropic bilinear model (Fereidoonnezhad, Dwivedi, et al., 2021; Fereidoonnezhad, Moerman, et al., 2021; Fereidoonnezhad et al., 2020) to replicate the experimental data of compression and tensile tests for whole blood clot analogues.

Table 12. The parameter set of the optimal anisotropic bilinear model (Fereidoonnezhad, Dwivedi, et al., 2021; Fereidoonnezhad, Moerman, et al., 2021; Fereidoonnezhad et al., 2020) to replicate the experimental data of compression and tensile tests for whole blood clot analogues.

D_{1m}	0.1
D_{2m}	0.4
E_{1m}	5e-5
E_{2m}	0.003
D_{1v}	0.27
D_{2v}	0.8
κ_1	0.0015
κ_2	0.06
D_{1f}	0.08
D_{2f}	0.016
E_{1f}	0.2
E_{2f}	0.4

3.2. Validation of the material model

Once the optimal anisotropic bilinear model is identified, the material parameters are assigned to the numerical clot analogue (as depicted in *Figure 13.*). Next, the tensile simulation is performed and the results are presented to compare with the experimental data. Initially, a mesh sensitivity study is conducted to determine the relationship between maximum principal stress and mesh density. The findings are presented in *Figure 22, Figure 23 and Table 13.*

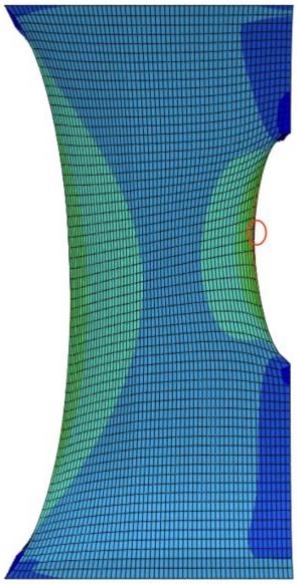

Figure 22. The location of the maximum principal stress occurrence in the tensile simulations for the mesh sensitivity study to identify optimal mesh density. The simulation is used to validate the optimal isotropic bilinear model (Fereidoonnezhad, Dwivedi, et al., 2021; Fereidoonnezhad, Moerman, et al., 2021; Fereidoonnezhad et al., 2020).

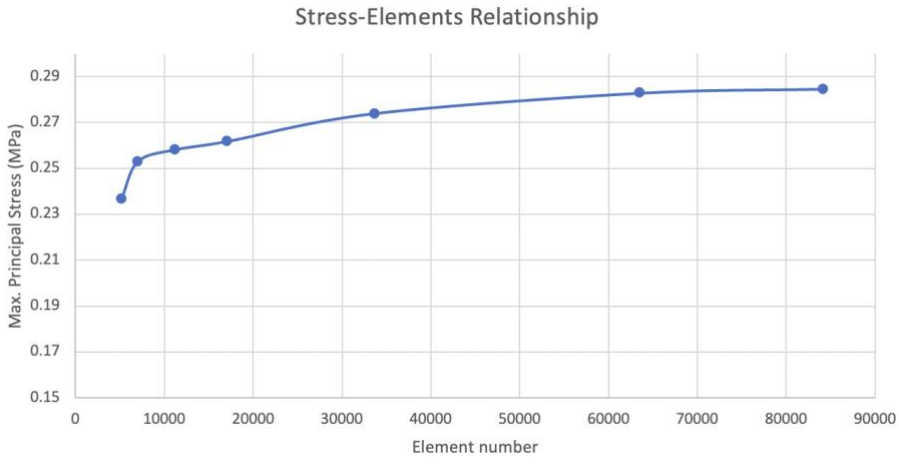

Figure 23. The relationship between elements and maximum principal stress in the tensile simulations for the mesh sensitivity study to identify optimal mesh density. The simulation is used to validate the

optimal isotropic bilinear model (Fereidoonnezhad, Dwivedi, et al., 2021; Fereidoonnezhad, Moerman, et al., 2021; Fereidoonnezhad et al., 2020).

Table 13. The relationship between elements, max. principal stress and computational time in the tensile simulations for the mesh sensitivity study to identify optimal mesh density. The simulation is used to validate the optimal isotropic bilinear model (Fereidoonnezhad, Dwivedi, et al., 2021; Fereidoonnezhad, Moerman, et al., 2021; Fereidoonnezhad et al., 2020).

Elements	Max. principal stress	Computational time
5193	0.2368	33 mins
7030	0.2531	44 mins
11172	0.2582	1 hr 6 mins
17034	0.2618	2 hr 10 mins
33643	0.274	4 hr 15 mins
63525	0.2829	8 hr 20 mins
84157	0.2847	11 hr 6 mins

The location of the maximum principal stress remains consistent across different mesh densities, as depicted in *Figure 22*. In addition, the value of the maximum principal stress appears to converge as the number of elements increases. Moreover, by taking the computational time into consideration, the element number of 33643 is selected since it provides a good accuracy in a relatively short period.

Therefore, a comparison can be made between the results of the in-silico model and experimental data. To begin with, the total reaction force of the in-silico model is collected and multiplied by a factor of two since only half of the clot was modeled. This enables the determination of the force-displacement curve, considering the known strain rate of 10%. Furthermore, the force-displacement curve of the experiment is plotted in the same figure, allowing for a visual comparison of the differences within the 0-65% elongation range. The trends of the two curves are similar, however, a notable deviation is evident between the computational simulation and the *in-vitro* tensile experiment *(Figure 24)*.

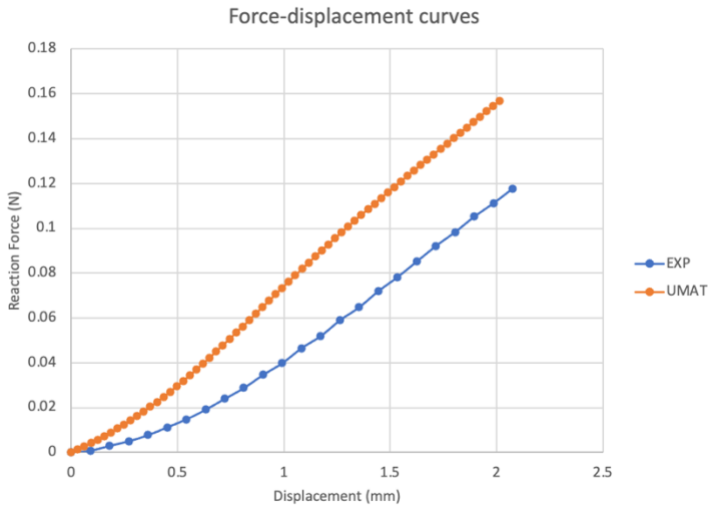

Figure 24. The comparison in terms of force-displacement curves of the tensile experiment and the numerical simulation to validate the anisotropic bilinear material model(Fereidoonnezhad, Dwivedi, et al., 2021; Fereidoonnezhad, Moerman, et al., 2021; Fereidoonnezhad et al., 2020).

Subsequently, screenshots of the simulation and experimental shapes at 0%, 25%, 45%, and 65% tension (corresponding to 0, 2.5, 4.5, and 6.5 seconds) are taken. Next, xyExtract is used to digitize the screenshots to acquire the coordinate data of the outlines. The coordinate data obtained is utilized by MATLAB to plot the shapes at the same tension in a single figure for the purpose of comparison *(Figure 25)*.

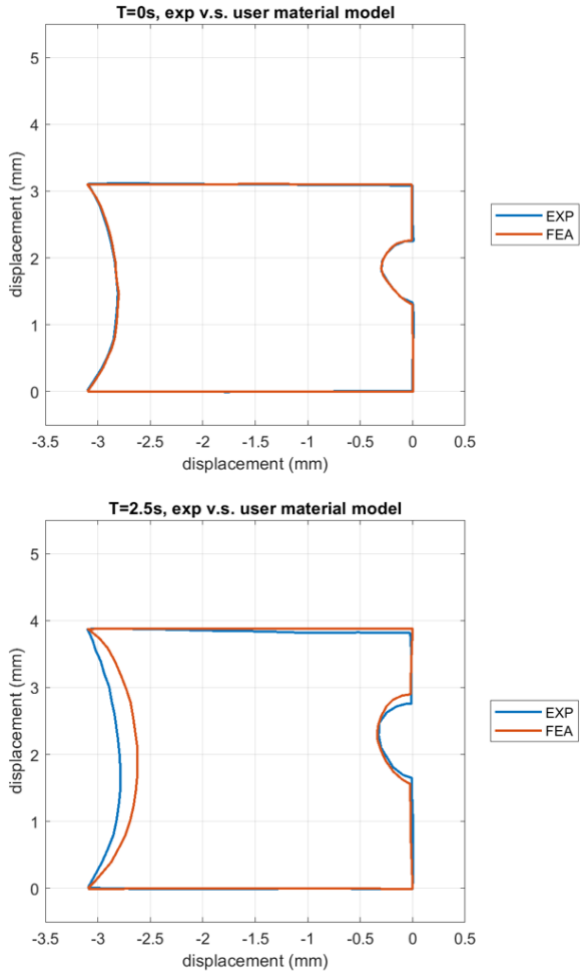

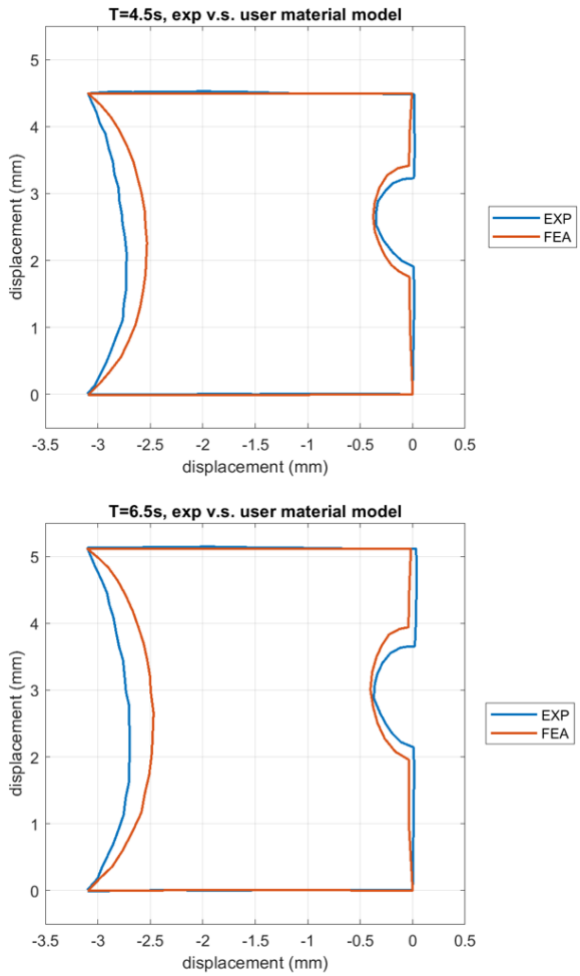

Figure 25. The comparison of shape changing processes between the tensile experiment and the tensile simulation to validate the anisotropic bilinear material model(Fereidoonnezhad, Dwivedi, et al., 2021; Fereidoonnezhad, Moerman, et al., 2021; Fereidoonnezhad et al., 2020).

According to the comparison, an obvious deviation is observed and the anisotropic bilinear model exhibits a greater shrinkage compared the tensile experiment, particularly at both the right and left sides.

3.3. Traction-separation curve study

The simulation results of modeling rigid clots and vessel wall are shown. The traction-separation curves obtained from each case are collected and presented in *Figure 26.*, aligning with the settings specified in *Table 3*. The fracture energy values, calculated from the area under the curves, align with the predefined settings as well.

Case 1:

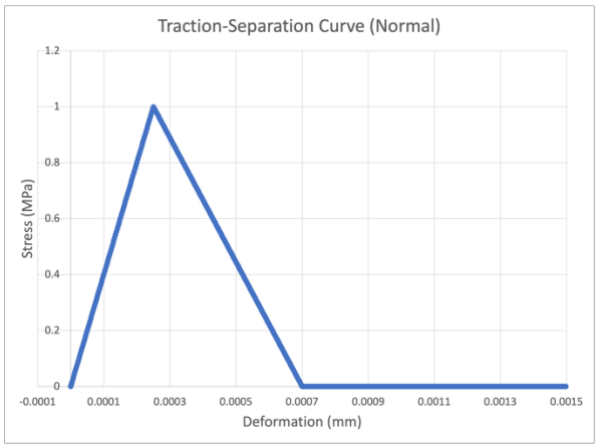

Case 2:

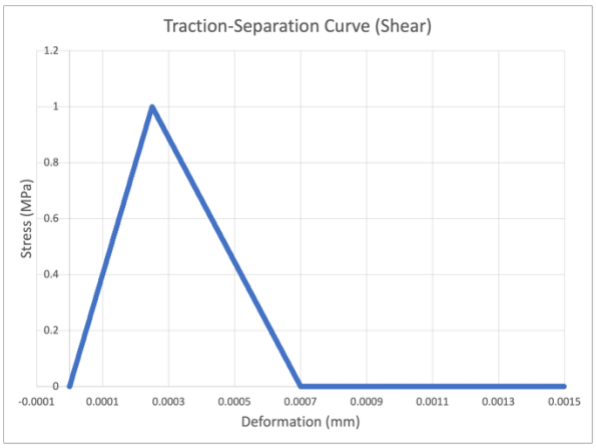

Case 3:

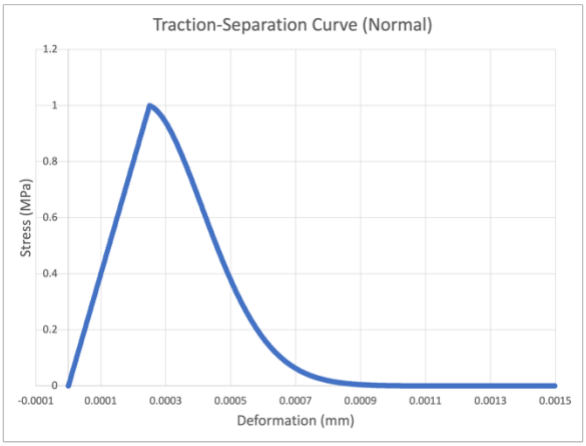

Case 4:

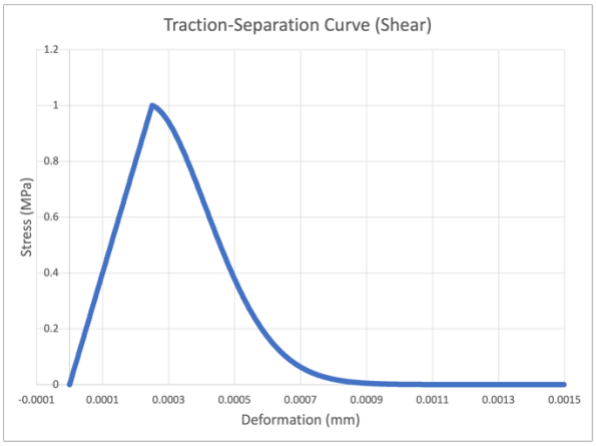

Case 5:

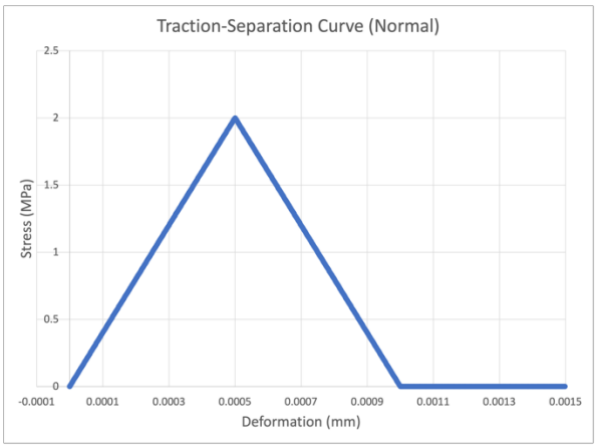

Case 6:

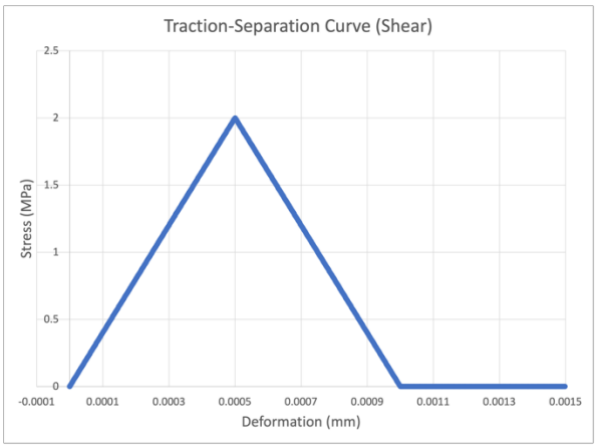

Case 7:

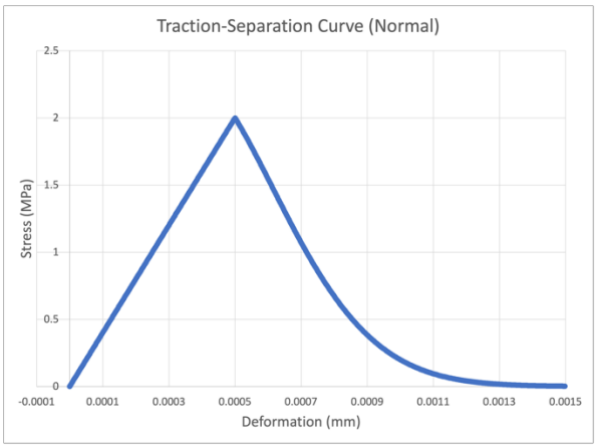

Case 8:

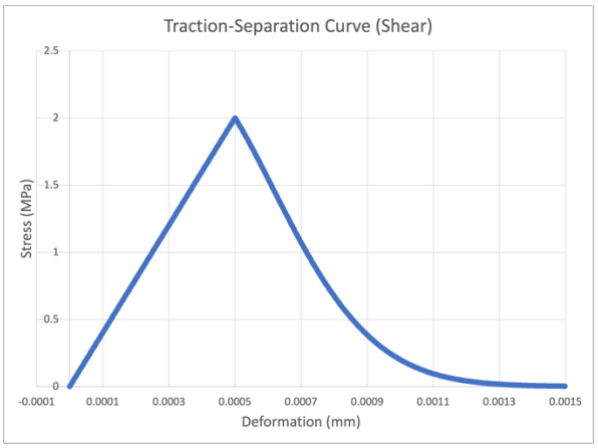

Figure 26. The resulting traction-separation curves of the simulations which validate the cohesive and damage behaviour in Abaqus using rigid clots and vessel wall

Upon replacing the clot material with the hyper foam model (*Table 4.*), the mesh sensitivity studies show that the location of the maximum principal stress remains consistent irrespective of the mesh density (*Figure 27*). Additionally, the resulting traction-separation curves exhibit complete similarity (*Figure 28* and *Figure 29*).

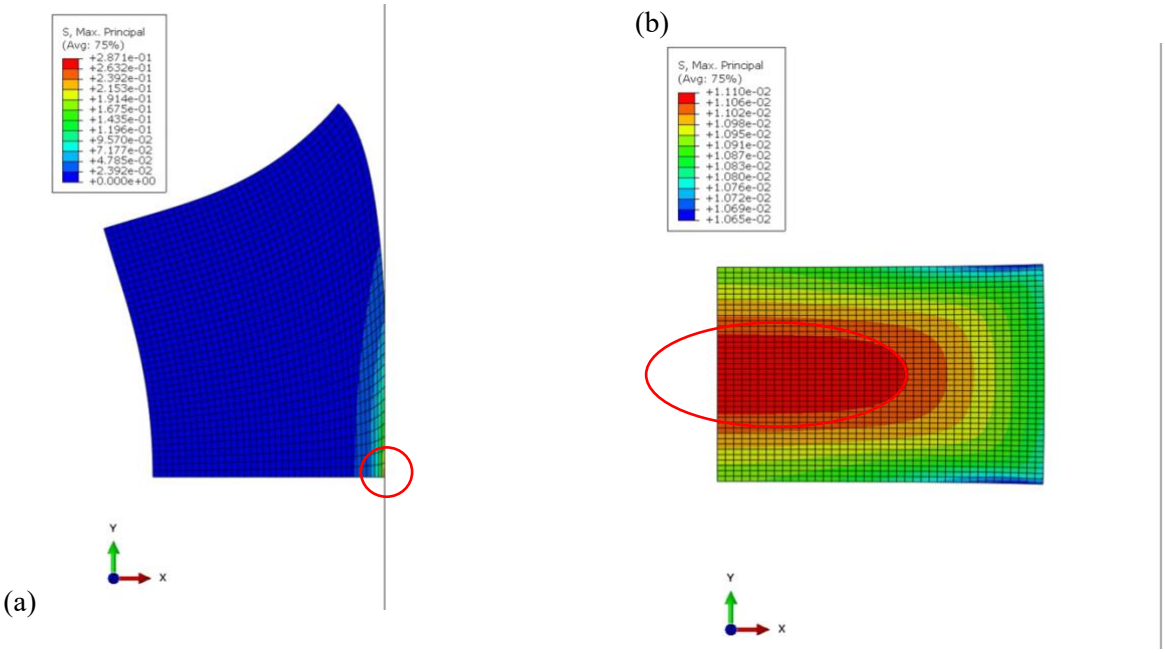

Figure 27. The location where the maximum principal stress occurs when (a) applying displacements in shear direction (b) applying displacements in normal direction to identify the optimal mesh density for CZM validation in Abaqus. The models consist of a hyper foam clot and a rigid vessel wall.

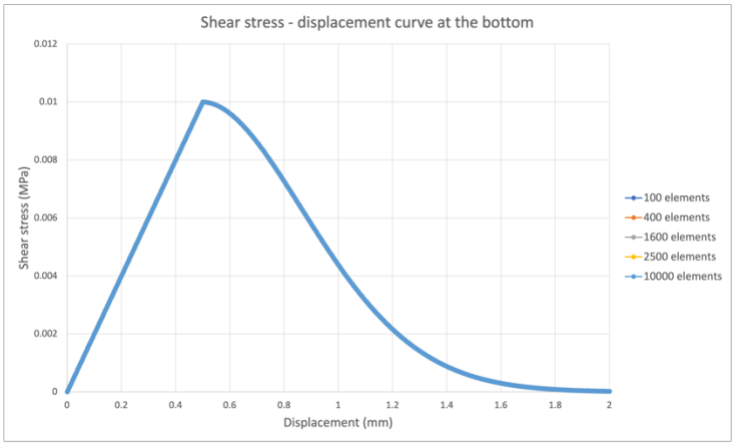

Figure 28. The resulting traction-separation curves of simulations applying displacements in shear direction to the clot. The models consist of a hyper foam clot and a rigid vessel wall, and the interface is modeled as a cohesive zone.

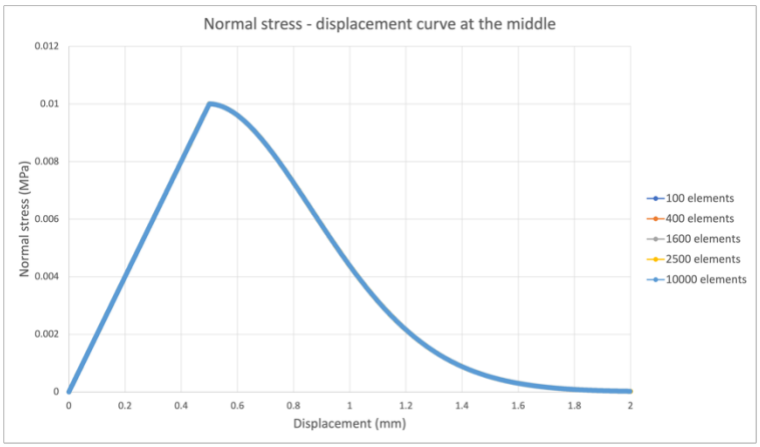

Figure 29. The resulting traction-separation curves of simulations applying displacements in normal direction to the clot. The models consist of a hyper foam clot and a rigid vessel wall, and the interface is modeled as a cohesive zone.

To visualize the stress and deformation distribution more effectively, the simulation is conducted with a chosen element number of 1600 (mesh density = 0.025 mm) for further analyses. Next, the parameter studies are performed for the maximum stress, fracture energy, and cohesive stiffness. The resulting curves obtained from these studies are identical to the predefined parameters listed in *Table 6*. Moreover, the areas under the curves align with the predefined fracture energy values. In addition, it is observed that when the K value is excessively high or the maximum stress is too low, the traction stress can exceed the predefined maximum stress (the damage initiation criterion). The resulting curves are presented in *Figure 30* and *Figure 31*.

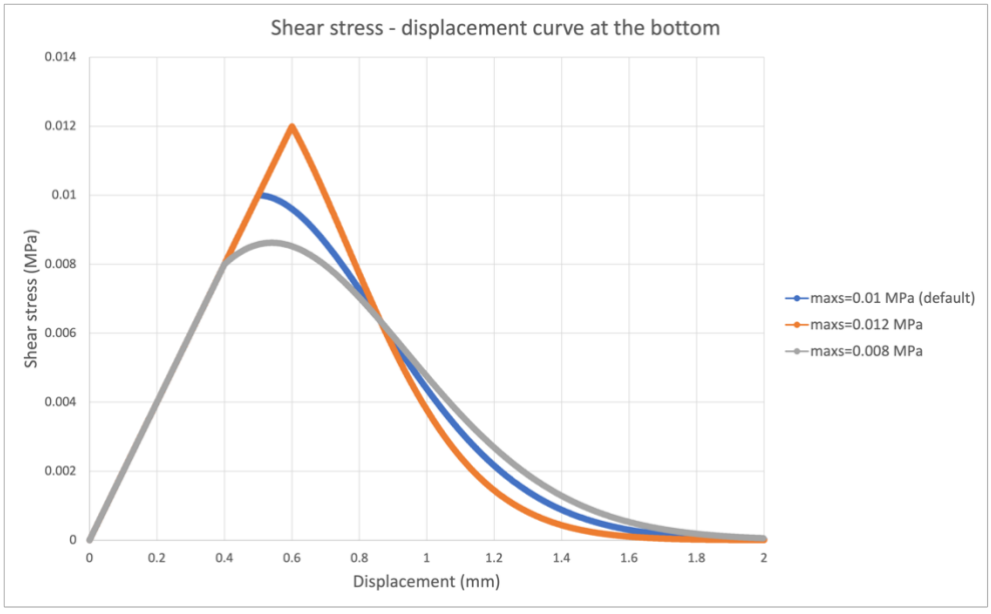

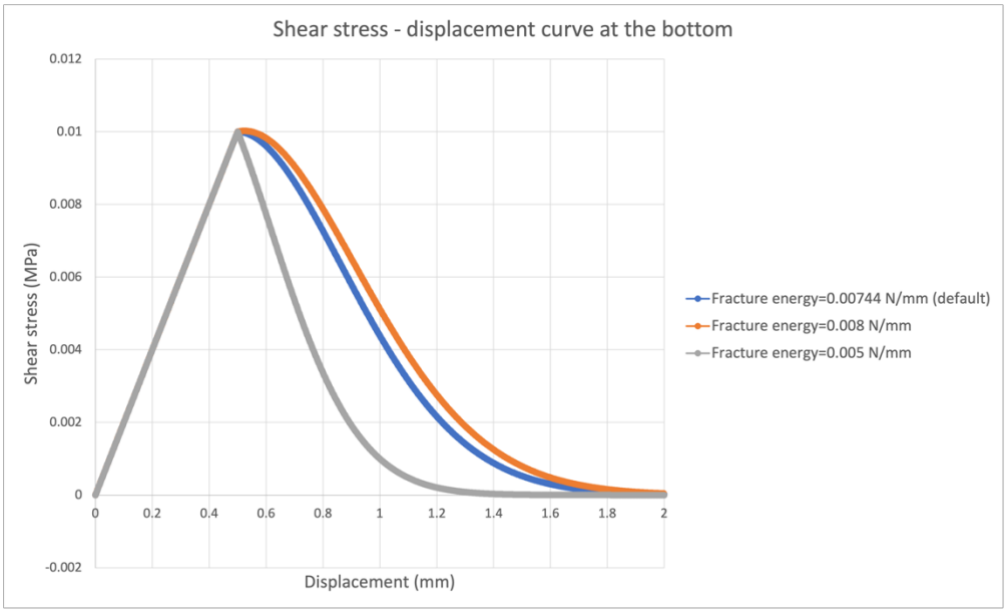

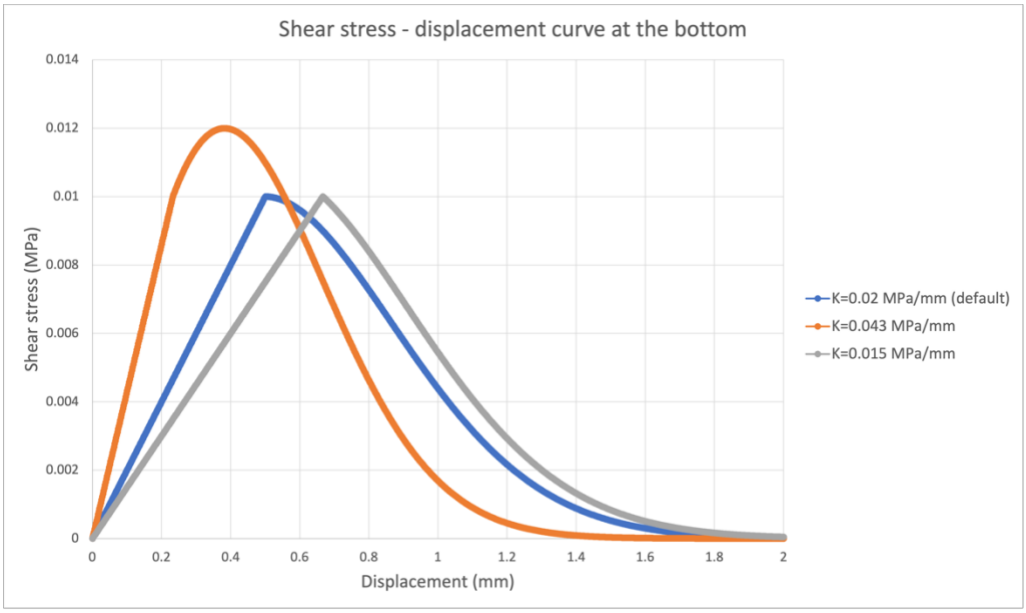

Figure 30. The resulting traction-separation curves in the cohesive interface when applying shear displacements to the hyper foam clot to study the influence of different damage parameters. The models consist of a hyper foam clot and a rigid vessel wall, and the interface is modeled as a cohesive zone. Parameters which are not specified are identical to the default values in Table 6.

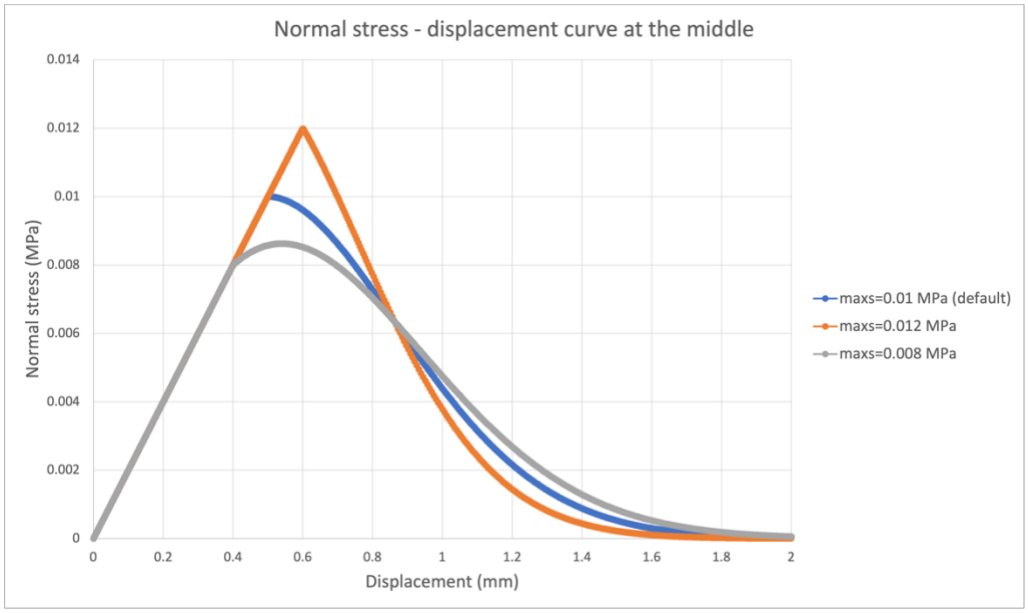
Normal stress - displacement curve at the middle
Normal stress (MPa)
0.014
0.012
0.01
0.008
0.006
0.004
0.002
0
0
0.2
0.4
0.6
0.8
1
1.2
1.4
1.6
1.8
2
Displacement (mm)
maxs=0.01 MPa (default)
maxs=0.012 MPa
maxs=0.008 MPa

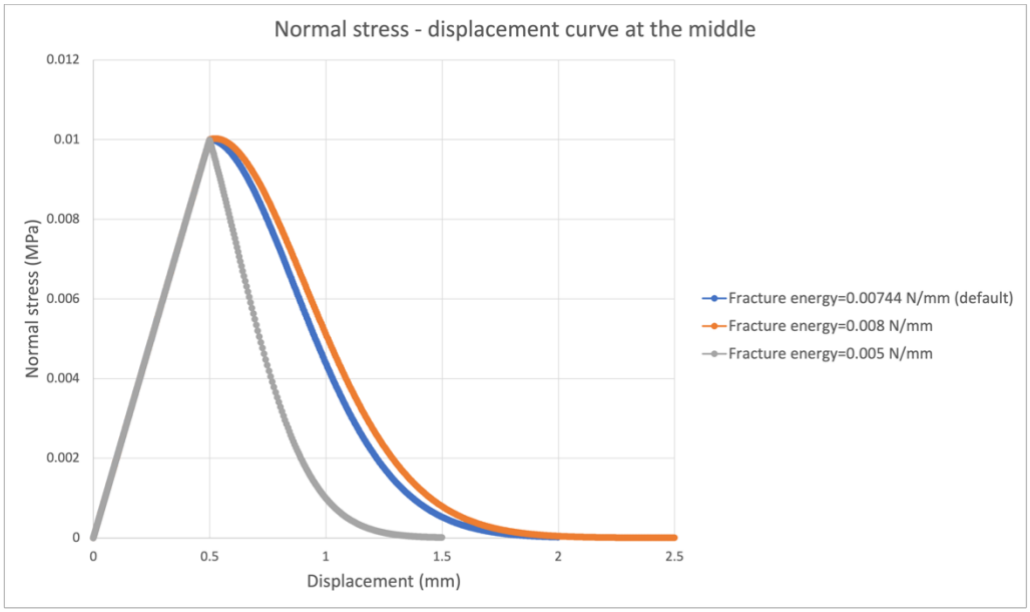
Normal stress - displacement curve at the middle
Normal stress (MPa)
0.012
0.01
0.008
0.006
0.004
0.002
0
0
0.5
1
1.5
2
2.5
Displacement (mm)
Fracture energy=0.00744 N/mm (default)
Fracture energy=0.008 N/mm
Fracture energy=0.005 N/mm

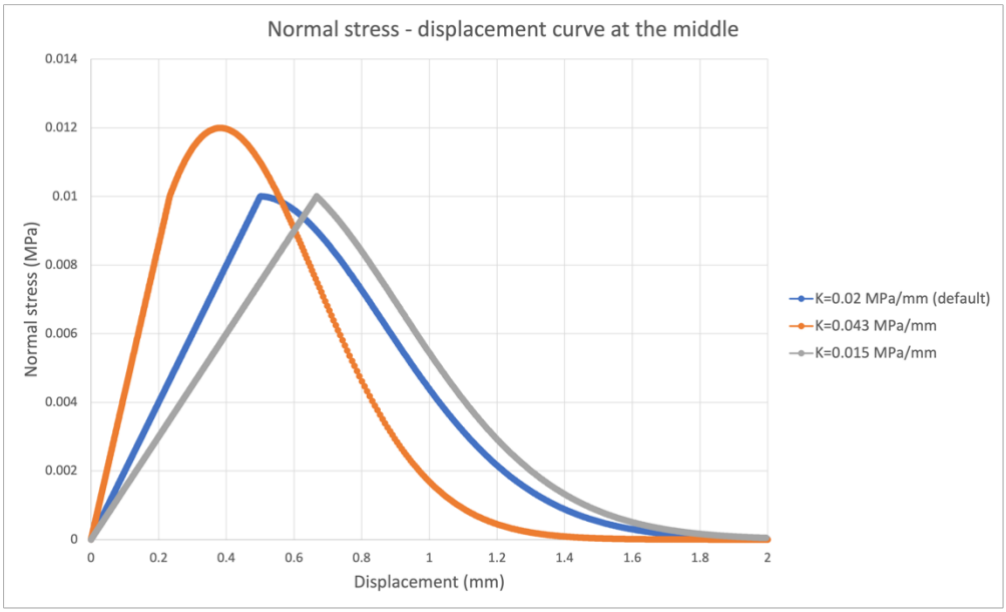

Figure 31. The resulting traction-separation curves in the cohesive interface when applying normal displacements to the hyper foam clot to study the influence of different damage parameters. The models consist of a hyper foam clot and a rigid vessel wall, and the interface is modeled as a cohesive zone. Parameters which are not specified are identical to the default values in Table 6.

Subsequently, the clot material is replaced with the anisotropic bilinear model (*Table 7.*). Once again, the mesh sensitivity studies indicate that the location of the maximum principal stress remains consistent regardless of the mesh density *(Figure 32)*. Moreover, the resulting traction-separation curves are completely identical *(Figure 33)*.

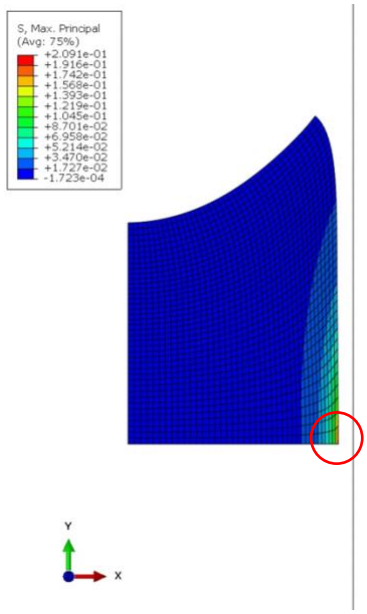

Figure 32. The location where the maximum principal stress occurs when applying displacements in shear direction in the axisymmetric model to identify the optimal mesh density for CZM validation in

Abaqus. The models consist of an anisotropic bilinear clot (Fereidoonnezhad, Dwivedi, et al., 2021; Fereidoonnezhad, Moerman, et al., 2021; Fereidoonnezhad et al., 2020) and a rigid vessel wall.

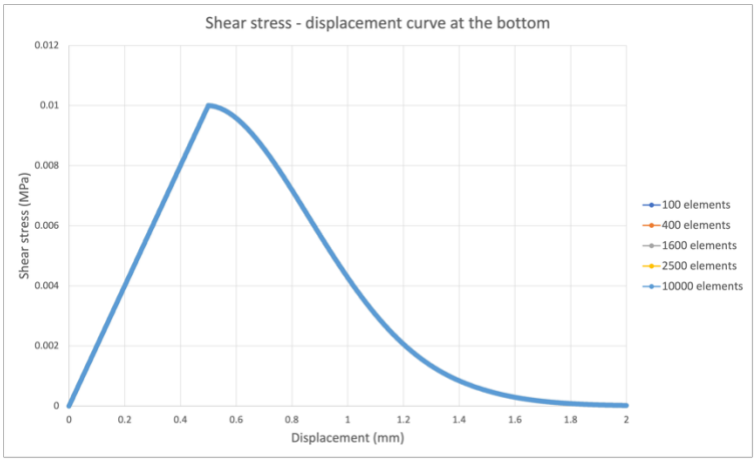

Figure 33. The resulting traction-separation curves of simulations applying displacements in shear direction to the clot in the axisymmetric model. The models consist of a anisotropic bilinear clot (Fereidoonnezhad, Dwivedi, et al., 2021; Fereidoonnezhad, Moerman, et al., 2021; Fereidoonnezhad et al., 2020) and a rigid vessel wall, and the interface is modeled as a cohesive zone.

For the same reason, the element number of 1600 (mesh density = 0.025 mm) is selected for further analyses. The subsequent parameter studies investigate the effects of maximum stress, fracture energy, and cohesive stiffness. The resulting curves obtained from these studies closely match the predefined parameters outlined in *Table 6.* Furthermore, the areas under the curves align with the predetermined fracture energy values. It is worth noting that in cases where the cohesive stiffness (K value) is excessively high or the maximum stress is too low, the traction stress may surpass the predefined maximum stress (the damage initiation criterion). The resulting curves are shown in *Figure 34.*

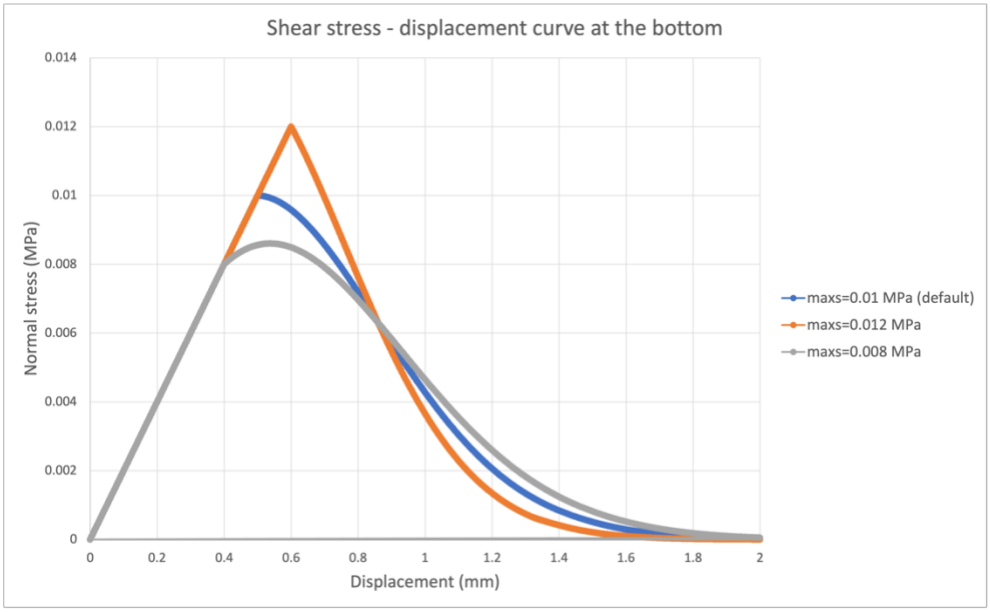

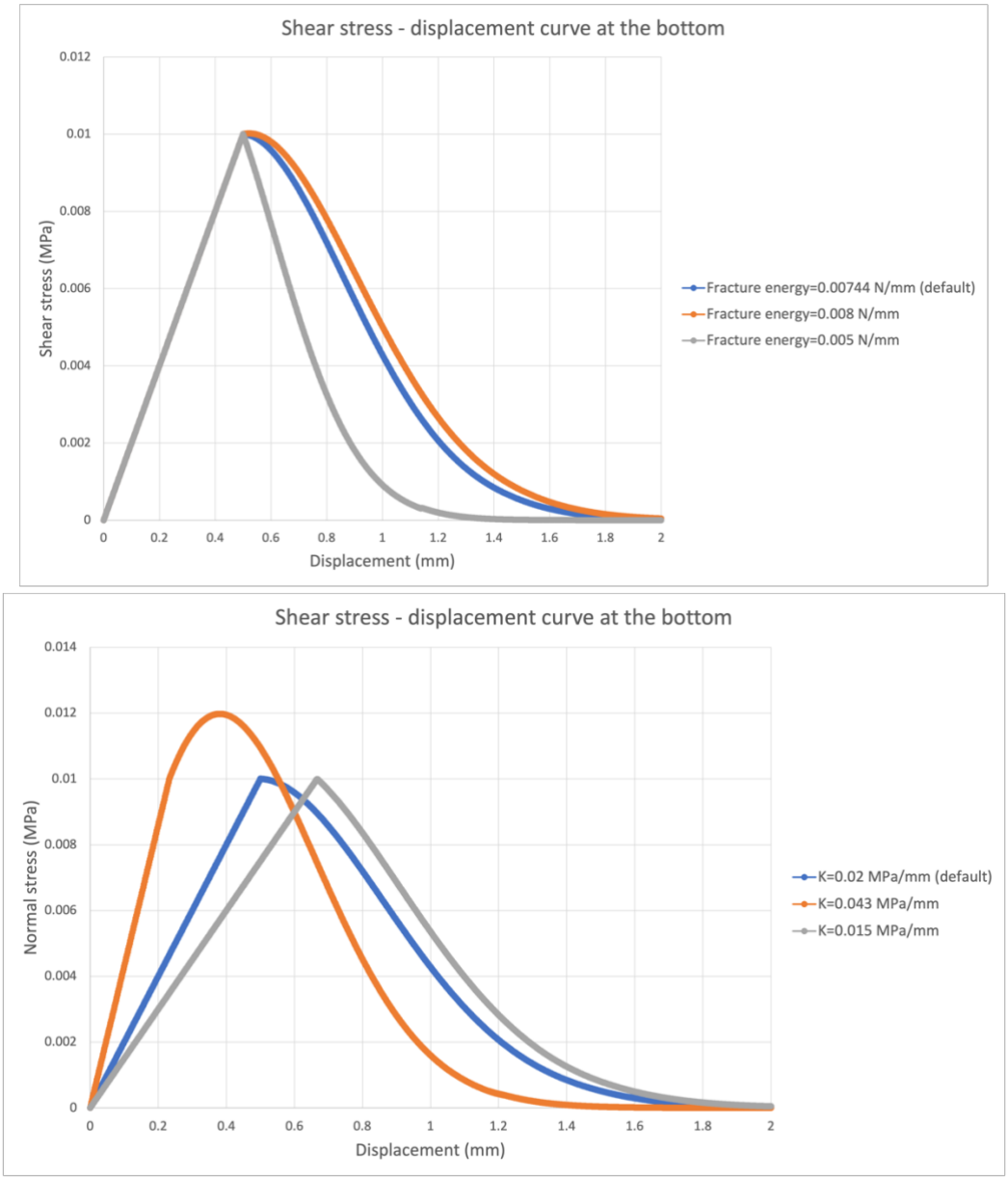

Figure 34. The resulting traction-separation curves in the cohesive interface when applying shear displacements to the anisotropic bilinear clot to study the influence of different damage parameters. The models consist of an isotropic bilinear clot (Fereidoonnezhad, Dwivedi, et al., 2021; Fereidoonnezhad, Moerman, et al., 2021; Fereidoonnezhad et al., 2020) and a rigid vessel wall, and the interface is modeled as a cohesive zone. Parameters which are not specified are identical to the default values in Table 6.

3.4. Aspiration thrombectomy simulations

A mesh sensitivity analysis using 40%H clot was conducted to determine the relationship between the displacement at the center of the clot bottom and the number of elements. The maximum principal stress is consistently found at the same location, regardless of mesh density *(Figure 35.)*, and displacement tends to stabilize *(Figure 36)*. As a result, a mesh density of 0.02 mm (4692 elements) is chosen.

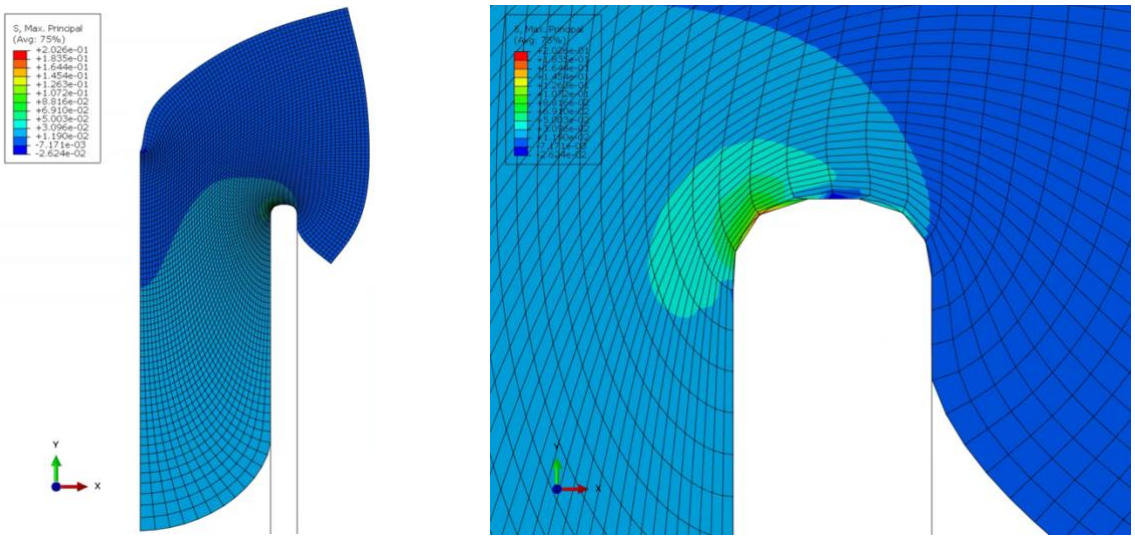

Figure 35. The outcome of the simulation using a 40%H clot in the mesh sensitivity study for the parameter study of clot dimensions. The zoom-in view (right) shows where the max. principal stress occurs

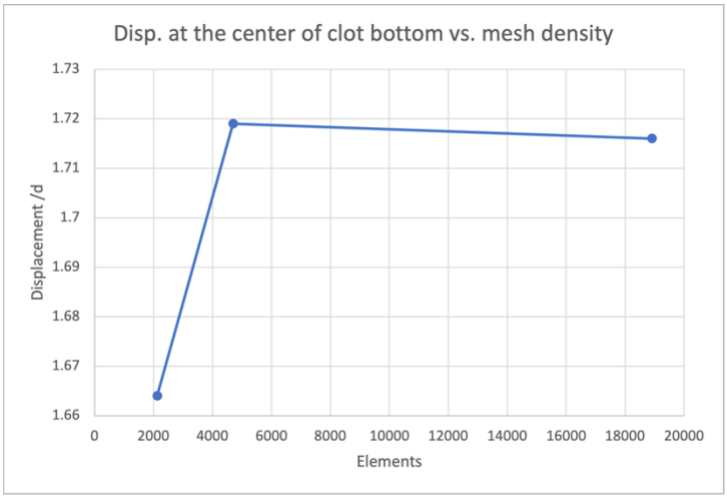

Figure 36. The relationship between the deformation at the clot bottom center and the mesh density in the mesh sensitivity study for the parameter study of clot dimensions. The clot composition is 40%H.

In the 40%H clot cases, the entire clot is aspirated into the aspiration catheter when the ratio D/d (clot diameter divided by catheter diameter) was less than 1.1. However, when D/d is increased to greater than 1.1 and lower than 1.8, the clot models experienced tremendous compression and self-contact, leading to convergence issues in the simulations. As a result, the relationship between the clot diameter and the

displacement at the clot bottom center could only be plotted when D/d ≥ 1.8. The relationship is shown in *Figure 37.*

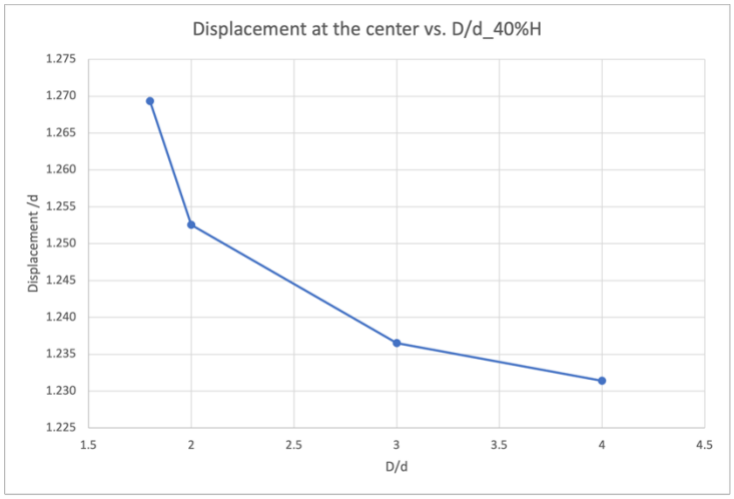

Figure 37. The relationship between the deformation at the clot bottom center and the clot diameter when a suction pressure of 0.02 MPa is applied. The clot composition is 40%H (All the values are divided by the catheter diameter to make them dimensionless). The clot length was set to be twice as that of the catheter diameter.

As for the influence of the clot length, the clot models again suffer significant compression, self-contact, and leads to converge issues when the ratio L/d (clot length divided by catheter diameter) was less than 1. Thus, meaningful results regarding the relationship between the clot diameter and the displacement at the clot bottom center could only be obtained when L/d ≥ 1. The relationship is shown in *Figure 38.*

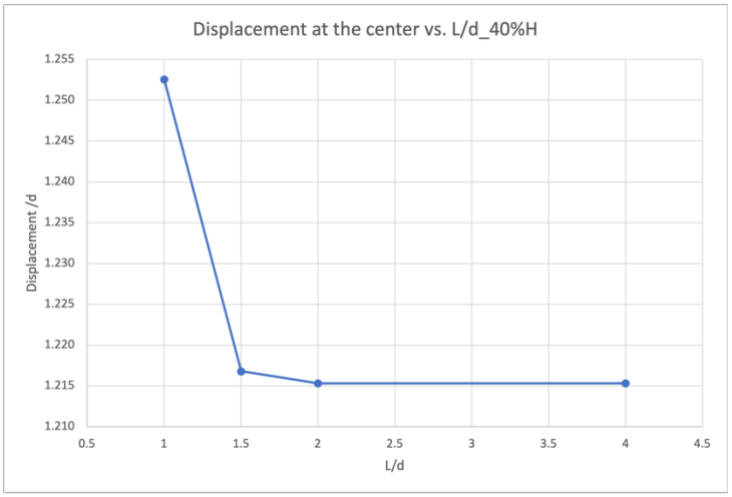

Figure 38. The relationship between the deformation at the clot bottom center and the clot length when a suction pressure of 0.02 MPa is applied. The clot composition is 40%H (All the values are divided by the catheter diameter to make them dimensionless). The clot diameter was set to be twice as that of the catheter diameter.

Furthermore, in the 5%H clot cases, the entire clot is aspirated into the aspiration catheter when the ratio D/d was less than 1.1. Nonetheless, when D/d was increased to greater than 1.1 and lower than 1.7, the converge issues of enormous compression and self-contact occurred. In conclusion, the relationship between the clot diameter and the displacement at the clot bottom center could only be plotted when D/d ≥ 1.7. The relationship is shown in *Figure 39.*

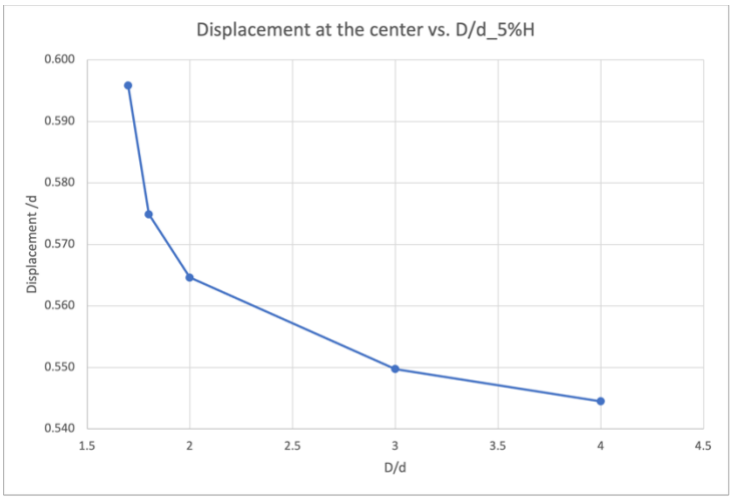

Figure 39. The relationship between the deformation at the clot bottom center and the clot diameter when a suction pressure of 0.02 MPa is applied. The clot composition is 5%H (All the values are divided by the catheter diameter to make them dimensionless). The clot length was set to be twice as that of the catheter diameter.

In terms of the clot length, the clot models once again suffer the identical converge issues when the ratio L/d was less than 1. Thus, meaningful results regarding the relationship between the clot diameter and the displacement at the clot bottom center could only be obtained when L/d ≥ 1. The relationship is shown in *Figure 40.*

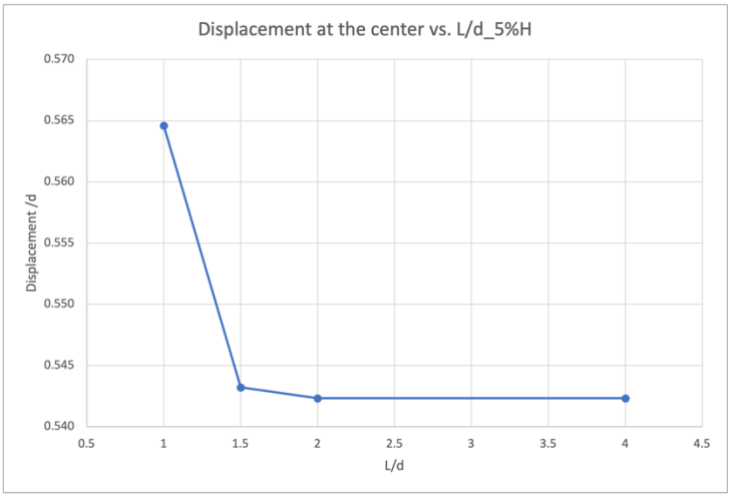

Figure 40. The relationship between the deformation at the clot bottom center and the clot length when a suction pressure of 0.02 MPa is applied. The clot composition is 5%H (All the values are divided by

the catheter diameter to make them dimensionless). The clot diameter was set to be twice as that of the catheter diameter.

Additionally, as depicted in *Figure 41.* And *Figure 42.*, it is evident that stress and strain levels remain notably low in the outer and distal sections of the clot. This implies that these areas are minimally influenced by aspiration and have little impact on the deformation.

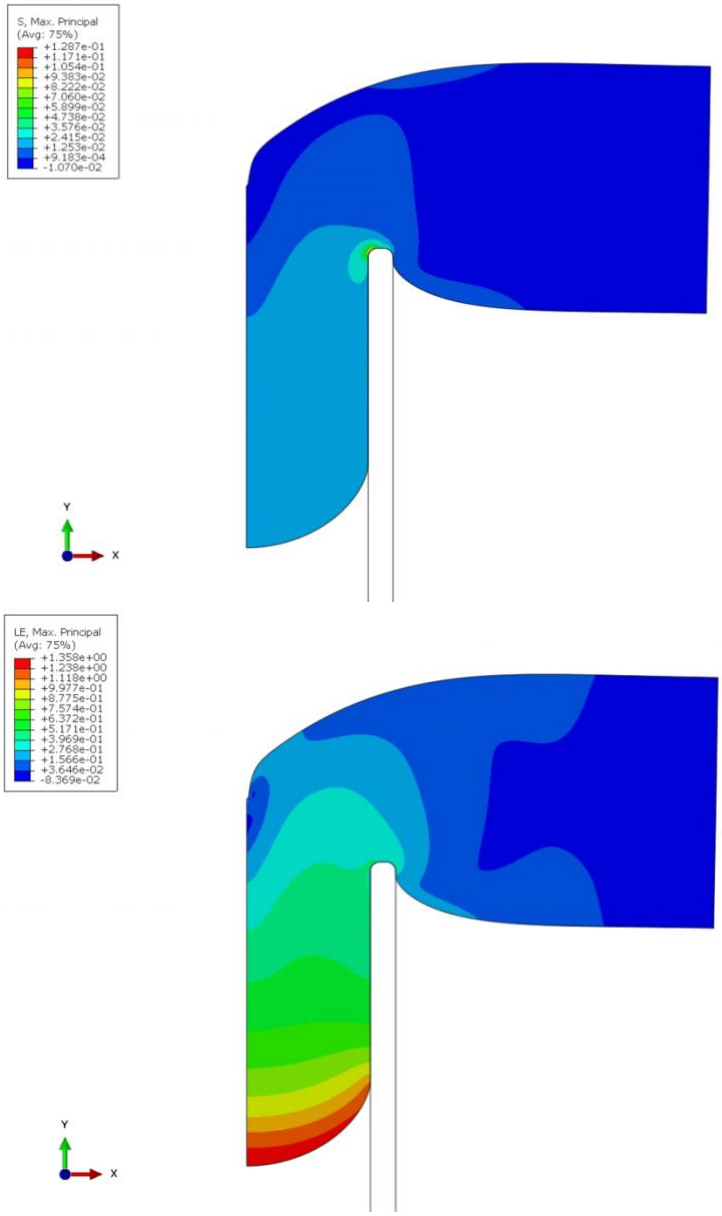

Figure 41. The distribution of max. principal stress (top) and max. principal strain (bottom) for D/d=4 in 40%H clot case. The deformation and stress level at the outer part of the clot is significantly lower than the inner part which closes to the catheter

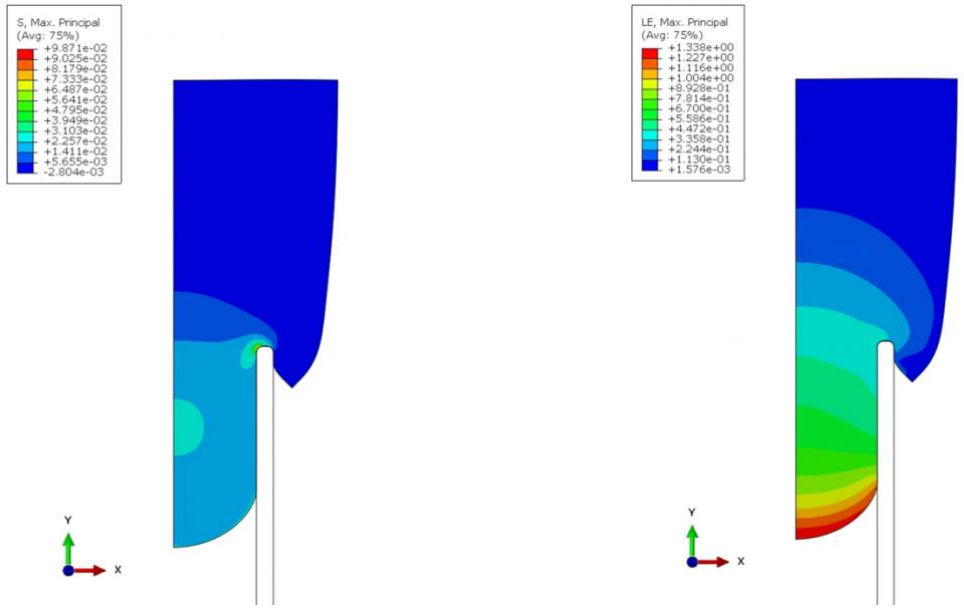

Figure 42. The distribution of max. principal stress (left) and max. principal strain (right) for L/d=2 in 40%H clot case. The deformation and stress level at the outer part of the clot is significantly lower than the inner part which closes to the catheter

Following that, a parameter study of the CZM coefficients in the aspiration simulation, along with the rigid vessel wall, was conducted. For all cases, except when D = 2.74 mm and d = 1.37 mm, a larger catheter with an inner diameter of 2.62 mm was incorporated, as the clot is entirely aspirated when D/d < 1.1. As for the clot length, a value four times that of the original catheter diameter was utilized. This decision was based on the average clot length being approximately 12.0 mm (Consoli et al., 2018), and a length greater than four times the catheter diameter did not significantly affect the performance, as illustrated in *Figure 38. and Figure 40.*

In the case of D/d = 2, four distinct scenarios are investigated: (i) adopting damage criteria for clots (Fereidoonnezhad, Dwivedi, et al., 2021), (ii) reduced maximum nominal stress, (iii) decreased fracture energy, and (iv) reduced maximum nominal stress combined with decreased fracture energy. The simulation configurations and results are listed and shown in *Table 14.,Table 15., Figure 43., and Figure 44.*

Table 14. The simulation configurations, results in terms of the displacement at the clot bottom center, and notes for D/d=2 in CZ parameter study of aspiration simulation for 40%H clot case

Damage initiation criterion	Fracture energy (N/mm)	The displacement at the center of the clot bottom, divided by d (1.37 mm)	Note
maxs = 0.01 MPa	0.00744	1.097	The damage criteria for the clot itself
maxs = 0.0015 MPa	0.00744	1.098	Little damage in CZ (0-3.5%)
maxs = 0.01 MPa	0.00006	1.097	No damage in CZ
maxs = 0.0015 MPa	0.00006	1.253	CZ fully damaged

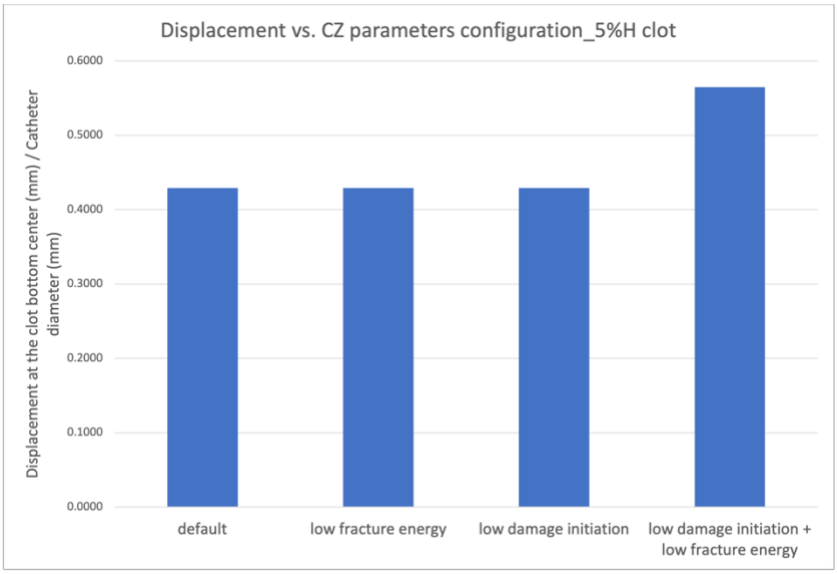

Figure 43. The displacements at the clot bottom center for different simulation scenarios for D/d=2 in CZ parameter study of aspiration simulation for 40%H clot case

Table 15. The simulation configurations, results in terms of the displacement at the clot bottom center, and notes for D/d=2 in CZ parameter study of aspiration simulation for 5%H clot case

Damage initiation criterion	Fracture energy (N/mm)	The displacement at the center of the clot bottom, divided by d (1.37 mm)	Note
maxs = 0.045 MPa	0.0219	0.4292	The damage criteria for the clot itself
maxs = 0.002 MPa	0.0219	0.4292	Little damage in CZ (0-0.7%)
maxs = 0.045 MPa	0.00011	0.4292	No damage in CZ
maxs = 0.002 MPa	0.00011	0.5646	CZ fully damaged

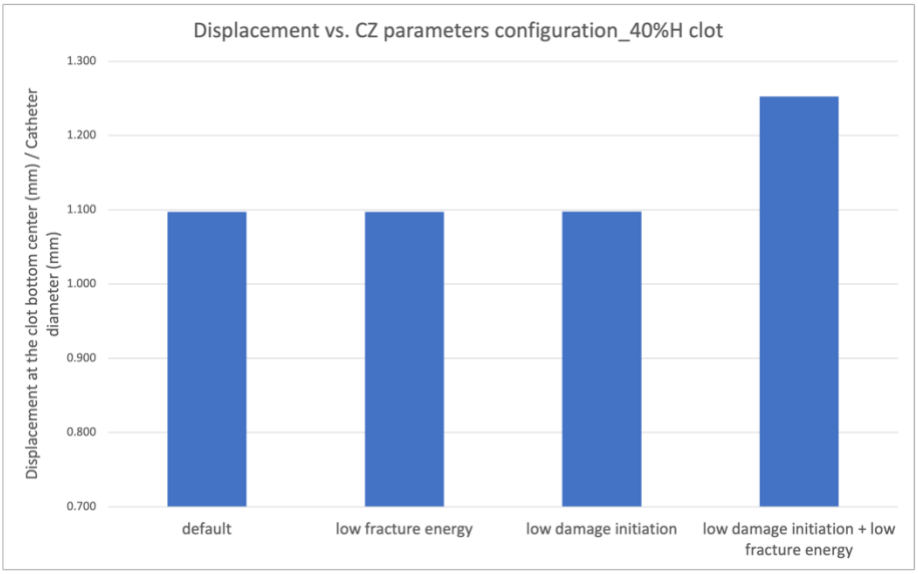

Figure 44. The displacements at the clot bottom center for different simulation scenarios for D/d=2 in CZ parameter study of aspiration simulation for 5%H clot case

Consequently, solely decreasing either the maximum nominal stress or the fracture energy does not lead to the evolution of damage in the cohesive zone or an increase in displacement at the center of the clot bottom. It is essential to decrease both the damage initiation criterion and the fracture energy to facilitate clot separation. Nevertheless, even with the decrease in both criteria, the clot remains unextracted despite the full damage to the cohesive zone.

Hence, for the case of catheter diameter = 2.62 mm, only two scenarios are examined: the clot damage criteria and the reduction of both criteria. The setups and outcomes are presented in *Table 16. and Table 17.*

Table 16. The simulation configurations, results in terms of the displacement at the clot bottom center, and notes for large catheter case in CZ parameter study of aspiration simulation for 40%H clot case

Damage initiation criterion	Fracture energy (N/mm)	The displacement at the center of the clot bottom, divided by d (2.62 mm)	Note
maxs = 0.01 MPa	0.00744	0.9107	1. The damage criteria for the clot itself 2. No damage in CZ
maxs = 0.0015 MPa	0.00006	Whole clot aspirated	

Table 17. The simulation configurations, results in terms of the displacement at the clot bottom center, and notes for large catheter case in CZ parameter study of aspiration simulation for 5%H clot case

Damage initiation criterion	Fracture energy (N/mm)	The displacement at the center of the clot bottom, divided by d (2.62 mm)	Note

maxs = 0.01 MPa	0.0219	0.3161	1. The damage criteria for the clot itself 2. No damage in CZ
maxs = 0.002 MPa	0.00011	Whole clot aspirated	

As a result, the thrombi can be entirely aspirated using the CZ coefficients outlined in *Table 16*. for the 40%H clot and *Table 17* for 5%H clot. Therefore, for the parameter study of L_1 and L_2, these parameters are utilized in cohesive zone modeling.

3.5. Proposing a new catheter design

Subsequently, the analysis of L_1 and L_2 parameters, which correspond to the catheter and stent design, is conducted and the results are presented in this section. In simulations involving the 5%H clot, it is evident that all thrombi detach from the vessel wall and completely enter the catheter simultaneously, irrespective of the specific values assigned to L_1 and L_2. This pattern is consistently observed in scenarios involving the 40%H clot as well. Two examples are illustrated in *Figure 45*. and *Figure 46*.

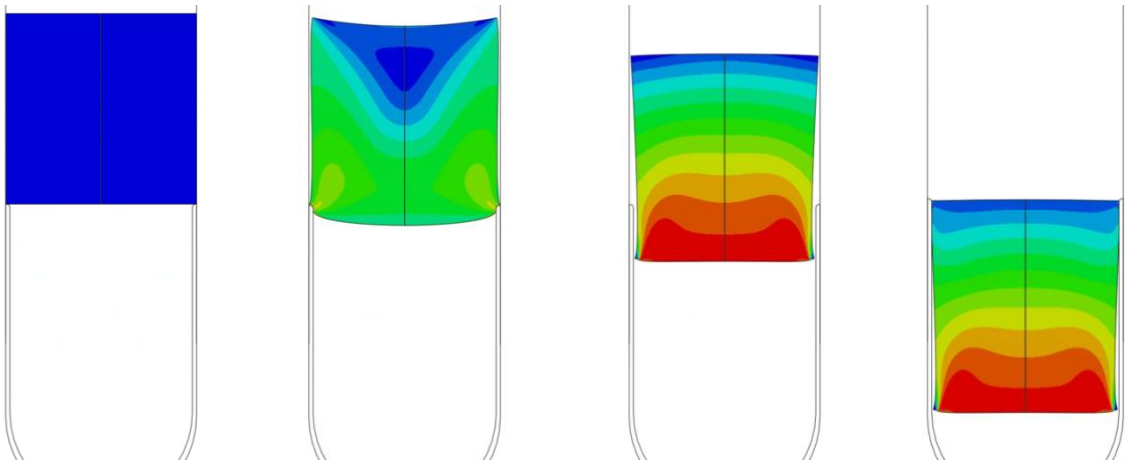

Figure 45. The aspiration process (from the left to the right, the distribution of deformation is shown) of 5%H clot when L_1 = 5 mm and L_2 = 2 mm. The deformation and separation start in parallel. Next, the clot separates from the vessel wall completely and enters the catheter.

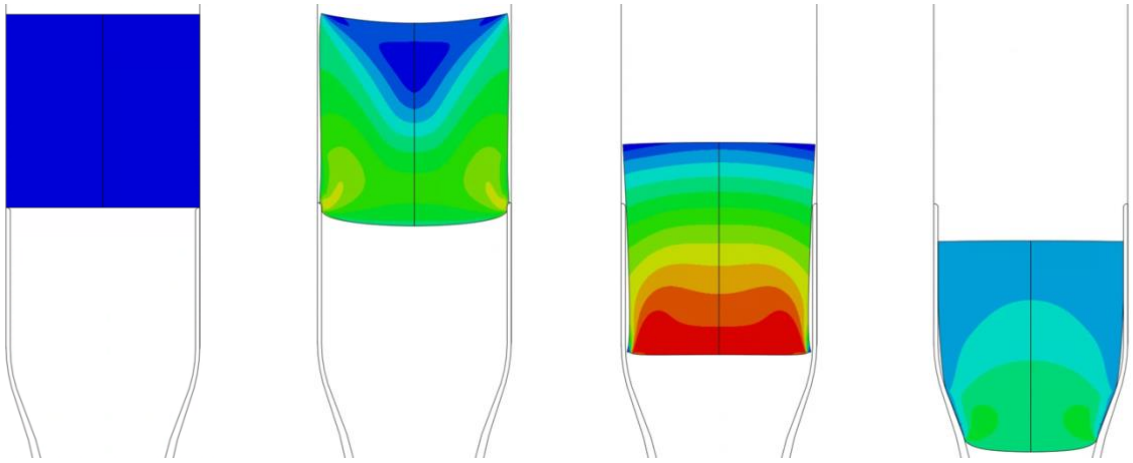

Figure 46. The aspiration process (from the left to the right, the distribution of deformation is shown) of 5%H clot when L_1 = 5 mm and L_2 = 3 mm. The deformation and separation start in parallel. Next, the clot separates from the vessel wall completely and enters the catheter.

Chapter 4. Discussion and Limitation

In this study, we investigated the capability of the anisotropic bilinear model, a hyper-elastic model, to replicate the mechanical behaviour of blood clots in tensile and compressive loadings. The model provides flexibility for users to adjust the stress-strain curve, enabling a precise alignment with the experimental data. However, notable deviations become evident when attempting to predict the behavior, including deformation and force-displacement curves, of another clot analogue in a tensile test. This variance could potentially be attributed to inconsistent clot sample thickness resulting from contraction during the production process. Consequently, such difference in thickness between the actual sample and numerical model could contribute to the observed deviations. Furthermore, the considerable heterogeneity in human clots, as documented in various studies (Chueh et al., 2011; Staessens & De Meyer, 2021), may significantly vary among patients and even within the same clot (Alkarithi et al., 2021; Liu et al., 2020). Therefore, distinct properties between the computational clot and the experimental clot might contribute to the observed differences. To obtain an optimal material parameter set, it is essential to carry out predictions based on a series of *in-vivo* experiments.

Following that, recognizing the significance of the clot-vessel interface, we utilized cohesive zone modeling (Good et al., 2020; Oyekole et al., 2021) to simulate the interface computationally. We carried out validation studies for rigid, hyper foam, and anisotropic bilinear clots with a rigid vessel wall to demonstrate Abaqus' ability to incorporate predetermined parameters, including CZ stiffness, damage initiation criteria, and fracture energy, into the cohesive zone. Generally, these models accurately capture CZ characteristics when simulating the interaction between a rigid vessel wall and a clot. Nonetheless, a specific scenario was observed where the traction exceeds the maximum nominal stress. This phenomenon is attributed to an increased CZ stiffness causing the cohesive interface to resist separation more strongly. As a result, this leads to a tighter connection between the clot and the vessel, resulting in elevated tractions even beyond the point where the damage should initiate. This observation emphasizes the need for cautious selection of CZ coefficients to prevent unintended phenomena.

The analysis of clot dimensions shows that the suction pressure exerted by the catheter affects smaller clots more significantly. In contrast, enlarging the clot diameter or length results in a reduction of displacement at the center of the clot bottom. Furthermore, the trends indicate the presence of specific thresholds beyond which increasing the dimensions no longer affects the displacement. Which means that larger clots demonstrate low sensitivity to the suction pressure, particularly in their outer and distal regions. In other words, these parts of the clot contribute little to the deformation induced by aspiration. Consequently, increasing the catheter diameter results in more substantial deformation, potentially enabling complete clot removal. This observation is further validated by incorporating the vessel wall. In the study, challenges in clot extraction emerge when the clot diameter-to-catheter diameter ratio equals two. On the other hand, a decrease in this ratio (as exemplified by a catheter diameter of 2.62 mm and a clot diameter of 2.74 mm) enables the complete removal of the clot in a single attempt. However, this achievement is contingent upon the damage criteria of the interface being substantially lower than that of the clot when the aspiration pressure is 0.02 MPa. The outcomes suggest that a strategy for improving clot removal in medical practice involves the increase the catheter diameter. This approach aligns with the observed trends in the research

(Chitsaz et al., 2018; Hu & Stiefel, 2016), where larger catheter diameters enable the aspiration catheter to target a wider region of the clot and deliver suction force close to the clot-vessel interface (Talayero et al., 2019; Talayero et al., 2020).

Therefore, the final phase of this project integrates an expandable stent to extend beyond the catheter tip. This approach expands the area of suction force application while avoiding navigation challenges during the medical practice. Exploring the optimization of this design reveals that as far as the aspiration area, clot size, and CZ parameters remain consistent, the gap between the catheter tip and the proximal face of the clot becomes unimportant. In addition, the specific location at which the stent reaches the desired diameter expansion does not influence the efficacy of aspiration.

Regarding the limitations of the project, it is important to note that a suction pressure of 20 kPa was uniformly applied in all aspiration simulations to prevent significant deformation and convergence issues. However, in clinical applications, aspiration systems can apply negative pressures up to 98.9 kPa (as in the case of Penumbra) (Penumbra). Additionally, the clot fragmentation, crucial in aspiration thrombectomy, is not included in this study and should be explored in future research. Furthermore, the precise criteria governing damage initiation and evolution at the clot-vessel interface remain unknown. Moreover, the influence of the blood flow was not taken into consideration in the models. These factors could play important roles and exert substantial influence on the aspiration procedure. Therefore, incorporating these features into future simulation studies could provide intriguing insights.

Chapter 5. Conclusion

The thesis includes a comprehensive exploration, encompassing the identification of an appropriate clot material model, the validation of this model, validation of the CZM implementation in Abaqus, a parameter study investigating the interplay between clot dimensions and catheter diameter ratios, and the formulation of computational models for aspiration thrombectomy. The aim of these studies is to optimize the design of catheters for the clot removal procedure.

Through the simulations and experiments, it is demonstrated that the anisotropic bilinear model has the potentially replicate the clot behaviours, yet further experiments and predictions are required to obtain an optimal clot model. Additionally, Abaqus could precisely model the cohesive zone using predefined parameters, though it is important to pick these measurements carefully. Furthermore, the impact of clot dimensions is identified. Most important of all, the first-pass recanalization might potentially be accomplished through using an expandable stent in conjunction with an aspiration catheter. Notably, so long as the suction area in direct clot contact reaches a certain threshold, the distance between the catheter tip and the proximal face of the clot insignificantly affects clinical outcomes. Given the intricate nature of catheter positioning in medical practice, the practicality of these findings is noteworthy. Given the difficulty in accurately positioning the catheter tip during medical procedures, these findings are seen as applicable in real-world scenarios. Therefore, the objective is considered achieved.

To improve the current simulation models, a crucial part is to integrate critical factors such as authentic aspiration pressure, clot fracture mechanics, and practical damage criteria for clot-vessel interface. These adjustments would lead the simulation closer to replicating real medical scenarios, yielding meaningful insights. Eventually, this thesis has established a groundwork for future research pursuits.

References

Alkarithi, G., Duval, C., Shi, Y., Macrae, F. L., & Ariëns, R. A. S. (2021). Thrombus Structural Composition in Cardiovascular Disease. *Arteriosclerosis, Thrombosis, and Vascular Biology*, *41*(9), 2370-2383. https://doi.org/doi:10.1161/ATVBAHA.120.315754

Baek, J.-H., Kim, B. M., Kang, D.-H., Heo, J. H., Nam, H. S., Kim, Y. D., Hwang, Y.-H., Kim, Y.-W., Kim, Y.-S., Kim, D. J., Kwak, H. S., Roh, H. G., Lee, Y.-J., Kim, S. H., Baik, S. K., Jeon, P., Yoo, J., Suh, S. H., Kim, B., . . . Jeon, H.-J. (2019). Balloon Guide Catheter Is Beneficial in Endovascular Treatment Regardless of Mechanical Recanalization Modality. *Stroke*, *50*(6), 1490-1496. https://doi.org/doi:10.1161/STROKEAHA.118.024723

Bathias, C., & Pineau, A. (2013). *Fatigue of Materials and Structures: Fundamentals*. Wiley. https://books.google.nl/books?id=xD9wuQ0Jl64C

Brouwer, P. A., Brinjikji, W., & De Meyer, S. F. (2018). Clot Pathophysiology: Why Is It Clinically Important? *Neuroimaging Clinics of North America*, *28*(4), 611-623. https://doi.org/https://doi.org/10.1016/j.nic.2018.06.005

Brown, A. E. X., Litvinov, R. I., Discher, D. E., Purohit, P. K., & Weisel, J. W. (2009). Multiscale Mechanics of Fibrin Polymer: Gel Stretching with Protein Unfolding and Loss of Water. *Science*, *325*(5941), 741-744. https://doi.org/doi:10.1126/science.1172484

Bustamante-Góez, L., Chica-Arrieta, E., & Villarraga-Ossa, J. (2019). Evaluación de la relación tracción-separación cohesiva según la variación de rigidez. *Revista UIS Ingenierías*, *18*(2), 67-76. https://doi.org/10.18273/revuin.v18n2-2019006

Cahalane, R., Boodt, N., Akyildiz, A. C., Giezen, J.-a., Mondeel, M., van der Lugt, A., Marquering, H., & Gijsen, F. (2021). A review on the association of thrombus composition with mechanical and radiological imaging characteristics in acute ischemic stroke. *Journal of Biomechanics*, *129*, 110816. https://doi.org/https://doi.org/10.1016/j.jbiomech.2021.110816

Chitsaz, A., Nejat, A., & Nouri, R. (2018). Three-Dimensional Numerical Simulations of Aspiration Process: Evaluation of Two Penumbra Aspiration Catheters Performance. *Artificial Organs*, *42*(12), E406-E419. https://doi.org/https://doi.org/10.1111/aor.13300

Chueh, J. Y., Wakhloo, A. K., Hendricks, G. H., Silva, C. F., Weaver, J. P., & Gounis, M. J. (2011). Mechanical Characterization of Thromboemboli in Acute Ischemic Stroke and Laboratory Embolus Analogs. *American Journal of Neuroradiology*, *32*(7), 1237-1244. https://doi.org/10.3174/ajnr.A2485

Colombo, M., Luraghi, G., Cestariolo, L., Ravasi, M., Airoldi, A., Chiastra, C., & Pennati, G. (2020). Impact of lower limb movement on the hemodynamics of femoropopliteal arteries: A computational study. *Medical Engineering & Physics*, *81*, 105-117. https://doi.org/https://doi.org/10.1016/j.medengphy.2020.05.004

Consoli, A., Rosi, A., Coskun, O., Nappini, S., Maria, F. D., Renieri, L., Limbucci, N., Rodesch, G., Mangiafico, S., Decroix, J.-P., Kyheng, M., Labreuche, J., & Lapergue, B. (2018). Thrombectomy for M1-Middle Cerebral Artery Occlusion. *Stroke*, *49*(5), 1286-1289. https://doi.org/doi:10.1161/STROKEAHA.117.018987

Deshaies, E. M. (2013). Tri-axial system using the Solitaire-FR and Penumbra Aspiration Microcatheter for acute mechanical thrombectomy. *Journal of Clinical Neuroscience*, *20*(9), 1303-1305. https://doi.org/https://doi.org/10.1016/j.jocn.2012.10.037

Dutra, B. G., Tolhuisen, M. L., Alves, H. C. B. R., Treurniet, K. M., Kappelhof, M., Yoo, A. J., Jansen, I. G. H., Dippel, D. W. J., Zwam, W. H. v., Oostenbrugge, R. J. v., Rocha, A. J. d., Lingsma, H. F., Lugt, A. v. d., Roos, Y. B. W. E. M., Marquering, H. A., & Majoie, C. B. L. M. (2019). Thrombus Imaging Characteristics and Outcomes in Acute Ischemic Stroke Patients Undergoing

Endovascular Treatment. *Stroke*, *50*(8), 2057-2064. https://doi.org/doi:10.1161/STROKEAHA.118.024247

Fanous, A. A., & Siddiqui, H. A. (2016). Mechanical thrombectomy: Stent retrievers vs. aspiration catheters [journal article]. *Cor et Vasa*, *58*(2), e193-e203. http://dx.doi.org/10.1016/j.crvasa.2016.01.004

Fereidoonnezhad, B., Dwivedi, A., Johnson, S., McCarthy, R., & McGarry, P. (2021). Blood clot fracture properties are dependent on red blood cell and fibrin content. *Acta Biomaterialia*, *127*, 213-228. https://doi.org/https://doi.org/10.1016/j.actbio.2021.03.052

Fereidoonnezhad, B., & McGarry, P. (2022). A new constitutive model for permanent deformation of blood clots with application to simulation of aspiration thrombectomy. *Journal of Biomechanics*, *130*, 110865. https://doi.org/https://doi.org/10.1016/j.jbiomech.2021.110865

Fereidoonnezhad, B., Moerman, K. M., Johnson, S., McCarthy, R., & McGarry, P. J. (2021). A new compressible hyperelastic model for the multi-axial deformation of blood clot occlusions in vessels. *Biomechanics and Modeling in Mechanobiology*, *20*(4), 1317-1335. https://doi.org/10.1007/s10237-021-01446-4

Fereidoonnezhad, B., O'Connor, C., & McGarry, J. P. (2020). A new anisotropic soft tissue model for elimination of unphysical auxetic behaviour. *Journal of Biomechanics*, *111*, 110006. https://doi.org/https://doi.org/10.1016/j.jbiomech.2020.110006

Good, B. C., Simon, S., Manning, K., & Costanzo, F. (2020). Development of a computational model for acute ischemic stroke recanalization through cyclic aspiration. *Biomechanics and Modeling in Mechanobiology*, *19*(2), 761-778. https://doi.org/10.1007/s10237-019-01247-w

Goyal, M., Menon, B. K., van Zwam, W. H., Dippel, D. W. J., Mitchell, P. J., Demchuk, A. M., Dávalos, A., Majoie, C. B. L. M., van der Lugt, A., de Miquel, M. A., Donnan, G. A., Roos, Y. B. W. E. M., Bonafe, A., Jahan, R., Diener, H.-C., van den Berg, L. A., Levy, E. I., Berkhemer, O. A., Pereira, V. M., . . . Jovin, T. G. (2016). Endovascular thrombectomy after large-vessel ischaemic stroke: a meta-analysis of individual patient data from five randomised trials. *The Lancet*, *387*(10029), 1723-1731. https://doi.org/https://doi.org/10.1016/S0140-6736(16)00163-X

Gralla, J., Schroth, G., Remonda, L., Nedeltchev, K., Slotboom, J., & Brekenfeld, C. (2006). Mechanical Thrombectomy for Acute Ischemic Stroke. *Stroke*, *37*(12), 3019-3024. https://doi.org/doi:10.1161/01.STR.0000248457.55493.85

Grech, R., Mizzi, A., Pullicino, R., Thornton, J., & Downer, J. (2015). Functional outcomes and recanalization rates of stent retrievers in acute ischaemic stroke: A systematic review and meta-analysis. *The Neuroradiology Journal*, *28*(2), 152-171. https://doi.org/10.1177/1971400915576678

He, D., Kim, D. A., Ku, D. N., & Hu, Y. (2022). Viscoporoelasticity of coagulation blood clots. *Extreme Mechanics Letters*, *56*, 101859. https://doi.org/https://doi.org/10.1016/j.eml.2022.101859

Hu, Y. C., & Stiefel, M. F. (2016). Force and aspiration analysis of the ADAPT technique in acute ischemic stroke treatment. *Journal of NeuroInterventional Surgery*, *8*(3), 244-246. https://doi.org/10.1136/neurintsurg-2014-011563

Humphries, W., Hoit, D., Doss, V. T., Elijovich, L., Frei, D., Loy, D., Dooley, G., Turk, A. S., Chaudry, I., Turner, R., Mocco, J., Morone, P., Fiorella, D., Siddiqui, A., Mokin, M., & Arthur, A. S. (2015). Distal aspiration with retrievable stent assisted thrombectomy for the treatment of acute ischemic stroke. *Journal of NeuroInterventional Surgery*, *7*(2), 90-94. https://doi.org/10.1136/neurintsurg-2013-010986

Johnson, S., McCarthy, R., Gilvarry, M., McHugh, P. E., & McGarry, J. P. (2021). Investigating the Mechanical Behavior of Clot Analogues Through Experimental and Computational Analysis. *Annals of Biomedical Engineering*, *49*(1), 420-431. https://doi.org/10.1007/s10439-020-02570-5

Kaesmacher, J., Boeckh-Behrens, T., Simon, S., Maegerlein, C., Kleine, J. F., Zimmer, C., Schirmer, L., Poppert, H., & Huber, T. (2017). Risk of Thrombus Fragmentation during Endovascular Stroke Treatment. *American Journal of Neuroradiology*, *38*(5), 991-998. https://doi.org/10.3174/ajnr.A5105

Kusner, J., Luraghi, G., Khodaee, F., Rodriguez Matas, J. F., Migliavacca, F., Edelman, E. R., & Nezami, F. R. (2021). Understanding TAVR device expansion as it relates to morphology of the bicuspid aortic valve: A simulation study. *PLOS ONE*, *16*(5), e0251579. https://doi.org/10.1371/journal.pone.0251579

Liang, X., Chernysh, I., Purohit, P. K., & Weisel, J. W. (2017). Phase transitions during compression and decompression of clots from platelet-poor plasma, platelet-rich plasma and whole blood. *Acta Biomaterialia*, *60*, 275-290. https://doi.org/https://doi.org/10.1016/j.actbio.2017.07.011

Ling, C. (2023). *Internship report - in-silico study of clot mechanical behaviour*.

Litvinov, R. I., & Weisel, J. W. (2017). Fibrin mechanical properties and their structural origins. *Matrix Biology*, *60-61*, 110-123. https://doi.org/https://doi.org/10.1016/j.matbio.2016.08.003

Liu, R., Jin, C., Wang, L., Yang, Y., Fan, Y., & Wang, W. (2022). Simulation of stent retriever thrombectomy in acute ischemic stroke by finite element analysis. *Computer Methods in Biomechanics and Biomedical Engineering*, *25*(7), 740-749. https://doi.org/10.1080/10255842.2021.1976761

Liu, Y., Zheng, Y., Reddy, A. S., Gebrezgiabhier, D., Davis, E., Cockrum, J., Gemmete, J. J., Chaudhary, N., Griauzde, J. M., Pandey, A. S., Shih, A. J., & Savastano, L. E. (2020). Analysis of human emboli and thrombectomy forces in large-vessel occlusion stroke. *Journal of Neurosurgery JNS*, 1-9. https://doi.org/https://doi.org/10.3171/2019.12.JNS192187

Luraghi, G., Bridio, S., Rodriguez Matas, J. F., Dubini, G., Boodt, N., Gijsen, F. J. H., van der Lugt, A., Fereidoonnezhad, B., Moerman, K. M., McGarry, P., Konduri, P. R., Arrarte Terreros, N., Marquering, H. A., Majoie, C. B. L. M., & Migliavacca, F. (2021). The first virtual patient-specific thrombectomy procedure. *Journal of Biomechanics*, *126*, 110622. https://doi.org/https://doi.org/10.1016/j.jbiomech.2021.110622

Luraghi, G., Matas, J. F. R., Beretta, M., Chiozzi, N., Iannetti, L., & Migliavacca, F. (2021). The impact of calcification patterns in transcatheter aortic valve performance: a fluid-structure interaction analysis. *Computer Methods in Biomechanics and Biomedical Engineering*, *24*(4), 375-383. https://doi.org/10.1080/10255842.2020.1817409

Luraghi, G., Rodriguez Matas, J. F., Dubini, G., Berti, F., Bridio, S., Duffy, S., Dwivedi, A., McCarthy, R., Fereidoonnezhad, B., McGarry, P., Majoie, C. B. L. M., & Migliavacca, F. (2021). Applicability assessment of a stent-retriever thrombectomy finite-element model. *Interface Focus*, *11*(1), 20190123. https://doi.org/doi:10.1098/rsfs.2019.0123

McCarthy, R., Mirza, M., Johnson, S., Dwivedi, A., Gunning, G., Vale, D., & Gilvarry, M. (2022). Aspects of ischemic stroke biomechanics derived using ex-vivo and in-vitro methods relating to mechanical thrombectomy. *Journal of Biomechanics*, *131*, 110900. https://doi.org/https://doi.org/10.1016/j.jbiomech.2021.110900

Menon, B. K., Al-Ajlan, F. S., Najm, M., Puig, J., Castellanos, M., Dowlatshahi, D., Calleja, A., Sohn, S.-I., Ahn, S. H., Poppe, A., Mikulik, R., Asdaghi, N., Field, T. S., Jin, A., Asil, T., Boulanger, J.-M., Smith, E. E., Coutts, S. B., Barber, P. A., . . . Investigators, f. t. I. S. (2018). Association of Clinical, Imaging, and Thrombus Characteristics With Recanalization of Visible Intracranial Occlusion in Patients With Acute Ischemic Stroke. *JAMA*, *320*(10), 1017-1026. https://doi.org/10.1001/jama.2018.12498

Migliori, S., Chiastra, C., Bologna, M., Montin, E., Dubini, G., Genuardi, L., Aurigemma, C., Mainardi, L., Burzotta, F., & Migliavacca, F. (2020). Application of an OCT-based 3D reconstruction framework to the hemodynamic assessment of an ulcerated coronary artery plaque. *Medical Engineering & Physics*, *78*, 74-81. https://doi.org/https://doi.org/10.1016/j.medengphy.2019.12.006

Münster, S., Jawerth, L. M., Leslie, B. A., Weitz, J. I., Fabry, B., & Weitz, D. A. (2013). Strain history dependence of the nonlinear stress response of fibrin and collagen networks. *Proceedings of the National Academy of Sciences*, *110*(30), 12197-12202. https://doi.org/doi:10.1073/pnas.1222787110

Nguyen, T. N., Malisch, T., Castonguay, A. C., Gupta, R., Sun, C.-H. J., Martin, C. O., Holloway, W. E., Mueller-Kronast, N., English, J. D., Linfante, I., Dabus, G., Marden, F. A., Bozorgchami, H., Xavier, A., Rai, A. T., Froehler, M. T., Badruddin, A., Taqi, M., Abraham, M. G., . . . Zaidat, O. O. (2014). Balloon Guide Catheter Improves Revascularization and Clinical Outcomes With the Solitaire Device. *Stroke*, *45*(1), 141-145. https://doi.org/doi:10.1161/STROKEAHA.113.002407

Ospel, J. M., van der Lugt, A., Gounis, M., Goyal, M., & Majoie, C. B. L. M. (2021). A clinical perspective on endovascular stroke treatment biomechanics. *Journal of Biomechanics*, *127*, 110694. https://doi.org/https://doi.org/10.1016/j.jbiomech.2021.110694

Ospel, J. M., Volny, O., Jayaraman, M., McTaggart, R., & Goyal, M. (2019). Optimizing fast first pass complete reperfusion in acute ischemic stroke – the BADDASS approach (BAlloon guiDe with large bore Distal Access catheter with dual aspiration with Stent-retriever as Standard approach). *Expert Review of Medical Devices*, *16*(11), 955-963. https://doi.org/10.1080/17434440.2019.1684263

Oyekole, O., Simon, S., Manning, K. B., & Costanzo, F. (2021). Modeling acute ischemic stroke recanalization through cyclic aspiration. *Journal of Biomechanics*, *128*, 110721. https://doi.org/https://doi.org/10.1016/j.jbiomech.2021.110721

Pearce, G., Perkinson, R. N. D., Wong, J., Roffe, C., Brooker, L., Jones, K., Dodd, M., Spence, J., Rai, M., & Brookfield, P. (2010). In Vitro Testing of a New Aspiration Thrombus Device. *Journal of Stroke and Cerebrovascular Diseases*, *19*(2), 121-129. https://doi.org/https://doi.org/10.1016/j.jstrokecerebrovasdis.2009.03.017

Penumbra, I. *Penumbra Engine: Penumbra Inc*. Retrieved August, 2023 from https://www.penumbrainc.com/au/products/penumbra-engine/

The Penumbra Pivotal Stroke Trial. (2009). *Stroke*, *40*(8), 2761-2768. https://doi.org/doi:10.1161/STROKEAHA.108.544957

Powers, W. J., Rabinstein, A. A., Ackerson, T., Adeoye, O. M., Bambakidis, N. C., Becker, K., Biller, J., Brown, M., Demaerschalk, B. M., Hoh, B., Jauch, E. C., Kidwell, C. S., Leslie-Mazwi, T. M., Ovbiagele, B., Scott, P. A., Sheth, K. N., Southerland, A. M., Summers, D. V., & Tirschwell, D. L. (2018). 2018 Guidelines for the Early Management of Patients With Acute Ischemic Stroke: A Guideline for Healthcare Professionals From the American Heart Association/American Stroke Association. *Stroke*, *49*(3), e46-e99. https://doi.org/doi:10.1161/STR.0000000000000158

Rai, A. T., Hogg, J. P., Cline, B., & Hobbs, G. (2013). Cerebrovascular geometry in the anterior circulation: an analysis of diameter, length and the vessel taper. *J Neurointerv Surg*, *5*(4), 371-375. https://doi.org/10.1136/neurintsurg-2012-010314

Rausch, M. K., & Humphrey, J. D. (2016). A microstructurally inspired damage model for early venous thrombus. *Journal of the Mechanical Behavior of Biomedical Materials*, *55*, 12-20. https://doi.org/https://doi.org/10.1016/j.jmbbm.2015.10.006

Rausch, M. K., Sugerman, G. P., Kakaletsis, S., & Dortdivanlioglu, B. (2021). Hyper-viscoelastic damage modeling of whole blood clot under large deformation. *Biomechanics and Modeling in Mechanobiology*, *20*(5), 1645-1657. https://doi.org/10.1007/s10237-021-01467-z

Romero, G., Talayero, C., Pearce, G., & Wong, J. (2020). Modeling of blood clot removal with aspiration Thrombectomy devices. *Journal of Mechanical Engineering and Sciences*, *14*(1), 6238 - 6250. https://doi.org/10.15282/jmes.14.1.2020.03.0488

Santos, E. M. M., Marquering, H. A., Blanken, M. D. d., Berkhemer, O. A., Boers, A. M. M., Yoo, A. J., Beenen, L. F., Treurniet, K. M., Wismans, C., Noort, K. v., Lingsma, H. F., Dippel, D. W. J., Lugt, A. v. d., Zwam, W. H. v., Roos, Y. B. W. E. M., Oostenbrugge, R. J. v., Niessen, W. J., Majoie, C. B., Fransen, P. S. S., . . . Csizmadia, M. (2016). Thrombus Permeability Is Associated With Improved Functional Outcome and Recanalization in Patients With Ischemic Stroke. *Stroke*, *47*(3), 732-741. https://doi.org/doi:10.1161/STROKEAHA.115.011187

Simon, S., Grey, C. P., Massenzo, T., Simpson, D. G., & Longest, P. W. (2014). Exploring the efficacy of cyclic vs static aspiration in a cerebral thrombectomy model: an initial proof of concept study.

Journal of NeuroInterventional Surgery, *6*(9), 677-683. https://doi.org/10.1136/neurintsurg-2013-010941

Simons, N., Mitchell, P., Dowling, R., Gonzales, M., & Yan, B. (2015). Thrombus composition in acute ischemic stroke: A histopathological study of thrombus extracted by endovascular retrieval. *Journal of Neuroradiology*, *42*(2), 86-92. https://doi.org/https://doi.org/10.1016/j.neurad.2014.01.124

Soleimani, S., Dubini, G., & Pennati, G. (2014). Possible Benefits of Catheters With Lateral Holes in Coronary Thrombus Aspiration: A Computational Study for Different Clot Viscosities and Vacuum Pressures. *Artificial Organs*, *38*(10), 845-855. https://doi.org/https://doi.org/10.1111/aor.12274

Soleimani, S., Dubini, G., & Pennati, G. (2016). Performance of a thrombectomy device for aspiration of thrombus with various sizes based on a computational fluid dynamic modeling. *Biomedical Engineering / Biomedizinische Technik*, *61*(3), 337-344. https://doi.org/doi:10.1515/bmt-2014-0013

Staessens, S., & De Meyer, S. F. (2021). Thrombus heterogeneity in ischemic stroke. *Platelets*, *32*(3), 331-339. https://doi.org/10.1080/09537104.2020.1748586

Sugerman, G. P., Kakaletsis, S., Thakkar, P., Chokshi, A., Parekh, S. H., & Rausch, M. K. (2021). A whole blood thrombus mimic: Constitutive behavior under simple shear. *Journal of the Mechanical Behavior of Biomedical Materials*, *115*, 104216. https://doi.org/https://doi.org/10.1016/j.jmbbm.2020.104216

Sugerman, G. P., Parekh, S. H., & Rausch, M. K. (2020). Nonlinear, dissipative phenomena in whole blood clot mechanics [10.1039/D0SM01317J]. *Soft Matter*, *16*(43), 9908-9916. https://doi.org/10.1039/D0SM01317J

Talayero, C., Romero, G., Pearce, G., & Wong, J. (2018). Simulation of Blood Clot Removal by Aspiration Thrombectomy in Cerebral Vessels usingGeometry Optimization of the Aspiration Device. *International Journal of Simulation: Systems, Science and Technology*, *19*, 18.11-18.16. https://doi.org/10.5013/IJSSST.a.19.05.18

Talayero, C., Romero, G., Pearce, G., & Wong, J. (2019). Numerical modelling of blood clot extraction by aspiration thrombectomy. Evaluation of aspiration catheter geometry. *Journal of Biomechanics*, *94*, 193-201. https://doi.org/https://doi.org/10.1016/j.jbiomech.2019.07.033

Talayero, C., Romero, G., Pearce, G., & Wong, J. (2020). Thrombectomy aspiration device geometry optimization for removal of blood clots in cerebral vessels. *Journal of Mechanical Engineering and Sciences*, *14*(1), 6229 - 6237. https://doi.org/10.15282/jmes.14.1.2020.02.0487

Tashiro, K., Shobayashi, Y., Ota, I., & Hotta, A. (2021). Finite element analysis of blood clots based on the nonlinear visco-hyperelastic model. *Biophysical Journal*, *120*(20), 4547-4556. https://doi.org/https://doi.org/10.1016/j.bpj.2021.08.034

Tutwiler, V., Maksudov, F., Litvinov, R. I., Weisel, J. W., & Barsegov, V. (2021). Strength and deformability of fibrin clots: Biomechanics, thermodynamics, and mechanisms of rupture. *Acta Biomaterialia*, *131*, 355-369. https://doi.org/https://doi.org/10.1016/j.actbio.2021.06.046

Tutwiler, V., Singh, J., Litvinov, R. I., Bassani, J. L., Purohit, P. K., & Weisel, J. W. (2020). Rupture of blood clots: Mechanics and pathophysiology. *Science Advances*, *6*(35), eabc0496. https://doi.org/doi:10.1126/sciadv.abc0496

Walter, K. (2022). What Is Acute Ischemic Stroke? *JAMA*, *327*(9), 885-885. https://doi.org/10.1001/jama.2022.1420

WHO. (2020). *The top 10 causes of death.* World Health Organization. https://www.who.int/news-room/fact-sheets/detail/the-top-10-causes-of-death

Withey, P. A. (1997). Fatigue failure of the de Havilland comet I. *Engineering Failure Analysis*, *4*, 147-154.

Yuki, I., Kan, I., Vinters, H. V., Kim, R. H., Golshan, A., Vinuela, F. A., Sayre, J. W., Murayama, Y., & Vinuela, F. (2012). The Impact of Thromboemboli Histology on the Performance of a Mechanical

Thrombectomy Device. *American Journal of Neuroradiology*, *33*(4), 643-648. https://doi.org/10.3174/ajnr.A2842

Zaccaria, A., Danielli, F., Gasparotti, E., Fanni, B. M., Celi, S., Pennati, G., & Petrini, L. (2020). Left atrial appendage occlusion device: Development and validation of a finite element model. *Medical Engineering & Physics*, *82*, 104-118. https://doi.org/https://doi.org/10.1016/j.medengphy.2020.05.019

Zaidat, O. O., Castonguay, A. C., Linfante, I., Gupta, R., Martin, C. O., Holloway, W. E., Mueller-Kronast, N., English, J. D., Dabus, G., Malisch, T. W., Marden, F. A., Bozorgchami, H., Xavier, A., Rai, A. T., Froehler, M. T., Badruddin, A., Nguyen, T. N., Taqi, M. A., Abraham, M. G., . . . Nogueira, R. G. (2018). First Pass Effect. *Stroke*, *49*(3), 660-666. https://doi.org/doi:10.1161/STROKEAHA.117.020315

Appendix

A. The MATLAB script for the parameter study for the anisotropic bilinear model

a) MPI_main.m

```
% This Matlab script run abaqus simulation, extract the results, and
% compare the results with the experimental data
%
% Developed by Behrooz Fereidoonnezhad
% Last update: April 2022
% Email: b.fereidoonnezhad@tudelft.nl

%Define working directory
    defaultFolder='C:\MPI_template2';
    compilerPath='"C:\Program Files
(x86)\IntelSWTools\compilers_and_libraries_2016.4.246\windows\bin\ifortvars.b
at"';
    visualStudioPath='"C:\Program Files (x86)\Microsoft Visual Studio
12.0\VC\bin\vcvars32.bat"';
%     visualStudioPath='"C:\Program Files (x86)\Microsoft Visual
Studio\2019\Community\VC\Auxiliary\Build\vcvars32.bat"';
    umatScriptName='umat_axisym-3D_BL3_Jan2021.for';
    pythonScriptName='ExtractResults.py';
    pythonScriptName_temp='ExtractResults_temp.py';
    abaqusInpFileName1='CompressionTest_newmodel';

%%Experimental data
% compression and tension test data (Nominal strain-Nominal stress)
% -80% - 65%
    stress_exp = [-0.069903968, -0.045201755, -0.029383145, -0.019576559, -
0.013404511, -0.009305387, -0.006526755, -0.004589725, -0.003204398, -
0.002280752, -0.001674755, -0.001227625, -0.000926664, -0.000715112, -
0.000520546, -0.000393737, -0.000259023, -0.000156686, -0.0000765, 0.000065,
0.000898904, 0.002259057, 0.003907429, 0.005638952, 0.007440334, 0.009585846,
0.011455498, 0.013476002, 0.015194814,    0.017059254,      0.018768492,
      0.020700644,      0.022369141];
    strain_exp = [-0.8, -0.757894737,     -0.715789474,     -0.673684211,
      -0.631578947,     -0.589473684,     -0.547368421,     -0.505263158,
      -0.463157895,     -0.421052632,     -0.378947368,     -0.336842105,
      -0.294736842,     -0.252631579,     -0.210526316,     -0.168421053,
      -0.126315789,     -0.084210526,     -0.042105263,     0,
      0.051784211,      0.103568421,      0.155352632,      0.207136842,
      0.258921053,      0.310705263,      0.362489474,      0.414273684,
      0.466057895,      0.517842105,      0.569626316,      0.621410526,
      0.673194737];

    model=5;%neo Hooke=1, Ogden=2, Yeoh=3, hyperfoam=4,  BL3=5

    objectiveStruct.defaultFolder=defaultFolder;
    objectiveStruct.compilerPath=compilerPath;
    objectiveStruct.visualStudioPath=visualStudioPath;
    objectiveStruct.umatScriptName=umatScriptName;
    objectiveStruct.abaqusInpFileName=abaqusInpFileName1;
    objectiveStruct.pythonScriptName=pythonScriptName;
```

```
    objectiveStruct.pythonScriptName_temp=pythonScriptName_temp;

% Experimental data
  objectiveStruct.stress=stress_exp;
  objectiveStruct.strain=strain_exp;
%   objectiveStruct.SD=SD_exp;
  objectiveStruct.model=model;

%   The material parameters
  x0 = [0.1, 0.4,  0.00005, 0.003, 5., 0.27, 0.8, 0.0015, 0.06, 0.08, 0.016,
0.2, 0.4, 2, 2, 90., 45., 90., -45., 0.01];

%  Lower and upper boundary for optimization
%   lb = [0.2, 0.95,  0.005, 0.09, 5., 0.2, 0.3, 0.04, 0.06, 0.008, 0.02,
0.1, 0.2, 2, 2, 90., 45., 90., -45., 0.01]
%   ub = [0.2, 0.95,  0.005, 0.09, 5., 0.2, 0.3, 0.04, 0.06, 0.008, 0.02,
0.1, 0.2, 2, 2, 90., 45., 90., -45., 0.01]

%Optimization settings if needed
maxNumberIterations=10000; %Maximum number of optimization iterations
maxNumberFunctionEvaluations=maxNumberIterations*100; %Maximum number of
function evaluations, N.B. multiple evaluations are used per iteration
functionTolerance=1e-2; %Tolerance on objective function value
parameterTolerance=1e-3; %Tolerance on parameter variation
displayTypeIterations='iter';

OPT_options = optimoptions(@lsqnonlin,'Algorithm','levenberg-marquardt');
OPT_options =
optimoptions(OPT_options,'MaxFunEvals',maxNumberFunctionEvaluations,...
                    'MaxIter',maxNumberIterations,...
                    'TolFun',functionTolerance,...
                    'TolX',parameterTolerance,...
                    'Display',displayTypeIterations,...
                    'FinDiffRelStep',1e-3,...
                    'DiffMaxChange',Inf);

% Optimization
% [x_opt,resnorm,residual,exitflag]= lsqnonlin(@(x)
MPI_CompressionTest_2(x,objectiveStruct),x0,[lb],[ub],OPT_options);

% Manually fitting
[errVec,U1,RF1,RF2,RF3,DET]=MPI_CompressionTest_2(x0,objectiveStruct);

% save('MPI_BL_Ogden_Yeoh_hyperfoam.mat','U1_BL','RF1_BL','DET_BL',...
%
'U1_ogden','RF1_ogden','DET_ogden',...
%                                         'U1_yeoh','RF1_yeoh','DET_yeoh',...
%
'U1_hyperfoam','RF1_hyperfoam','DET_hyperfoam');

%% Plot
%%Experimental data
eps_exp=strain_exp;
 P_exp=stress_exp;
 % Plot Settings
    fontSize=30;
    fontSizeInner=fontSize+10;
```

```
    fontSizeLabel=fontSize+5;
    faceAlpha1=0.8;
    faceAlpha2=1;
    edgeColor=0.25*ones(1,3);
    edgeWidth=1.5;
    markerSize=55;
    lineWidth=6;
    gridAlpha=0.3;
    LineWidthAxis=2;
    plotType =1;  % =1 for separate figures, =2 for subplot

    colorVec{1} = [1 0 0];  %red
    colorVec{2} = [0 0 1];  %blue
    colorVec{3} = [0, 0.5, 0];  %Green
    colorVec{4} = [0.4940, 0.1840, 0.5560];  %Purple
    colorVec{5} = [0.9290, 0.6940, 0.1250];  % Orange
    colorVec{6} = [0 0 0];  %black

    cFigure % comment this line if multiple curves in a single figure wanted
(from the 2nd curve)
    hold on
%     errorbar(eps_exp,P_exp,SDV,'.-
k','MarkerSize',markerSize,'LineWidth',lineWidth/2,'CapSize',18);\

% Comment the next line if multiple curves in a single figure wanted (from
the 2nd curve)
    plot(eps_exp,P_exp,'.-k','MarkerSize',markerSize,'LineWidth',lineWidth/2)
    plot(U1,RF1,'-','Color',colorVec{1},'LineWidth',lineWidth); % change the
value in colorVec{} to get different color
%     plot(U1,RF1,'-','Color',colorVec{2},'LineWidth',lineWidth);
%     plot(U1,RF1,'-','Color',colorVec{3},'LineWidth',lineWidth);

    ha=gca;
    ha.FontSize=fontSize;
    xlabel('Nominal axial
strain','FontSize',fontSizeLabel,'Interpreter','Latex');
    ylabel('Nominal axial stress $(\rm
MPa)$','FontSize',fontSizeLabel,'Interpreter','Latex');
    leg=legend({'Experiment','Proposed
model'},'Location','south','FontSize',0.7*fontSize,'Interpreter','Latex');
    leg.EdgeColor='none';
    axis tight;
    axis square
    box on;

% Show the specific range if needed
%     axis([-0.7 0.65 -0.02 0.025])

%     if nset==3
%         text(-1.07, 0, 'A','FontSize',40,'FontWeight','bold');
%     elseif nset==2
%         text(-1.2, 0, 'C','FontSize',40,'FontWeight','bold');
%     else
%         text(-1.2, 0, 'E','FontSize',40,'FontWeight','bold');
%     end

%     axes('Position',[0.25 0.48 0.25 0.25]);
```

```
 drawnow;
```

b) MPI_CompressionTest_2.m

```
function [errVec,U1,RF1,RF2,RF3,DET]=MPI_CompressionTest_2(x,objectiveStruct)
tic

props=x;

% show parameters
% fopen('parameters.txt');
% fprintf('mu1', 'alpha1', 'mu2', 'alpha2', 'nu1', 'nu2');

% if exist('x_opt') == 0
%     fprintf('-----------');
% else
%     fprintf(x_opt(1), x_opt(2), x_opt(3), x_opt(4), x_opt(5), x_opt(6));
% end

% fprintf('-----------');

defaultFolder=objectiveStruct.defaultFolder
compilerPath=objectiveStruct.compilerPath;
visualStudioPath=objectiveStruct.visualStudioPath;
umatScriptName=objectiveStruct.umatScriptName;
abaqusInpFileName1=objectiveStruct.abaqusInpFileName;
pythonScriptName=objectiveStruct.pythonScriptName;
pythonScriptName_temp=objectiveStruct.pythonScriptName_temp;
model=objectiveStruct.model;

% Experimental data
  stress_exp=objectiveStruct.stress;
  strain_exp=objectiveStruct.strain;
%   SD_exp=objectiveStruct.SD;

% for hh1=1:1
    abaqusInpFileName = [abaqusInpFileName1,'.inp'];
    abaqusInpFileNameTemp = [abaqusInpFileName1,'_temp.inp'];
    abaqusJobName = abaqusInpFileName1;
    lockFileName=fullfile(defaultFolder,[abaqusJobName,'.lck']);

     %%Modify inp file
             %Material Parameters
%                %Read in inp file into cell array
               T2=txtfile2cell(fullfile(defaultFolder,abaqusInpFileName));

             if model==1  %neo Hooke
               %Find target line
               scanTarget1 = '*Hyperelastic, neo hooke';
               textLineMaterial1 =
find(~cellfun(@isempty,regexp(T2,scanTarget1)));
               formatSpecNow='%6.7e, %6.7e';
               T2{textLineMaterial1+1}=sprintf(formatSpecNow,props(1:2));
               %Write new file

cell2txtfile(fullfile(defaultFolder,abaqusInpFileNameTemp),T2);
```

```
            elseif model==2  %Ogden (abaqus)
                %Find target line
                scanTarget1 = '*Hyperelastic, ogden, n=2';
                textLineMaterial1 =
find(~cellfun(@isempty,regexp(T2,scanTarget1)));
                formatSpecNow='%6.7e, %6.7e, %6.7e, %6.7e, %6.7e, %6.7e';
                T2{textLineMaterial1+1}=sprintf(formatSpecNow,props(1:6));
                %Write new file

cell2txtfile(fullfile(defaultFolder,abaqusInpFileNameTemp),T2);
            elseif model==3  % Yeoh (abaqus)
                %Find target line
                scanTarget1 = '*Hyperelastic, yeoh';
                textLineMaterial1 =
find(~cellfun(@isempty,regexp(T2,scanTarget1)));
                formatSpecNow='%6.7e, %6.7e, %6.7e, %6.7e, %6.7e, %6.7e';
                T2{textLineMaterial1+1}=sprintf(formatSpecNow,props(1:6));
                %Write new file

cell2txtfile(fullfile(defaultFolder,abaqusInpFileNameTemp),T2);
            elseif model==4  % hyperfoam (abaqus)
                %Find target line
                scanTarget1 = '*Hyperfoam, n=2';
                textLineMaterial1 =
find(~cellfun(@isempty,regexp(T2,scanTarget1)));
                formatSpecNow='%6.7e, %6.7e, %6.7e, %6.7e, %6.7e, %6.7e';
                T2{textLineMaterial1+1}=sprintf(formatSpecNow,props(1:6));
                %Write new file

cell2txtfile(fullfile(defaultFolder,abaqusInpFileNameTemp),T2);

            elseif model==5  %BLM_BLV_BLF (BL3)
                %Find target line

                   scanTarget1 = ['*User Material,
constants=',num2str(length(props))];
                   textLineMaterial1 =
find(~cellfun(@isempty,regexp(T2,scanTarget1)));
                %Overwrite text line in cell
                    formatSpecNow='%6.7e, %6.7e, %6.7e, %6.7e, %6.7e, %6.7e,
%6.7e, %6.7e';

T2{textLineMaterial1+1}=sprintf(formatSpecNow,props(1:8));
                    formatSpecNow='%6.7e, %6.7e,%6.7e, %6.7e,%6.7e, %i, %i,
%6.7e';

T2{textLineMaterial1+2}=sprintf(formatSpecNow,props(9:16));
                    formatSpecNow='%6.7e, %6.7e, %6.7e, %6.7e';

T2{textLineMaterial1+3}=sprintf(formatSpecNow,props(17:20));
                %Write new file

cell2txtfile(fullfile(defaultFolder,abaqusInpFileNameTemp),T2);

             elseif model==6  %Ogden N=4(abaqus)
                %Find target line
                scanTarget1 = '*Hyperelastic, ogden, n=4';
```

```
                textLineMaterial1 =
find(~cellfun(@isempty,regexp(T2,scanTarget1)));
                formatSpecNow='%6.7e, %6.7e, %6.7e, %6.7e, %6.7e, %6.7e,
%6.7e, %6.7e';
                T2{textLineMaterial1+1}=sprintf(formatSpecNow,props(1:8));
                formatSpecNow='%6.7e, %6.7e, %6.7e, %6.7e';
                T2{textLineMaterial1+2}=sprintf(formatSpecNow,props(9:12));
                %Write new file

cell2txtfile(fullfile(defaultFolder,abaqusInpFileNameTemp),T2);

             elseif model==7  %Hyper Foam N=4(abaqus)
                %Find target line
                scanTarget1 = '*Hyperfoam, n=4';
                textLineMaterial1 =
find(~cellfun(@isempty,regexp(T2,scanTarget1)));
                formatSpecNow='%6.7e, %6.7e, %6.7e, %6.7e, %6.7e, %6.7e,
%6.7e, %6.7e';
                T2{textLineMaterial1+1}=sprintf(formatSpecNow,props(1:8));
                formatSpecNow='%6.7e, %6.7e, %6.7e, %6.7e';
                T2{textLineMaterial1+2}=sprintf(formatSpecNow,props(9:12));
                %Write new file

cell2txtfile(fullfile(defaultFolder,abaqusInpFileNameTemp),T2);

            end

                if exist(lockFileName,'file')
                    warning('Lockfile found and deleted')
                    delete(lockFileName);
                end
% end

    oldPath=pwd; %Get current working directory
    cd(defaultFolder) %Set new working directory to match save patch

%
    %Run the job
    if model==5
%         batchFileString = ['abaqus job=',abaqusJobName,'
inp=',abaqusInpFileNameTemp,' user=',umatScriptName,' cpus=4','
interactive'];
        batchFileString = ['abaqus job=',abaqusJobName,'
inp=',abaqusInpFileNameTemp,' user=',umatScriptName,' cpus=4','
interactive'];

    else
%         batchFileString = ['abaqus job=',abaqusJobName{1},'
inp=',abaqusInpFileNameTemp,' cpus=4 & ', 'abaqus job=',abaqusJobName{2},'
inp=',abaqusInpFileNameTemp{2},' cpus=4',' interactive'];
%         batchFileString = ['abaqus job=',abaqusJobName,'
inp=',abaqusInpFileNameTemp,' user=',umatScriptName,' cpus=1','
interactive'];
        batchFileString = ['abaqus job=',abaqusJobName,'
inp=',abaqusInpFileNameTemp,' cpus=4',' interactive'];
    end
```

```
        batFileName = fopen('temp1.bat','w');

        fprintf(batFileName,batchFileString)

%         runString = ['cd "',defaultFolder,'" && ', visualStudioPath,' &
',compilerPath,' intel64 vs2013 & "',defaultFolder,'\temp1.bat"',' &&
"C:\WINDOWS\system32\cmd.exe" /k exit'];
        runString = ['cd ',defaultFolder, ' &
"',defaultFolder,'\temp1.bat"',' & "C:\WINDOWS\system32\cmd.exe" /k exit'];
        system(runString)
        fclose(batFileName);
        cd(oldPath); %Restore working directory

%% Post-processing
%%%%%%%%%%%%%%%%%%%%%%%%%%%%%%%%%%%%%%%%%%%%%%%%%%%%%%%%%%%%%%%%%%%%%%%
                        % Visualization of the abaqus results
%%%%%%%%%%%%%%%%%%%%%%%%%%%%%%%%%%%%%%%%%%%%%%%%%%%%%%%%%%%%%%%%%%%%%%%

% for hh1=1:1
    abaqusJobName1 = abaqusInpFileName1;
    lockFileName1=fullfile(defaultFolder,[abaqusJobName1,'.lck']);
    AbaqusResultsFileName = [abaqusJobName1,'_Results','.txt'];

 % Modify python script
    %Read in python script into cell array
    T2=txtfile2cell(fullfile(defaultFolder,pythonScriptName));
    %Find target line
    scanTarget4 = 'from textRepr import *';
    textLineMaterial1 = find(~cellfun(@isempty,regexp(T2,scanTarget4)));
    %Overwrite text line in cell
%     AbaqusResultsFileName = [abaqusJobName,'_Results','.txt'];
    T2{textLineMaterial1+2}=['outFile =
open(''',abaqusJobName1,'_Results','.txt'',''w+'')'];
    T2{textLineMaterial1+3}=['odbFileNameFull =
''',(fullfile(defaultFolder,[abaqusJobName1,'.odb''']))];
%     T2{textLineMaterial1+8}=['    U2_proximal =
val.fieldOutputs[''U''].values[',num2str(proximalNode-1),'].data[1]'];
%     T2{textLineMaterial1+9}=['    U2_distal =
val.fieldOutputs[''U''].values[',num2str(distalNode-1),'].data[1]'];
%     T2{textLineMaterial1+10}=['    U2_central =
val.fieldOutputs[''U''].values[',num2str(centralNode-1),'].data[1]'];
%
%     %Write new file
    cell2txtfile(fullfile(defaultFolder,pythonScriptName_temp),T2);

% run the python script to get the results from odb file
        if exist(lockFileName1,'file')
            warning('Lockfile found and deleted')
            delete(lockFileName1);
        end

        batchFileStringODB = ['abaqus cae -noGUI ',pythonScriptName_temp];
        batFileName1 = fopen(fullfile(defaultFolder,'temp2.bat'),'w');
        fprintf(batFileName1,batchFileStringODB);
%         runString = ['cd "',defaultFolder,'" && ', visualStudioPath,' &
',compilerPath,' intel64 vs2013 & "',defaultFolder,'\temp2.bat"',' &&
"C:\WINDOWS\system32\cmd.exe" /k exit'];
```

```
        runString = ['cd ',defaultFolder, ' &
"',defaultFolder,'\temp2.bat"',' & "C:\WINDOWS\system32\cmd.exe" /k exit'];
        system(runString)
        fclose(batFileName1);
        cd(oldPath); %Restore working directory

    % post-processing
        clear U2 data_f data
        fileName = fullfile(defaultFolder,AbaqusResultsFileName);
        fid1=fopen(fileName,'r');
        data_f=textscan(fid1,'%f','delimiter', ',','Whitespace','');
        data_f=data_f{:,1};
        data(1,1:numel(data_f))=data_f;

    kk=0;
    clear U1 U2 U3 RF1 RF2 RF3 DET

%     for ii =1:6:size(data,2)-5 % -0.8~1.0
%     for ii =1:6:size(data,2)-50 % -0.8~0.68
    for ii =1:6:size(data,2)-50 % -0.67~0.68
        kk=kk+1;
        U1(kk)=data(1,ii);
        U2(kk)=data(1,ii+1);
        U3(kk)=data(1,ii+2);
        RF1(kk)=data(1,ii+3);
        RF2(kk)=data(1,ii+4);
        RF3(kk)=data(1,ii+5);
        DET(kk)=(1+U1(kk))*(1+U2(kk))*(1+U3(kk));

    end

%   end

    fclose(fid1)

errVec1=0;

%Resample experimental data to same number of Frames in simulation
   %Removing potential double points
      [strain_exp,indUni1,~]=unique(strain_exp);
      stress_exp=stress_exp(indUni1);
      stress_exp_re=interp1(strain_exp,stress_exp,U1,'pchip');
   %Calculate error
      errVec=abs((stress_exp_re-RF1));
%       errVec=abs((stress_exp_re-RF1)/(stress_exp_re));
      norm(stress_exp_re-RF1)
      NRMSE_stress =norm(stress_exp_re-RF1)/abs(mean(stress_exp));
%%Calculate R-squared (Coefficent of determination)
      dev_exp=abs(stress_exp-mean(stress_exp));
      SS_total = (norm(dev_exp))^2;
      SS_res = (norm(errVec))^2;
      R2_sigma = 1-SS_res/SS_total;

toc
```

B. The anisotropic bilinear model

```
      SUBROUTINE UMAT(STRESS,STATEV,DDSDDE,SSE,SPD,SCD,
     1 RPL,DDSDDT,DRPLDE,DRPLDT,
     2 STRAN,DSTRAN,TIME,DTIME,TEMP,DTEMP,PREDEF,DPRED,CMNAME,
     3 NDI,NSHR,NTENS,NSTATV,PROPS,NPROPS,COORDS,DROT,PNEWDT,
     4 CELENT,DFGRD0,DFGRD1,NOEL,NPT,LAYER,KSPT,KSTEP,KINC)
C
      INCLUDE 'ABA_PARAM.INC'
C
      CHARACTER*80 CMNAME
      DIMENSION STRESS(NTENS),STATEV(NSTATV),
     1 DDSDDE(NTENS,NTENS),DDSDDT(NTENS),DRPLDE(NTENS),
     2 STRAN(NTENS),DSTRAN(NTENS),TIME(2),PREDEF(1),DPRED(1),
     3 PROPS(NPROPS),COORDS(3),DROT(3,3),DFGRD0(3,3),DFGRD1(3,3),
     4 DFGRD1_m(3,3)
C
C LOCAL ARRAYS
C ----------------------------------------------------------------
C XKIRCH1 - KIRCHHOFF STRESS
C DFP - INCREMENT OF THE PERTURBED DEF. GRAD.
C DFGRD_PERT - PERTURBED DEF. GRAD.
C XKIRCH_PERT - PERTURBED KIRCHHOFF STRESS
C CMJ - (:,:,I,J) COMPONENTS OF MATERIAL JACOBIAN
C CMJVEC - ABOVE IN VECTOR FORM
C ILIST, JLIST - SET OF THE COMPONENTS TO BE PERTURBED UPON
C DUMSTRSS - DUMMY STRESS TENSOR
C XMMAT - ARRAY OF THE UNIT VECTORS DESCRIBING THE FIBRE DIRECTION
C ----------------------------------------------------------------
C
      DIMENSION XKIRCH1(3,3), DFP(3,3), DFGRD_PERT(3,3),XKIRCH_PERT(3,3)
     1 ,CMJ(3,3), CMJVEC(NTENS), ilist(6), jlist(6), DUMSTRSS(3,3),
     1 XMMAT(3,2), XMDUM(3,1), XMDUM1(3,1), XI4(2),XALPHAR(2),XBETAR(2)
C
C     ARRAYS FOR THE POLAR DECOMPOSITION
C
      DIMENSION spolF(3,3), spolC(3,3), spolCS(3,3), spolUINV(3,3),
     & U(3,3), R(3,3), RT(3,3)
C
      PARAMETER(ZERO=0.D0, ONE=1.D0, TWO=2.D0, THREE=3.D0, FOUR=4.D0,
     1 SIX=6.D0)
C
C ----------------------------------------------------------------
C UMAT FOR COMPRESSIBLE HYPERELASTIC MODEL DEVELOPED BY Behrooz
Fereidoonnezhad,
C
C
C 3D CONTINUUM ELEMENTS
C ----------------------------------------------------------------
C
C    ** PROPERTIES **
C
C PROPS(1) - E
C PROPS(2) - NU
C PROPS(3) - K1
C PROPS(4) - K2
C PROPS(5) - KAPPA (FIBRE DISPERSION)
```

```
C PROPS(6) - THETA1 (ORIENTATION ANGLE OF THE 1ST FIBRE FAMILY)
C PROPS(7) - THETA2 (ORIENTATION ANGLE OF THE 1ST FIBRE FAMILY)
C
C
C    ** STATE DEPENDENT VARIABLES **
C
C STATEV(1) - I1
C STATEV(2) - I2
C STATEV(3) - I3
C STATEV(4) - I4
C STATEV(5) - I6
C STATEV(6) - J
C
C ------------------------------------------------------------------
C     NUMBER OF FIBRE FAMILIES
C ------------------------------------------------------------------
C
C        NANISO = 2
C
C ------------------------------------------------------------------
C     MATERIAL PROPERTIES
C ------------------------------------------------------------------
C
      ! Isotropic parameters
        xD1t  = PROPS(1) ! first transitional strain for matrix (tension)
        xD2t  = PROPS(2) ! second transitional strain for matrix (tension)
        xE1   = PROPS(3) ! lower strain stiffness for matrix
        xE2t  = PROPS(4) ! higher strain stiffness for matrix
        xE2c = xE2t ! symmetric behavior for compression and tension
        xscale = PROPS(5) ! do not concern this one
        xD1v = PROPS(6) ! first transitional strain for volumetric
        xD2v = PROPS(7) ! first transitional strain for volumetric
        xkappa1 = PROPS(8) ! bulk modulus for lower stain
        xkappa2 = PROPS(9) ! bulk modulus for higher strain
C
      ! Anisotropic parameters
        xE1f = PROPS(10) ! lower stiffness for fibers
        xE2f = PROPS(11) ! higher stiffness for fibers
        xD1f = PROPS(12) ! first transitional strain for fibers
        xD2f = PROPS(13) ! second transitional strain for fibers
        NANISO = PROPS(14) ! equals 2, should not be changed
        iswitch=int(props(15)) ! equals 2, should not be changed
        ALPHAD1 = PROPS(16) ! Used to define the first main fiber direction
        BETAD1 = PROPS(17) ! Used to define the first main fiber direction
        ALPHAD2 = PROPS(18) ! Used to define the second main fiber direction
        BETAD2 = PROPS(19) ! Used to define the second main fiber direction
        xbb = PROPS(20) ! concentrated distribution: 200; diperse
distribution: 0.01
C
        xP = (xE1f - xE2f)/(2.d0*(xD1f-xD2f))
        xQ = xE1f - (xD1f*(xE1f-xE2f))/(xD1f-xD2f)
        xR = xE1f*xD1f - xP*(xD1f**2.d0) - xQ*xD1f
C
        XPI = 3.14159265359d0
        XBETAR(1) = BETAD1*XPI/180.d0
        XALPHAR(1)= ALPHAD1*XPI/180.d0
        XBETAR(2) = BETAD2*XPI/180.d0
```

```
        XALPHAR(2)= ALPHAD2*XPI/180.d0
C
        XMMAT(1,1)= sin(xalphar(1))*cos(xbetar(1))    ! mean fiber direction
        XMMAT(2,1)= sin(xalphar(1))*sin(xbetar(1))
        XMMAT(3,1)= cos(xalphar(1))
C
        XMMAT(1,2)= sin(xalphar(2))*cos(xbetar(2))
        XMMAT(2,2)= sin(xalphar(2))*sin(xbetar(2))
        XMMAT(3,2)= cos(xalphar(2))
        iter=0
C
C-------------------------------------------------------------------------
C     POLAR DECOMPOSITION
C-------------------------------------------------------------------------
C
      spolF=dfgrd1
      DO  J=1,3
        DO  I = 1,3
          spolC(I,J)= 0.0D0
          DO  K=1,3
            spolC(I,J)= spolC(I,J) + spolF(K,I)*spolF(K,J)
          ENDDO
        ENDDO
      ENDDO

      DO  J=1,3
        DO  I=1,3
          spolCS(I,J)= 0.0D0
          DO K=1,3
            spolCS(I,J)= spolCS(I,J) + spolC(I,K)*spolC(K,J)
          ENDDO
        ENDDO
      ENDDO

      spolC1= spolC(1,1) + spolC(2,2) + spolC(3,3)
      spolC2= 0.5D0 * (spolC1**2.0D0 - (spolCS(1,1)+spolCS(2,2)+
     +    spolCS(3,3)))
      spolC3= spolC(1,1) * (spolC(2,2)*spolC(3,3)-spolC(2,3)*spolC(3,2))
     1    +spolC(1,2) * (spolC(2,3)*spolC(3,1)-spolC(2,1)*spolC(3,3))
     2    +spolC(1,3) * (spolC(2,1)*spolC(3,2)-spolC(2,2)*spolC(3,1))
      spolU3= SQRT(spolC3)
      spolX1=2.0**5.0 /27.0*(2.0*spolC1**3.0-9.0*spolC1*spolC2+
     &27.0*spolC3)
      spolX2= 2.**10.0 /27.0*(4.0*spolC2**3.0-spolC1**2.0*spolC2**2.0 +
     &4.0*spolC1**3.0*spolC3-18.0*spolC1*spolC2*spolC3+27.0*spolC3**2.0)

      IF (spolX2.LT.0.) spolX2= 0.0
      F1= spolX1 + SQRT(spolX2)
      IFLAG2= 0
      IFLAG1= 0
      IF (F1.LT.0.0) IFLAG1= 1
      F2= spolX1 - SQRT(spolX2)
      IF (F2.LT.0.0) IFLAG2= 1
      IF (IFLAG2.EQ.1) F2= -F2
      IF (IFLAG1.EQ.1) F1= -F1
      spolX3= -2.0/3.0*spolC1 + F1**(1.0/3.0) + F2**(1.0/3.0)
      IF (IFLAG1.EQ.1) spolX3= -2.0/3.0*spolC1 + F2**(1.0/3.0) -
```

```
     +                     F1**(1.0/3.0)
      IF (IFLAG2.EQ.1) spolX3= -2.0/3.0*spolC1 + F1**(1.0/3.0) -
     +                     F2**(1.0/3.0)
      B= -2.0*spolC1
      IF (spolX3.EQ.B) THEN
      U1= SQRT(spolC1+2.0*SQRT(spolC2))
      ELSE
      U1= 0.5 * (SQRT(2.0*spolC1+spolX3) + SQRT(2.0*spolC1 -
     +    spolX3+16.0*SQRT(spolC3)/SQRT(2.0*spolC1+spolX3)))
      ENDIF
      U2= SQRT(spolC2+2.0*spolU3*U1)
      B1= spolU3**2.0 * (spolU3+U1*spolC1) +
     &U1**2.0 * (U1*spolC3+spolU3*spolC2)
      B2= U1 * (U1*U2-spolU3) / B1
      B3=-(U1*U2-spolU3) * (spolU3+U1*spolC1) / B1
      B4= (U2*spolU3*(spolU3+U1*spolC1) +
     &U1**2.0 * (U2*spolC2+spolC3))/B1

      DO  J=1,3
        DO  I=1,3
          spolUINV(I,J)= B2*spolCS(I,J) + B3*spolC(I,J)
          IF (I.EQ.J)   spolUINV(I,J)= spolUINV(I,J) + B4
        ENDDO
      ENDDO

      DO  J=1,3
        DO  I=1,3
          R(I,J)=0.0
          DO  K=1,3
            R(I,J)= R(I,J) + spolF(I,K)*spolUINV(K,J)
          ENDDO
        ENDDO
      ENDDO
      DO  I=1,3
        DO  J=1,3
          RT(I,J) = R(J,I)
        ENDDO
      ENDDO

      U=0.0
       DO I=1,3
            DO J=1,3
                DO M=1,3
                         !U(I,J)=U(I,J)+RT(I,M)*spolF(M,J)      ! old version
                         U(I,J)=U(I,J)+spolF(I,M)*RT(M,J)     ! modified
                ENDDO
            ENDDO
       ENDDO
C
C-----------------------------------------------------------------
C  CALCULATE THE ROTATED, a_0' VECTORS
C-----------------------------------------------------------------
C
      IF (iswitch.EQ.1) then
      DO IAN = 1,2
        XMDUM(:,1) = XMMAT(:,IAN)
!                  (M, N, L, A, KA, B, KB, C, KC)
```

```
        !call KMTMS(3, 3, 1, RT, 3, XMDUM, 3, XMDUM1, 3)
         call KMTMS(3, 3, 1, RT, XMDUM, XMDUM1)
         XMMAT(:,IAN) = XMDUM1(:,1)
       END DO
C
       write(6,*) '*Orientation is defined!'
C
        DFGRD1_m=0.0
        DO I=1,3
             DO J=1,3
                 DO M=1,3

                          DFGRD1_m(I,J)=DFGRD1_m(I,J)+R(I,M)*U(M,J)     !
modified
                 ENDDO
             ENDDO
       ENDDO
       !DFGRD1_m = U
C
       ELSE IF (iswitch.EQ.2) then
             XMMAT(:,IAN)=XMMAT(:,IAN)
             DFGRD1_m = DFGRD1
       ELSE
            WRITE (6,*) '*** ERROR: Global or local coordinate system must be'
            WRITE (6,*) 'specified in PROPS(15),=1 for local, =2 for global'
C          STOP
       ENDIF
C
C-----------------------------------------------------------------
C  ZERO THE TANGENT MATRIX
C-----------------------------------------------------------------
C
       DO I=1,NTENS
       DO J=1,NTENS
         DDSDDE(I,J) = ZERO
       END DO
       END DO
C-----------------------------------------------------------------
C CALCULATE THE STRESS
C-----------------------------------------------------------------
C
    !call kstress_calc(DFGRD1, C10, D1, xA, xB, xP, xQ, xR,
    !1   xD1, xD2, xbb, XKIRCH1, XJ1, XALPHAR, XBETAR, NANISO,
    !2   XI1, XI2, XI3, XI4)
      call kstress_calc(DFGRD1_m,PROPS,NPROPS,NANISO,
     1 XKIRCH1,XJ1,XI1,XI2,XI3,XI4,nphase)
C
         STATEV(1) = XI1
         STATEV(2) = XI2
         STATEV(3) = XI3
         STATEV(4) = XI4(1)
         STATEV(5) = XI4(2)
         STATEV(6) = XJ1
         STATEV(7) = nphase
C
C-----------------------------------------------------------------
C CONVERT KIRCHHOFF STRESS TO CAUCHY STRESS
```

```
C-----------------------------------------------------------------
      DUMSTRSS = XKIRCH1 / XJ1

      call kmatrix2vector(DUMSTRSS, STRESS, NTENS)
C
      !write(6,*) '-------'
      !write(6,*) 'inc=', kinc
      !write(6,*) 'Props=', props
      !write(6,*) 'XJ1=', XJ1
      !write(6,*) 'DROT=', DROT
C
C*****************************************************************
C
C-----------------------------------------------------------------
C CALCULATE THE PERTURBATION OF THE KIRCHHOFF STRESS
C-----------------------------------------------------------------
C
      eps = 1.0e-08
C
      ilist(1) = 1; ilist(2) = 2; ilist(3) = 3
      ilist(4) = 1; ilist(5) = 1; ilist(6) = 2
      jlist(1) = 1; jlist(2) = 2; jlist(3) = 3
      jlist(4) = 2; jlist(5) = 3; jlist(6) = 3
C
C
      Perturbation: DO iter = 1,NTENS
C
        ii = ilist(iter)
        jj = jlist(iter)
C
          call kdelF(ii, jj, DFGRD1_m, eps, DFP)
C
C-----------------------------------------------------------------
C CREATE THE PERTURBATION OF THE DEFORMATION GRADIENT
C-----------------------------------------------------------------
C
          DFGRD_PERT = DFGRD1_m + DFP
C
C-----------------------------------------------------------------
C CALCULATE THE STRESS BASED ON THIS NEW DEFORMATION GRADIENT
C-----------------------------------------------------------------
C
    !    call kstress_calc(DFGRD_PERT, C10, D1, xA, xB, xP, xQ, xR,xD1,
    !1     xD2, xbb, XKIRCH_PERT, XJP, XALPHAR,XBETAR,
    !2     NANISO, XI1, XI2, XI3, XI4)
      call kstress_calc(DFGRD_PERT,PROPS,NPROPS,NANISO,
     1 XKIRCH_PERT, XJP,XI1,XI2,XI3,XI4,nphase)

C
C-----------------------------------------------------------------
C DIFFERENCE BETWEEN THE PERTURBED(i,j) AND UNPERT. STRESS
C-----------------------------------------------------------------
C
          do i = 1,3
          do j = 1,3
            CMJ(i,j) = XKIRCH_PERT(i,j) - XKIRCH1(i,j)
          end do
```

```
          end do
C
          CMJ = CMJ/XJ1/eps
C
C-----------------------------------------------------------------
C VECTORISE AND INSERT INTO THE DDSDDE MATRIX
C-----------------------------------------------------------------
C
          call kmatrix2vector(CMJ, CMJVEC, NTENS)

          do insert = 1,NTENS

            DDSDDE(insert,iter) = CMJVEC(insert)

          end do
C
       end do Perturbation
C
      RETURN
      contains
C
C-------------------------------------------------------------------------
-
C           SUBROUTINES
C-------------------------------------------------------------------------
-
C
C * KSTRESS_CALC -   Calculate the Kirchhoff stress based on the deformation
C                   gradient and the elastic constants C10 and D1.
C
C * KDELF        -   Calculate the increment of the deformation gradient for
C                   a given perturbation in (i,j), with epsilon
C
C * KPRINTER     -   Print out a matrix of any size
C
C * KMTMS      -   Multiply two 2nd order tensors
C
C * KMATRIX2VECTOR     -   Convert a 3x3 matrix to a 6x1 vector
C
C * KDOTPROD           - Dot product of two vectors
C
C-------------------------------------------------------------------------
-
C
      subroutine kstress_calc(DGRAD,PROPS,NPROPS,NANISO,XKIRCH,
     1      DET,XI1,XI2,XI3,XI4,nphase)
C
      INCLUDE 'ABA_PARAM.INC'
C
      intent(in) :: DGRAD, PROPS, NPROPS, NANISO
      intent(out):: XKIRCH, DET, XI1, XI2, XI3, XI4, nphase
C
      dimension DGRAD(3,3), BMAT(3,3), XKIRCH(3,3),
     1 B2MAT(3,3),aoa(3,3),
     2 XANISOK(3,3),XANISOTOT(3,3),XI4(NANISO),XALPHAR(NANISO),
     3 XBETAR(NANISO),PROPS(NPROPS)
C
```

```
        parameter(n_phi=20, n_omega=10, nseg = (n_omega-1)*n_phi+1)
C
        dimension phi_vec(n_phi), omega_vec(n_omega), xm0i(3,1),
     1 xn0i_mat(nseg,3), xn0i(3,1), rho_vec(nseg), area_vec(nseg),
     2 rot_mat_E2(3,3),rot_mat_E3(3,3),rot_mat(3,3),xm0i_rot(3,1),
     3 xn0i_pre_rot(3,1),xn0i_rot(3,1),xn0i_rot_mat(nseg,3),xn1i(3,1),
     4 rho_mat(n_omega,n_phi), rot_mat1(3,3)
    !4 xn0i_rot_vec(3,1),
C
        DOUBLE PRECISION  XMMAT(3,2),
     1 XMM(3),DUMMY1(3),BBAR(6),BBARP(3),BBARN(3,3),
     2 BBARMAT(3,3),XKIRCH1(3,3),STRAIN(3),
     3 SBAR(3),Cauchy(3,3), BBARNT(3,3),SISOP(3,3)
C
        real(8) ::kiso(6),lambda2(3),na(3,3),B_a(3),
     1 n11(6),n22(6),n33(6),lambda_bar(3),lambda(3)
C
       ! Isotropic parameters
         xD1t  = PROPS(1)
         xD2t  = PROPS(2)
         xE1   = PROPS(3)
         xE2t  = PROPS(4)
         xE2c = xE2t
         xscale = PROPS(5)
         xD1v = PROPS(6)
         xD2v = PROPS(7)
         xkappa1 = PROPS(8)
         xkappa2 = PROPS(9)

       ! Anisotropic parameters
         xE1f = PROPS(10)
         xE2f = PROPS(11)
         xD1f = PROPS(12)
         xD2f = PROPS(13)
         !NANISO = PROPS(14)
         !iswitch=int(props(15))
         ALPHAD1 = PROPS(16)
         BETAD1 = PROPS(17)
         ALPHAD2 = PROPS(18)
         BETAD2 = PROPS(19)
         xbb = PROPS(20)
C
         xP = (xE1f - xE2f)/(2.d0*(xD1f-xD2f))
         xQ = xE1f - (xD1f*(xE1f-xE2f))/(xD1f-xD2f)
         xR = xE1f*xD1f - xP*(xD1f**2.d0) - xQ*xD1f
C
!         xPm = (xE1m - xE2m)/(2.d0*(xD1m-xD2m))
!         xQm = xE1m - (xD1m*(xE1m-xE2m))/(xD1m-xD2m)
!         xRm = xE1m*xD1m - xPm*(xD1m**2.d0) - xQm*xD1m
!C
!         xPv = (xkappa1 - xkappa2)/(2.d0*(xD1v-xD2v))
!         xQv = xkappa1 - (xD1v*(xkappa1-xkappa2))/(xD1v-xD2v)
!         xRv = xkappa1*xD1v - xPv*(xD1v**2.d0) - xQv*xD1v
C
         XPI = 3.14159265359d0
         XBETAR(1) = BETAD1*XPI/180.d0
         XALPHAR(1)= ALPHAD1*XPI/180.d0
```

```
        XBETAR(2) = BETAD2*XPI/180.d0
        XALPHAR(2)= ALPHAD2*XPI/180.d0
C
C JACOBIAN
C
        DET=DGRAD(1, 1)*DGRAD(2, 2)*DGRAD(3, 3)
     1   -DGRAD(1, 2)*DGRAD(2, 1)*DGRAD(3, 3)
     2   +DGRAD(1, 2)*DGRAD(2, 3)*DGRAD(3, 1)
     3   +DGRAD(1, 3)*DGRAD(3, 2)*DGRAD(2, 1)
     4   -DGRAD(1, 3)*DGRAD(3, 1)*DGRAD(2, 2)
     5   -DGRAD(2, 3)*DGRAD(3, 2)*DGRAD(1, 1)
      nphase = 0 ! what state is the aniso part in
C
C     ZERO MATRICES
        DO I=1,3
        DO J=1,3
            BMAT(I,J) = ZERO
        END DO
        END DO
C
C CALCULATE LEFT CAUCHY-GREEN DEFORMATION TENSOR
C
        DO I=1,3
            DO J=1,3
                DO K = 1,3
                    BMAT(I,J) = BMAT(I,J) + DGRAD(I,K)*DGRAD(J,K)
                END DO
            END DO
        END DO
C
C-----------------------------------------------------------------------
C     CALCULCATE THE INVARIANTS
C-----------------------------------------------------------------------
C
        XI1 = BMAT(1,1)+BMAT(2,2)+BMAT(3,3)
C
        CALL KMTMS(3, 3, 3, BMAT, BMAT,B2MAT)
C
        TRB2 = B2MAT(1,1)+B2MAT(2,2)+B2MAT(3,3)
C
        XI2 = 0.5d0*((XI1**2.d0) - TRB2)
C
        XI3=BMAT(1, 1)*BMAT(2, 2)*BMAT(3, 3)
     1   -BMAT(1, 2)*BMAT(2, 1)*BMAT(3, 3)
     2   +BMAT(1, 2)*BMAT(2, 3)*BMAT(3, 1)
     3   +BMAT(1, 3)*BMAT(3, 2)*BMAT(2, 1)
     4   -BMAT(1, 3)*BMAT(3, 1)*BMAT(2, 2)
     5   -BMAT(2, 3)*BMAT(3, 2)*BMAT(1, 1)
C
C-----------------------------------------------------------------------
C     CALCULATE THE ISOTROPIC PORTION OF THE KIRCH STRESS
C-----------------------------------------------------------------------
C
C   Bilinear_erf
C
      par1 = ONE/(DET**(TWO/THREE))
      BBARMAT = par1*BMAT
```

```
      BBAR(1) = BBARMAT(1,1)
      BBAR(2) = BBARMAT(2,2)
      BBAR(3) = BBARMAT(3,3)
      BBAR(4) = BBARMAT(1,2)
      BBAR(5) = BBARMAT(1,3)     ! to be checked, the order
      BBAR(6) = BBARMAT(2,3)
!
      !    Calculate eigenvalues la2(a) and eigenvectors n_a(3,3) of b
!     (Note: Jacobian algorithm destroys upper triangular components
12,13,23)
!
      call kDSYEVJ3(BMAT,na,lambda2)
!
      !write(6,*) 'na=', na
!
      lambda(1) = lambda2(1)**0.5d0
      lambda(2) = lambda2(2)**0.5d0
      lambda(3) = lambda2(3)**0.5d0
C
      lambda_bar = DET**(-ONE/THREE)*lambda
C
      DO KK=1,3
          strain(KK) = lambda_bar(KK) - 1.d0
      END Do
C
C Calculate Sbar=lambda*(dPsi/dlambda) (erf)
C
!        Do I=1,3
!            if (strain(I) .le. 0.d0) then
!                xD1c = -props(1)
!                xD2c = -props(2)
!            else
!                xD1c = props(1)
!                xD2c = props(2)
!            endif
!C
!            xmuc = xD1c + 0.5d0*(xD2c-xD1c)
!            xac = xE2c-xE1
!            xbc = (xD2c-xD1c)/xscale
!C
!        !fxc = erf((strain(I)-xmuc)/(xbc*sqrt(2)))
!        xfD1c = erf((xD1c-xmuc)/(xbc*sqrt(2.d0)))
!        xfD2c = erf((xD2c-xmuc)/(xbc*sqrt(2.d0)))
!        xintfxc=  erf((sqrt(2.d0)*(xmuc - strain(I)))/(2.d0*xbc))
!     &                   *(xmuc-strain(I)) + (sqrt(2.d0)*xbc
!     &     *exp(-(xmuc-strain(I))**2.d0/(2.d0*xbc**2.d0)))/sqrt(XPI)
!
!        xintfx0c = erf((sqrt(2.d0)*(xmuc-0.d0))/(2.d0*xbc))*
!     &                  (xmuc-0.d0) + (sqrt(2.d0)*xbc*
!     &       exp(-(xmuc - 0.d0)**2.d0/(2.d0*xbc**2.d0)))/sqrt(XPI)
!        xintconstc=xac/(xfD2c-xfD1c)*xintfx0c   ! constant of integration to
force s=0 at epsilon=0
!C
!        Sbar(I)=xE1*strain(I)
!     &       + xac/(xfD2c-xfD1c)*(xintfxc-xfD1c*strain(I))-xintconstc
!      END DO
C
```

```
C
C Calculate Sbar=lambda*(dPsi/dlambda)
C
      Do I=1,3
            if (strain(I) .le. 0.d0) then
                xD1c = -props(1)
                xD2c = -props(2)
            else
                xD1c = props(1)
                xD2c = props(2)
            endif

       xPm = (xE1 - xE2c)/(2.d0*(xD1c-xD2c))
       xQm =  xE1 - (xD1c*(xE1-xE2c))/(xD1c-xD2c)
       xRm =  xE1*xD1c - xPm*(xD1c**2.d0) - xQm*xD1c

          if(abs(strain(I))<=abs(xD1c)) then
               Sbar(I) = xE1*strain(I)
          elseif (abs(strain(I))<=abs(xD2c)) then
               Sbar(I) = xPm*(strain(I)**2.d0)+xQm*strain(I)+xRm
          else
               Sbar(I) = xE2c*(strain(I)-xD2c) +
     &              (xPm*xD2c**2.d0 + xQm*xD2c + xRm)
          endif

       ENDDO

       !    Calculate the stress coefficients B_a
       DO J=1,3
          B_a(J) = (Sbar(J) - ONE/THREE*(Sbar(1)+Sbar(2)+Sbar(3)))
       END DO
!
!    Calculate the eigenvector dyadic products (eigenvalue bases)
!
!    n11
       n11(1) = na(1,1)*na(1,1)
       n11(2) = na(2,1)*na(2,1)
       n11(3) = na(3,1)*na(3,1)
       n11(4) = na(1,1)*na(2,1)
       n11(5) = na(1,1)*na(3,1)
       n11(6) = na(2,1)*na(3,1)
!    n22
       n22(1) = na(1,2)*na(1,2)
       n22(2) = na(2,2)*na(2,2)
       n22(3) = na(3,2)*na(3,2)
       n22(4) = na(1,2)*na(2,2)
       n22(5) = na(1,2)*na(3,2)
       n22(6) = na(2,2)*na(3,2)
!    n33
       n33(1) = na(1,3)*na(1,3)
       n33(2) = na(2,3)*na(2,3)
       n33(3) = na(3,3)*na(3,3)
       n33(4) = na(1,3)*na(2,3)
       n33(5) = na(1,3)*na(3,3)
       n33(6) = na(2,3)*na(3,3)
!
       Do kk2=1,6
```

```
          kiso(kk2) = 0.d0
        ENDDO
C
        Do k1=1,NTENS
           kiso(k1) = (B_a(1)*n11(k1))+(B_a(2)*n22(k1))+(B_a(3)*n33(k1))
        ENDDO
C
          strainV = DET-ONE
          if (strainV .le. 0.d0) then
              xD1v = -props(6)
              xD2v = -props(7)
          else
              xD1v = props(6)
              xD2v = props(7)
          endif
C
          xPv = (xkappa1 - xkappa2)/(2.d0*(xD1v-xD2v))
          xQv = xkappa1 - (xD1v*(xkappa1-xkappa2))/(xD1v-xD2v)
          xRv = xkappa1*xD1v - xPv*(xD1v**2.d0) - xQv*xD1v
C
          if(abs(strainV)<=abs(xD1v))then
              COEFF3 = xkappa1*strainV
          elseif (abs(strainV)<=abs(xD2v))then
              COEFF3 = (xPv*(strainV**2.d0)+xQv*strainV+xRv)
          else
              COEFF3 = (xkappa2*(strainV-xD2v) +
     &           (xPv*xD2v**2.d0 + xQv*xD2v + xRv))
          endif
C
        !COEFF3 = BulkM*(DET-ONE)*DET
C
        DO J=1,3
            kiso(J)= kiso(J)+COEFF3
        ENDDO
C
        XKIRCH(1,1)=kiso(1)
        XKIRCH(2,2)=kiso(2)
        XKIRCH(3,3)=kiso(3)
        XKIRCH(1,2)=kiso(4)
        XKIRCH(1,3)=kiso(5)
        XKIRCH(2,3)=kiso(6)
        XKIRCH(2,1)=XKIRCH(1,2)
        XKIRCH(3,1)=XKIRCH(1,3)
        XKIRCH(3,2)=XKIRCH(2,3)
C
C-----------------------------------------------------------------------
C     Set up the fiber dispersion in the local coordinate system
C-----------------------------------------------------------------------
C
          phi_vec(1)=ZERO

          DO i=2,n_phi
              phi_vec(i)=phi_vec(i-1)+TWO*xpi/n_phi
          END DO
          omega_vec = ZERO

          DO ih=2,n_omega
```

```
            omega_vec(ih)=omega_vec(ih-1)+((XPI/TWO)/(n_omega-1))
          END DO
C
          xm0i(1,1) = ZERO
          xm0i(2,1) = ZERO
          xm0i(3,1) = ONE
C
          del_phi = phi_vec(2)-phi_vec(1)
          del_omega =((xpi/two)*(ONE/(n_omega-1)))
C
          xn0i_mat(1,1)=sin(omega_vec(1))*cos(phi_vec(1))
          xn0i_mat(1,2)=sin(omega_vec(1))*sin(phi_vec(1))
          xn0i_mat(1,3)=cos(omega_vec(1))
C
          area_1 = ((0.5d0*del_omega)**two)*xpi
C
          CALL kPDF3D1(xbb,xm0i,xm0i,xrho_1)
C
          rho_vec(1) = xrho_1
          area_vec(1) = area_1
          rho_mat(1,1:n_phi)=xrho_1
          count = 1
          area_tot = 0.d0
          DO ii = 2, n_omega
              DO jj = 1, n_phi

                  count = count + 1

                  xn0i(1,1) = sin(omega_vec(ii))*cos(phi_vec(jj))
                  xn0i(2,1) = sin(omega_vec(ii))*sin(phi_vec(jj))
                  xn0i(3,1) = cos(omega_vec(ii))

                  xn0i_mat(count,1) = xn0i(1,1)
                  xn0i_mat(count,2) = xn0i(2,1)
                  xn0i_mat(count,3) = xn0i(3,1)

                  if (ii<n_omega) then
                     area_seg = del_omega*sin(omega_vec(ii))*del_phi
                  else
                     area_seg = del_omega*sin(omega_vec(ii))*del_phi*0.5d0
                  endif

                  area_vec(count) = area_seg
                  area_tot = area_tot + area_seg

                  CALL kPDF3D1(xbb,xn0i,xm0i,xrho)

                  rho_vec(count) = xrho

                  rho_mat(ii,jj) = xrho

                  xrho_tot = xrho_tot + xrho*area_seg

             END DO
          END DO

          area_tot = area_tot + area_1
```

```
        xrho_tot = xrho_tot + xrho_1*area_1

        xrho_tot_norm = xrho_tot/area_tot
C
C-------------------------------------------------------------------------
----------------------------------
C     Rotate the fiber dispersion in the local coodinate system to the global
coordinate system
C-------------------------------------------------------------------------
----------------------------------
C
! Need to rotate M (the local mean fiber direction the distribution is
distributed around)
! so that it maps to A (the global mean fiber direction of the fiber family)
C
      !xA0i(1) = sin(xalphar1)*cos(xbetar1)
      !xA0i(2) = sin(xalphar1)*sin(xbetar1)
      !xA0i(3) = cos(xalphar1)
C
      DO I=1,3
      DO J=1,3
          XANISOTOT(I,J) = ZERO
      END DO
      END DO
C
C  LOOP OVER THE NO OF FIBRE FAMILIES
C
      DO IANISO = 1,NANISO
          rot_mat_E2(1,1) = cos(xalphar(IANISO))
          rot_mat_E2(1,2) = 0.d0
          rot_mat_E2(1,3) = sin(xalphar(IANISO))
          rot_mat_E2(2,1) = 0.d0
          rot_mat_E2(2,2) = 1.d0
          rot_mat_E2(2,3) = 0.d0
          rot_mat_E2(3,1) = -sin(xalphar(IANISO))
          rot_mat_E2(3,2) = 0.d0
          rot_mat_E2(3,3) = cos(xalphar(IANISO))
C
          rot_mat_E3(1,1) = cos(xbetar(IANISO))
          rot_mat_E3(1,2) = -sin(xbetar(IANISO))
          rot_mat_E3(1,3) = 0.d0
          rot_mat_E3(2,1) = sin(xbetar(IANISO))
          rot_mat_E3(2,2) = cos(xbetar(IANISO))
          rot_mat_E3(2,3) = 0.d0
          rot_mat_E3(3,1) = 0.d0
          rot_mat_E3(3,2) = 0.d0
          rot_mat_E3(3,3) = 1.d0
C
      call KMTMS (3, 3, 3, rot_mat_E3, rot_mat_E2, rot_mat)
C
           DO i=1,3
              xm0i_rot(i,1) = 0.d0
              DO m=1,3
                  xm0i_rot(i,1) = xm0i_rot(i,1)+rot_mat(i,m)*xm0i(m,1)
               END DO
          END DO
C
```

```
            !counter = 0
C
          DO kk=1,nseg
                xn0i_pre_rot(1,1) = xn0i_mat(kk,1)
                xn0i_pre_rot(2,1) = xn0i_mat(kk,2)
                xn0i_pre_rot(3,1) = xn0i_mat(kk,3)
C
            DO i=1,3
             xn0i_rot(i,1) = 0.d0
             DO m=1,3
           xn0i_rot(i,1) = xn0i_rot(i,1)+rot_mat(i,m)*xn0i_pre_rot(m,1)
             END DO
            END DO
C
C    Calculate the Anisotropic Stress
C
            !call KMTMS (3, 3, 1, DGRAD, xn0i_rot, xn1i)
C
            DO i=1,3
             xn1i(i,1) = 0.d0
             DO m=1,3
                 !Do k=1,3
             xn1i(i,1) = xn1i(i,1) + DGRAD(i,m)*xn0i_rot(m,1)
             !    END DO
             END DO
           END DO
C
            DO I=1,3
                DO J=1,3
                    aoa(I,J) = xn1i(I,1)*xn1i(J,1)
                END DO
            END DO

             XI_F = aoa(1,1) + aoa(2,2) + aoa(3,3)

             if (kk==1) then
                XI4(IANISO) = XI_F
             endif
C
C-----------------------------------------------------------------------
C      INSTATE THE TENSION CONDITION
C-----------------------------------------------------------------------
C
            IF(XI_F>ONE) THEN
C
C    ZERO MATRICES
C
                DO I=1,3
                DO J=1,3
                    xanisok(i,j) = zero
                END DO
                END DO
C
C    CALCULATE THE VARIOUS PARTS OF THE EQUATION FOR KIRCHSTRESS
C
                fibeps = sqrt(XI_F)-1.d0
```

```
                if(fibeps<=xD1f)then
                    XANISOK = xE1f*fibeps*aoa
                    nphase = 1
                elseif (fibeps<=xD2f)then
                    XANISOK = (xP*(fibeps**2.d0) + xQ*fibeps + xR)*aoa
                    nphase = 2
                else
                    XANISOK = (xE2f*(fibeps-xD2f) +
     &              (xP*xD2f**2.d0 + xQ*xD2f + xR))*aoa
                    nphase = 3
                endif
C
            XANISOTOT = XANISOTOT +
     &         (1.d0/xrho_tot)*XANISOK*rho_vec(kk)*area_vec(kk)

      END IF
C
      END DO
C
      END DO
C
C
       XKIRCH = XKIRCH + XANISOTOT
C
CCCCC  non-equilibrium (viscoelastic) Stress


      return
      end subroutine kstress_calc

C-----------------------------------------------------------------------------
-

      subroutine kdelF(m, n, DGRAD, eps, DF)

      INCLUDE 'ABA_PARAM.INC'

      intent (in) :: DGRAD, eps, m, n
      intent (out):: DF

C Input: the index's i & j; The current deformation gradient (DGRAD). The
perturbation
C        increment (eps)
C
C Output: The perturbed increment DF
C
      dimension dyad1(3,3), dyad2(3,3), DGRAD(3,3), DF(3,3), DFp1(3,3)

c Zero the dyad matrices
c
      do i = 1,3
        do j = 1,3
            dyad1(i,j) = zero
            dyad2(i,j) = zero
        end do
      end do
```

```
c Place the 1's in the correct location
      dyad1(m,n) = 1.0
c
      dyad2(n,m) = 1.0
c
c      KMTMS (M, N, L, A, KA, B, KB, C, KC)
      !call KMTMS(3, 3, 3, dyad1, 3, DGRAD, 3, DFp1, 3)
      call KMTMS (3, 3, 3,dyad1, DGRAD, DFp1)
      DF = DFp1


      !call KMTMS(3, 3, 3, dyad2, 3, DGRAD, 3, DFp1, 3)
      call KMTMS (3, 3, 3, dyad2,DGRAD, DFp1)
      DF = DF + DFp1


      DF = 0.5*DF*eps

      end subroutine kdelF


c--------------------------------------------------------------------------
-

      subroutine kprinter(tens, m, n)

      INCLUDE 'ABA_PARAM.INC'

      intent(in):: tens, m, n

      dimension tens(m,n)

        write(6,*)
        do i = 1,m
        do j = 1,n
            write(6,'(e19.9)',advance='no'),tens(i,j)
        end do
        write(6,*)
        end do
        write(6,*)
      return
      end subroutine kprinter

c--------------------------------------------------------------------------
--
!
!      SUBROUTINE KMTMS (M, N, L, A, KA, B, KB, C, KC)
!      INCLUDE 'ABA_PARAM.INC'
!C
!      intent(in) :: M, N, L, A, KA, B, KB, KC
!      intent(out):: C
!C
!C
!C     PRODUCT OF REAL MATRICES
!C
!      DIMENSION A(KA,N), B(KB,L), C(KC,L)
!      DOUBLE PRECISION W
```

```
!C
!C
!      DO 30 J = 1,L
!         DO 20 I = 1,M
!            W = 0.D0
!            DO 10 K = 1,N
!               W = W + A(I,K) * B(K,J)
!   10       CONTINUE
!            C(I,J) = W
!   20    CONTINUE
!   30 CONTINUE
!      RETURN
!      END SUBROUTINE
!
c-------------------------------------------------------------------------------
--

      SUBROUTINE KMTMS (M, N, L, A, B, C)
      INCLUDE 'ABA_PARAM.INC'
C
      intent(in) :: M, N, L, A, B
      intent(out):: C
C
C
C     PRODUCT OF REAL MATRICES
C
      DIMENSION A(M,N), B(N,L), C(M,L)
      DOUBLE PRECISION W
C
C
      DO 30 I = 1,M
         DO 20 J = 1,L
            W = 0.D0
            DO 10 K = 1,N
               W = W + A(I,K) * B(K,J)
   10       CONTINUE
            C(I,J) = W
   20    CONTINUE
   30 CONTINUE
      RETURN
      END SUBROUTINE
c-------------------------------------------------------------------------


      subroutine kmatrix2vector(XMAT, VEC, NTENS)

      INCLUDE 'ABA_PARAM.INC'

      intent(in) :: XMAT, NTENS
      intent(out):: VEC

      dimension xmat(3,3), vec(NTENS)

        do i=1,3
            vec(i) = xmat(i,i)
        end do
```

```
        IF (NTENS==4) then
            vec(4) = xmat(1,2)
        ELSEIF (NTENS==6) then
            vec(4) = xmat(1,2)      !updated on Jan 2021!
            vec(5) = xmat(1,3)
            vec(6) = xmat(2,3)
        END IF

      end subroutine kmatrix2vector

C-----------------------------------------------------------------------

      subroutine kdotprod(A, B, dotp, n)

      INCLUDE 'ABA_PARAM.INC'

      intent(in) :: A, B, n
      intent(out):: dotp

      dimension A(n), B(n)
      dotp = 0.0

      do i = 1,n
        dotp = dotp + A(i)*B(i)
      end do

      end subroutine kdotprod
C
C-----------------------------------------------------------------------
C
      SUBROUTINE kPDF3D1(xbb,xn,xm,xrho)

      INCLUDE 'ABA_PARAM.INC'

      intent(in) :: xbb, xn, xm
      intent(out):: xrho
      dimension xn(3,1), xm(3,1)
      REAL  xpar
      XPI = 3.14159265359d0

      xpar = sqrt(2.d0*xbb)
      CALL kerfi1(xpar, xerr)

      xNdotM = xn(1,1)*xm(1,1)+xn(2,1)*xm(2,1)+xn(3,1)*xm(3,1)
      xq1 = 4.d0*(sqrt(xbb/(2.d0*xpi)))
      xq2 = (2.d0*xbb*(xNdotM**2.d0))
      xq3 = exp(xq2)
      xrho = xq1*xq3/xerr

      return
      end subroutine kPDF3D1
C
C-----------------------------------------------------------------------
C
      subroutine kerfi1(x, xerr1)
      INCLUDE 'ABA_PARAM.INC'
      INTEGER NMAX
```

```
      PARAMETER (NMAX=6,H=0.4d0,A1=2.d0/3.d0,A2=0.4d0,A3=2.d0/7.d0)

      INTEGER i,init,n0
      REAL d1,d2,e1,e2,sum,x2,xp,xx,c(NMAX),x
      SAVE init,c
      DATA init/0/

      if(init.eq.0)then
         init=1
         do i=1,NMAX
            c(i)=exp(-((2.d0*float(i)-1.d0)*H)**2.d0)
         enddo
      endif

      if (abs(x).lt.0.2) then
         x2=x**2.d0
         dawson=x*(1.d0-A1*x2*(1.d0-A2*x2*(1.d0-A3*x2)))
      else
         xx=abs(x)
         n0=2*nint(0.5*xx/H)
         xp=xx-float(n0)*H
         e1=exp(2.d0*xp*H)
         e2=e1**2.d0
         d1=float(n0+1)
         d2=d1-2.d0
         sum=0.d0
         do i=1,NMAX
            sum=sum+c(i)*(e1/d1+1.d0/(d2*e1))
            d1=d1+2.d0
            d2=d2-2.d0
            e1=e2*e1
         enddo

         dawson=0.5641895835*sign(exp(-xp**2.d0),x)*sum
      endif

      xerr1 = (2.d0/sqrt(XPI))*exp(x**2.d0)*dawson

      return
      END subroutine kerfi1

 !*********************************************************************
* ---------------------------------------------------------------------
-
* Numerical diagonalization of 3x3 matrcies
* Copyright (C) 2006  Joachim Kopp
* ---------------------------------------------------------------------
-
* This library is free software; you can redistribute it and/or
* modify it under the terms of the GNU Lesser General Public
* License as published by the Free Software Foundation; either
* version 2.1 of the License, or (at your option) any later version.
*
* This library is distributed in the hope that it will be useful,
* but WITHOUT ANY WARRANTY; without even the implied warranty of
* MERCHANTABILITY or FITNESS FOR A PARTICULAR PURPOSE.  See the GNU
```

```
* Lesser General Public License for more details.
*
* You should have received a copy of the GNU Lesser General Public
* License along with this library; if not, write to the Free Software
* Foundation, Inc., 51 Franklin Street, Fifth Floor, Boston, MA 02110-1301
USA
* ------------------------------------------------------------------------
-
      SUBROUTINE kDSYEVJ3(A, Q, W)
* ------------------------------------------------------------------------
-
* Calculates the eigenvalues and normalized eigenvectors of a symmetric 3x3
* matrix A using the Jacobi algorithm.
* The upper triangular part of A is destroyed during the calculation,
* the diagonal elements are read but not destroyed, and the lower
* triangular elements are not referenced at all.
* ------------------------------------------------------------------------
-
* Parameters:
*   A: The symmetric input matrix
*   Q: Storage buffer for eigenvectors
*   W: Storage buffer for eigenvalues
* ------------------------------------------------------------------------
-
*     .. Arguments ..
      DOUBLE PRECISION A(3,3)
      DOUBLE PRECISION Q(3,3)
      DOUBLE PRECISION W(3)

*     .. Parameters ..
      INTEGER          N
      PARAMETER        ( N = 3 )

*     .. Local Variables ..
      DOUBLE PRECISION SD, SO
      DOUBLE PRECISION S, C, T
      DOUBLE PRECISION G, H, Z, THETA
      DOUBLE PRECISION THRESH
      INTEGER          I, X, Y, R

*     Initialize Q to the identitity matrix
*     --- This loop can be omitted if only the eigenvalues are desired ---
      DO 10 X = 1, N
        Q(X,X) = 1.0D0
        DO 11, Y = 1, X-1
          Q(X, Y) = 0.0D0
          Q(Y, X) = 0.0D0
   11   CONTINUE
   10 CONTINUE

*     Initialize W to diag(A)
      DO 20 X = 1, N
        W(X) = A(X, X)
   20 CONTINUE

*     Calculate SQR(tr(A))
      SD = 0.0D0
```

```
      DO 30 X = 1, N
        SD = SD + ABS(W(X))
   30 CONTINUE
      SD = SD**2

*     Main iteration loop
      DO 40 I = 1, 50
*       Test for convergence
        SO = 0.0D0
        DO 50 X = 1, N
          DO 51 Y = X+1, N
            SO = SO + ABS(A(X, Y))
   51     CONTINUE
   50   CONTINUE
        IF (SO .EQ. 0.0D0) THEN
          RETURN
        END IF

        IF (I .LT. 4) THEN
          THRESH = 0.2D0 * SO / N**2
        ELSE
          THRESH = 0.0D0
        END IF

*       Do sweep
        DO 60 X = 1, N
          DO 61 Y = X+1, N
            G = 100.0D0 * ( ABS(A(X, Y)) )
            IF ( I .GT. 4 .AND. ABS(W(X)) + G .EQ. ABS(W(X))
     $                    .AND. ABS(W(Y)) + G .EQ. ABS(W(Y)) ) THEN
              A(X, Y) = 0.0D0
            ELSE IF (ABS(A(X, Y)) .GT. THRESH) THEN
*             Calculate Jacobi transformation
              H = W(Y) - W(X)
              IF ( ABS(H) + G .EQ. ABS(H) ) THEN
                T = A(X, Y) / H
              ELSE
                THETA = 0.5D0 * H / A(X, Y)
                IF (THETA .LT. 0.0D0) THEN
                  T = -1.0D0 / (SQRT(1.0D0 + THETA**2) - THETA)
                ELSE
                  T = 1.0D0 / (SQRT(1.0D0 + THETA**2) + THETA)
                END IF
              END IF

              C = 1.0D0 / SQRT( 1.0D0 + T**2 )
              S = T * C
              Z = T * A(X, Y)

*             Apply Jacobi transformation
              A(X, Y) = 0.0D0
              W(X)    = W(X) - Z
              W(Y)    = W(Y) + Z
              DO 70 R = 1, X-1
                T       = A(R, X)
                A(R, X) = C * T - S * A(R, Y)
                A(R, Y) = S * T + C * A(R, Y)
```

```
   70         CONTINUE
              DO 80, R = X+1, Y-1
                T       = A(X, R)
                A(X, R) = C * T - S * A(R, Y)
                A(R, Y) = S * T + C * A(R, Y)
   80         CONTINUE
              DO 90, R = Y+1, N
                T       = A(X, R)
                A(X, R) = C * T - S * A(Y, R)
                A(Y, R) = S * T + C * A(Y, R)
   90         CONTINUE

*             Update eigenvectors
*             --- This loop can be omitted if only the eigenvalues are
desired ---
              DO 100, R = 1, N
                T       = Q(R, X)
                Q(R, X) = C * T - S * Q(R, Y)
                Q(R, Y) = S * T + C * Q(R, Y)
  100         CONTINUE
            END IF
   61     CONTINUE
   60   CONTINUE
   40 CONTINUE

      PRINT *, "kDSYEVJ3: No convergence."

      END SUBROUTINE
* End of subroutine kDSYEVJ3
* ------------------------------------------------------------------------
-

      END
```

C. The input file for the clot tensile simulation

```
*Heading
** Job name: umat33643 Model name: Clot_Tension_hole_newmodel_33643
** Generated by: Abaqus/CAE 2020
*Preprint, echo=NO, model=NO, history=NO, contact=NO
**
** PARTS
**
*Part, name=Clot
*Node
** For the mesh and node settings, set the approximate global size to be
0.085 in Sizing control section in global seeds, the detail codes will not be
shown in this appendix

*Element, type=C3D8
** For the mesh and node settings, set the approximate global size to be
0.085 in Sizing control section in global seeds, the detail codes will not be
shown in this appendix
*Nset, nset=Clot, generate
     1,  37260,      1
*Elset, elset=Clot, generate
     1,  33643,      1
** Section: usermodel
*Solid Section, elset=Clot, material=Material-1
,
*End Part
**
**
** ASSEMBLY
**
*Assembly, name=Assembly
**
*Instance, name=Clot-1, part=Clot
*End Instance
**
*Nset, nset=Bottom, instance=Clot-1
     8,     9,    11,   179,   180,   181,   182,   183,   184,   185,   186,
187,   188,   189,   190,   191
   192,   193,   194,   195,   243,   244,   245,   246,   247,   248,   249,
250,   251,   252,   253,   254
   255,   256,   257,   258,   259,   260,   261,   262,   263,   264,   265,
266,  2078,  2079,  2081,  2249
  2250,  2251,  2252,  2253,  2254,  2255,  2256,  2257,  2258,  2259,  2260,
2261,  2262,  2263,  2264,  2265
  2313,  2314,  2315,  2316,  2317,  2318,  2319,  2320,  2321,  2322,  2323,
2324,  2325,  2326,  2327,  2328
  2329,  2330,  2331,  2332,  2333,  2334,  2335,  2336,  4148,  4149,  4151,
4319,  4320,  4321,  4322,  4323
  4324,  4325,  4326,  4327,  4328,  4329,  4330,  4331,  4332,  4333,  4334,
4335,  4383,  4384,  4385,  4386
  4387,  4388,  4389,  4390,  4391,  4392,  4393,  4394,  4395,  4396,  4397,
4398,  4399,  4400,  4401,  4402
  4403,  4404,  4405,  4406,  6218,  6219,  6221,  6389,  6390,  6391,  6392,
6393,  6394,  6395,  6396,  6397
  6398,  6399,  6400,  6401,  6402,  6403,  6404,  6405,  6453,  6454,  6455,
6456,  6457,  6458,  6459,  6460
```

6461, 6462, 6463, 6464, 6465, 6466, 6467, 6468, 6469, 6470, 6471,
6472, 6473, 6474, 6475, 6476
8288, 8289, 8291, 8459, 8460, 8461, 8462, 8463, 8464, 8465, 8466,
8467, 8468, 8469, 8470, 8471
8472, 8473, 8474, 8475, 8523, 8524, 8525, 8526, 8527, 8528, 8529,
8530, 8531, 8532, 8533, 8534
8535, 8536, 8537, 8538, 8539, 8540, 8541, 8542, 8543, 8544, 8545,
8546, 10358, 10359, 10361, 10529
10530, 10531, 10532, 10533, 10534, 10535, 10536, 10537, 10538, 10539, 10540,
10541, 10542, 10543, 10544, 10545
10593, 10594, 10595, 10596, 10597, 10598, 10599, 10600, 10601, 10602, 10603,
10604, 10605, 10606, 10607, 10608
10609, 10610, 10611, 10612, 10613, 10614, 10615, 10616, 12428, 12429, 12431,
12599, 12600, 12601, 12602, 12603
12604, 12605, 12606, 12607, 12608, 12609, 12610, 12611, 12612, 12613, 12614,
12615, 12663, 12664, 12665, 12666
12667, 12668, 12669, 12670, 12671, 12672, 12673, 12674, 12675, 12676, 12677,
12678, 12679, 12680, 12681, 12682
12683, 12684, 12685, 12686, 14498, 14499, 14501, 14669, 14670, 14671, 14672,
14673, 14674, 14675, 14676, 14677
14678, 14679, 14680, 14681, 14682, 14683, 14684, 14685, 14733, 14734, 14735,
14736, 14737, 14738, 14739, 14740
14741, 14742, 14743, 14744, 14745, 14746, 14747, 14748, 14749, 14750, 14751,
14752, 14753, 14754, 14755, 14756
16568, 16569, 16571, 16739, 16740, 16741, 16742, 16743, 16744, 16745, 16746,
16747, 16748, 16749, 16750, 16751
16752, 16753, 16754, 16755, 16803, 16804, 16805, 16806, 16807, 16808, 16809,
16810, 16811, 16812, 16813, 16814
16815, 16816, 16817, 16818, 16819, 16820, 16821, 16822, 16823, 16824, 16825,
16826, 18638, 18639, 18641, 18809
18810, 18811, 18812, 18813, 18814, 18815, 18816, 18817, 18818, 18819, 18820,
18821, 18822, 18823, 18824, 18825
18873, 18874, 18875, 18876, 18877, 18878, 18879, 18880, 18881, 18882, 18883,
18884, 18885, 18886, 18887, 18888
18889, 18890, 18891, 18892, 18893, 18894, 18895, 18896, 20708, 20709, 20711,
20879, 20880, 20881, 20882, 20883
20884, 20885, 20886, 20887, 20888, 20889, 20890, 20891, 20892, 20893, 20894,
20895, 20943, 20944, 20945, 20946
20947, 20948, 20949, 20950, 20951, 20952, 20953, 20954, 20955, 20956, 20957,
20958, 20959, 20960, 20961, 20962
20963, 20964, 20965, 20966, 22778, 22779, 22781, 22949, 22950, 22951, 22952,
22953, 22954, 22955, 22956, 22957
22958, 22959, 22960, 22961, 22962, 22963, 22964, 22965, 23013, 23014, 23015,
23016, 23017, 23018, 23019, 23020
23021, 23022, 23023, 23024, 23025, 23026, 23027, 23028, 23029, 23030, 23031,
23032, 23033, 23034, 23035, 23036
24848, 24849, 24851, 25019, 25020, 25021, 25022, 25023, 25024, 25025, 25026,
25027, 25028, 25029, 25030, 25031
25032, 25033, 25034, 25035, 25083, 25084, 25085, 25086, 25087, 25088, 25089,
25090, 25091, 25092, 25093, 25094
25095, 25096, 25097, 25098, 25099, 25100, 25101, 25102, 25103, 25104, 25105,
25106, 26918, 26919, 26921, 27089
27090, 27091, 27092, 27093, 27094, 27095, 27096, 27097, 27098, 27099, 27100,
27101, 27102, 27103, 27104, 27105
27153, 27154, 27155, 27156, 27157, 27158, 27159, 27160, 27161, 27162, 27163,
27164, 27165, 27166, 27167, 27168

```
 27169, 27170, 27171, 27172, 27173, 27174, 27175, 27176, 28988, 28989, 28991,
29159, 29160, 29161, 29162, 29163
 29164, 29165, 29166, 29167, 29168, 29169, 29170, 29171, 29172, 29173, 29174,
29175, 29223, 29224, 29225, 29226
 29227, 29228, 29229, 29230, 29231, 29232, 29233, 29234, 29235, 29236, 29237,
29238, 29239, 29240, 29241, 29242
 29243, 29244, 29245, 29246, 31058, 31059, 31061, 31229, 31230, 31231, 31232,
31233, 31234, 31235, 31236, 31237
 31238, 31239, 31240, 31241, 31242, 31243, 31244, 31245, 31293, 31294, 31295,
31296, 31297, 31298, 31299, 31300
 31301, 31302, 31303, 31304, 31305, 31306, 31307, 31308, 31309, 31310, 31311,
31312, 31313, 31314, 31315, 31316
 33128, 33129, 33131, 33299, 33300, 33301, 33302, 33303, 33304, 33305, 33306,
33307, 33308, 33309, 33310, 33311
 33312, 33313, 33314, 33315, 33363, 33364, 33365, 33366, 33367, 33368, 33369,
33370, 33371, 33372, 33373, 33374
 33375, 33376, 33377, 33378, 33379, 33380, 33381, 33382, 33383, 33384, 33385,
33386, 35198, 35199, 35201, 35369
 35370, 35371, 35372, 35373, 35374, 35375, 35376, 35377, 35378, 35379, 35380,
35381, 35382, 35383, 35384, 35385
 35433, 35434, 35435, 35436, 35437, 35438, 35439, 35440, 35441, 35442, 35443,
35444, 35445, 35446, 35447, 35448
 35449, 35450, 35451, 35452, 35453, 35454, 35455, 35456
*Elset, elset=Bottom, instance=Clot-1
    929,   954,   979,  1004,  1029,  1054,  1079,  1104,  1129,  1154,  1179,
1204,  1229,  1254,  1279,  1304
   1329,  1354,  1355,  1380,  1405,  1430,  1455,  1480,  1505,  1530,  1555,
1580,  1605,  1630,  1655,  1680
   1705,  1730,  1755,  1780,  1805,  1830,  1855,  1880,  1905,  1930,  1955,
2908,  2933,  2958,  2983,  3008
   3033,  3058,  3083,  3108,  3133,  3158,  3183,  3208,  3233,  3258,  3283,
3308,  3333,  3334,  3359,  3384
   3409,  3434,  3459,  3484,  3509,  3534,  3559,  3584,  3609,  3634,  3659,
3684,  3709,  3734,  3759,  3784
   3809,  3834,  3859,  3884,  3909,  3934,  4887,  4912,  4937,  4962,  4987,
5012,  5037,  5062,  5087,  5112
   5137,  5162,  5187,  5212,  5237,  5262,  5287,  5312,  5313,  5338,  5363,
5388,  5413,  5438,  5463,  5488
   5513,  5538,  5563,  5588,  5613,  5638,  5663,  5688,  5713,  5738,  5763,
5788,  5813,  5838,  5863,  5888
   5913,  6866,  6891,  6916,  6941,  6966,  6991,  7016,  7041,  7066,  7091,
7116,  7141,  7166,  7191,  7216
   7241,  7266,  7291,  7292,  7317,  7342,  7367,  7392,  7417,  7442,  7467,
7492,  7517,  7542,  7567,  7592
   7617,  7642,  7667,  7692,  7717,  7742,  7767,  7792,  7817,  7842,  7867,
7892,  8845,  8870,  8895,  8920
   8945,  8970,  8995,  9020,  9045,  9070,  9095,  9120,  9145,  9170,  9195,
9220,  9245,  9270,  9271,  9296
   9321,  9346,  9371,  9396,  9421,  9446,  9471,  9496,  9521,  9546,  9571,
9596,  9621,  9646,  9671,  9696
   9721,  9746,  9771,  9796,  9821,  9846,  9871, 10824, 10849, 10874, 10899,
10924, 10949, 10974, 10999, 11024
 11049, 11074, 11099, 11124, 11149, 11174, 11199, 11224, 11249, 11250, 11275,
11300, 11325, 11350, 11375, 11400
 11425, 11450, 11475, 11500, 11525, 11550, 11575, 11600, 11625, 11650, 11675,
11700, 11725, 11750, 11775, 11800
```

11825, 11850, 12803, 12828, 12853, 12878, 12903, 12928, 12953, 12978, 13003, 13028, 13053, 13078, 13103, 13128
13153, 13178, 13203, 13228, 13229, 13254, 13279, 13304, 13329, 13354, 13379, 13404, 13429, 13454, 13479, 13504
13529, 13554, 13579, 13604, 13629, 13654, 13679, 13704, 13729, 13754, 13779, 13804, 13829, 14782, 14807, 14832
14857, 14882, 14907, 14932, 14957, 14982, 15007, 15032, 15057, 15082, 15107, 15132, 15157, 15182, 15207, 15208
15233, 15258, 15283, 15308, 15333, 15358, 15383, 15408, 15433, 15458, 15483, 15508, 15533, 15558, 15583, 15608
15633, 15658, 15683, 15708, 15733, 15758, 15783, 15808, 16761, 16786, 16811, 16836, 16861, 16886, 16911, 16936
16961, 16986, 17011, 17036, 17061, 17086, 17111, 17136, 17161, 17186, 17187, 17212, 17237, 17262, 17287, 17312
17337, 17362, 17387, 17412, 17437, 17462, 17487, 17512, 17537, 17562, 17587, 17612, 17637, 17662, 17687, 17712
17737, 17762, 17787, 18740, 18765, 18790, 18815, 18840, 18865, 18890, 18915, 18940, 18965, 18990, 19015, 19040
19065, 19090, 19115, 19140, 19165, 19166, 19191, 19216, 19241, 19266, 19291, 19316, 19341, 19366, 19391, 19416
19441, 19466, 19491, 19516, 19541, 19566, 19591, 19616, 19641, 19666, 19691, 19716, 19741, 19766, 20719, 20744
20769, 20794, 20819, 20844, 20869, 20894, 20919, 20944, 20969, 20994, 21019, 21044, 21069, 21094, 21119, 21144
21145, 21170, 21195, 21220, 21245, 21270, 21295, 21320, 21345, 21370, 21395, 21420, 21445, 21470, 21495, 21520
21545, 21570, 21595, 21620, 21645, 21670, 21695, 21720, 21745, 22698, 22723, 22748, 22773, 22798, 22823, 22848
22873, 22898, 22923, 22948, 22973, 22998, 23023, 23048, 23073, 23098, 23123, 23124, 23149, 23174, 23199, 23224
23249, 23274, 23299, 23324, 23349, 23374, 23399, 23424, 23449, 23474, 23499, 23524, 23549, 23574, 23599, 23624
23649, 23674, 23699, 23724, 24677, 24702, 24727, 24752, 24777, 24802, 24827, 24852, 24877, 24902, 24927, 24952
24977, 25002, 25027, 25052, 25077, 25102, 25103, 25128, 25153, 25178, 25203, 25228, 25253, 25278, 25303, 25328
25353, 25378, 25403, 25428, 25453, 25478, 25503, 25528, 25553, 25578, 25603, 25628, 25653, 25678, 25703, 26656
26681, 26706, 26731, 26756, 26781, 26806, 26831, 26856, 26881, 26906, 26931, 26956, 26981, 27006, 27031, 27056
27081, 27082, 27107, 27132, 27157, 27182, 27207, 27232, 27257, 27282, 27307, 27332, 27357, 27382, 27407, 27432
27457, 27482, 27507, 27532, 27557, 27582, 27607, 27632, 27657, 27682, 28635, 28660, 28685, 28710, 28735, 28760
28785, 28810, 28835, 28860, 28885, 28910, 28935, 28960, 28985, 29010, 29035, 29060, 29061, 29086, 29111, 29136
29161, 29186, 29211, 29236, 29261, 29286, 29311, 29336, 29361, 29386, 29411, 29436, 29461, 29486, 29511, 29536
29561, 29586, 29611, 29636, 29661, 30614, 30639, 30664, 30689, 30714, 30739, 30764, 30789, 30814, 30839, 30864
30889, 30914, 30939, 30964, 30989, 31014, 31039, 31040, 31065, 31090, 31115, 31140, 31165, 31190, 31215, 31240
31265, 31290, 31315, 31340, 31365, 31390, 31415, 31440, 31465, 31490, 31515, 31540, 31565, 31590, 31615, 31640
32593, 32618, 32643, 32668, 32693, 32718, 32743, 32768, 32793, 32818, 32843, 32868, 32893, 32918, 32943, 32968

```
 32993, 33018, 33019, 33044, 33069, 33094, 33119, 33144, 33169, 33194, 33219,
33244, 33269, 33294, 33319, 33344
 33369, 33394, 33419, 33444, 33469, 33494, 33519, 33544, 33569, 33594, 33619
*Nset, nset=Clot, instance=Clot-1, generate
     1,  37260,      1
*Elset, elset=Clot, instance=Clot-1, generate
     1,  33643,      1
*Nset, nset=MiddlePlane, instance=Clot-1
     5,     6,    10,    11,   134,   135,   136,   137,   138,   139,   140,
141,   142,   143,   144,   145
   146,   220,   221,   222,   223,   224,   225,   226,   227,   228,   229,
230,   231,   232,   233,   234
   235,   236,  2075,  2076,  2080,  2081,  2204,  2205,  2206,  2207,  2208,
2209,  2210,  2211,  2212,  2213
  2214,  2215,  2216,  2290,  2291,  2292,  2293,  2294,  2295,  2296,  2297,
2298,  2299,  2300,  2301,  2302
  2303,  2304,  2305,  2306,  4145,  4146,  4150,  4151,  4274,  4275,  4276,
4277,  4278,  4279,  4280,  4281
  4282,  4283,  4284,  4285,  4286,  4360,  4361,  4362,  4363,  4364,  4365,
4366,  4367,  4368,  4369,  4370
  4371,  4372,  4373,  4374,  4375,  4376,  6215,  6216,  6220,  6221,  6344,
6345,  6346,  6347,  6348,  6349
  6350,  6351,  6352,  6353,  6354,  6355,  6356,  6430,  6431,  6432,  6433,
6434,  6435,  6436,  6437,  6438
  6439,  6440,  6441,  6442,  6443,  6444,  6445,  6446,  8285,  8286,  8290,
8291,  8414,  8415,  8416,  8417
  8418,  8419,  8420,  8421,  8422,  8423,  8424,  8425,  8426,  8500,  8501,
8502,  8503,  8504,  8505,  8506
  8507,  8508,  8509,  8510,  8511,  8512,  8513,  8514,  8515,  8516, 10355,
10356, 10360, 10361, 10484, 10485
 10486, 10487, 10488, 10489, 10490, 10491, 10492, 10493, 10494, 10495, 10496,
10570, 10571, 10572, 10573, 10574
 10575, 10576, 10577, 10578, 10579, 10580, 10581, 10582, 10583, 10584, 10585,
10586, 12425, 12426, 12430, 12431
 12554, 12555, 12556, 12557, 12558, 12559, 12560, 12561, 12562, 12563, 12564,
12565, 12566, 12640, 12641, 12642
 12643, 12644, 12645, 12646, 12647, 12648, 12649, 12650, 12651, 12652, 12653,
12654, 12655, 12656, 14495, 14496
 14500, 14501, 14624, 14625, 14626, 14627, 14628, 14629, 14630, 14631, 14632,
14633, 14634, 14635, 14636, 14710
 14711, 14712, 14713, 14714, 14715, 14716, 14717, 14718, 14719, 14720, 14721,
14722, 14723, 14724, 14725, 14726
 16565, 16566, 16570, 16571, 16694, 16695, 16696, 16697, 16698, 16699, 16700,
16701, 16702, 16703, 16704, 16705
 16706, 16780, 16781, 16782, 16783, 16784, 16785, 16786, 16787, 16788, 16789,
16790, 16791, 16792, 16793, 16794
 16795, 16796, 18635, 18636, 18640, 18641, 18764, 18765, 18766, 18767, 18768,
18769, 18770, 18771, 18772, 18773
 18774, 18775, 18776, 18850, 18851, 18852, 18853, 18854, 18855, 18856, 18857,
18858, 18859, 18860, 18861, 18862
 18863, 18864, 18865, 18866, 20705, 20706, 20710, 20711, 20834, 20835, 20836,
20837, 20838, 20839, 20840, 20841
 20842, 20843, 20844, 20845, 20846, 20920, 20921, 20922, 20923, 20924, 20925,
20926, 20927, 20928, 20929, 20930
 20931, 20932, 20933, 20934, 20935, 20936, 22775, 22776, 22780, 22781, 22904,
22905, 22906, 22907, 22908, 22909
```

22910, 22911, 22912, 22913, 22914, 22915, 22916, 22990, 22991, 22992, 22993,
22994, 22995, 22996, 22997, 22998
22999, 23000, 23001, 23002, 23003, 23004, 23005, 23006, 24845, 24846, 24850,
24851, 24974, 24975, 24976, 24977
24978, 24979, 24980, 24981, 24982, 24983, 24984, 24985, 24986, 25060, 25061,
25062, 25063, 25064, 25065, 25066
25067, 25068, 25069, 25070, 25071, 25072, 25073, 25074, 25075, 25076, 26915,
26916, 26920, 26921, 27044, 27045
27046, 27047, 27048, 27049, 27050, 27051, 27052, 27053, 27054, 27055, 27056,
27130, 27131, 27132, 27133, 27134
27135, 27136, 27137, 27138, 27139, 27140, 27141, 27142, 27143, 27144, 27145,
27146, 28985, 28986, 28990, 28991
29114, 29115, 29116, 29117, 29118, 29119, 29120, 29121, 29122, 29123, 29124,
29125, 29126, 29200, 29201, 29202
29203, 29204, 29205, 29206, 29207, 29208, 29209, 29210, 29211, 29212, 29213,
29214, 29215, 29216, 31055, 31056
31060, 31061, 31184, 31185, 31186, 31187, 31188, 31189, 31190, 31191, 31192,
31193, 31194, 31195, 31196, 31270
31271, 31272, 31273, 31274, 31275, 31276, 31277, 31278, 31279, 31280, 31281,
31282, 31283, 31284, 31285, 31286
33125, 33126, 33130, 33131, 33254, 33255, 33256, 33257, 33258, 33259, 33260,
33261, 33262, 33263, 33264, 33265
33266, 33340, 33341, 33342, 33343, 33344, 33345, 33346, 33347, 33348, 33349,
33350, 33351, 33352, 33353, 33354
33355, 33356, 35195, 35196, 35200, 35201, 35324, 35325, 35326, 35327, 35328,
35329, 35330, 35331, 35332, 35333
35334, 35335, 35336, 35410, 35411, 35412, 35413, 35414, 35415, 35416, 35417,
35418, 35419, 35420, 35421, 35422
35423, 35424, 35425, 35426
*Elset, elset=MiddlePlane, instance=Clot-1
  883, 884, 885, 886, 887, 888, 889, 890, 891, 892, 893,
894, 895, 896, 1955, 1956
 1957, 1958, 1959, 1960, 1961, 1962, 1963, 1964, 1965, 1966, 1967,
1968, 1969, 1970, 1971, 1972
 2862, 2863, 2864, 2865, 2866, 2867, 2868, 2869, 2870, 2871, 2872,
2873, 2874, 2875, 3934, 3935
 3936, 3937, 3938, 3939, 3940, 3941, 3942, 3943, 3944, 3945, 3946,
3947, 3948, 3949, 3950, 3951
 4841, 4842, 4843, 4844, 4845, 4846, 4847, 4848, 4849, 4850, 4851,
4852, 4853, 4854, 5913, 5914
 5915, 5916, 5917, 5918, 5919, 5920, 5921, 5922, 5923, 5924, 5925,
5926, 5927, 5928, 5929, 5930
 6820, 6821, 6822, 6823, 6824, 6825, 6826, 6827, 6828, 6829, 6830,
6831, 6832, 6833, 7892, 7893
 7894, 7895, 7896, 7897, 7898, 7899, 7900, 7901, 7902, 7903, 7904,
7905, 7906, 7907, 7908, 7909
 8799, 8800, 8801, 8802, 8803, 8804, 8805, 8806, 8807, 8808, 8809,
8810, 8811, 8812, 9871, 9872
 9873, 9874, 9875, 9876, 9877, 9878, 9879, 9880, 9881, 9882, 9883,
9884, 9885, 9886, 9887, 9888
10778, 10779, 10780, 10781, 10782, 10783, 10784, 10785, 10786, 10787, 10788,
10789, 10790, 10791, 11850, 11851
11852, 11853, 11854, 11855, 11856, 11857, 11858, 11859, 11860, 11861, 11862,
11863, 11864, 11865, 11866, 11867
12757, 12758, 12759, 12760, 12761, 12762, 12763, 12764, 12765, 12766, 12767,
12768, 12769, 12770, 13829, 13830

13831, 13832, 13833, 13834, 13835, 13836, 13837, 13838, 13839, 13840, 13841,
13842, 13843, 13844, 13845, 13846
14736, 14737, 14738, 14739, 14740, 14741, 14742, 14743, 14744, 14745, 14746,
14747, 14748, 14749, 15808, 15809
15810, 15811, 15812, 15813, 15814, 15815, 15816, 15817, 15818, 15819, 15820,
15821, 15822, 15823, 15824, 15825
16715, 16716, 16717, 16718, 16719, 16720, 16721, 16722, 16723, 16724, 16725,
16726, 16727, 16728, 17787, 17788
17789, 17790, 17791, 17792, 17793, 17794, 17795, 17796, 17797, 17798, 17799,
17800, 17801, 17802, 17803, 17804
18694, 18695, 18696, 18697, 18698, 18699, 18700, 18701, 18702, 18703, 18704,
18705, 18706, 18707, 19766, 19767
19768, 19769, 19770, 19771, 19772, 19773, 19774, 19775, 19776, 19777, 19778,
19779, 19780, 19781, 19782, 19783
20673, 20674, 20675, 20676, 20677, 20678, 20679, 20680, 20681, 20682, 20683,
20684, 20685, 20686, 21745, 21746
21747, 21748, 21749, 21750, 21751, 21752, 21753, 21754, 21755, 21756, 21757,
21758, 21759, 21760, 21761, 21762
22652, 22653, 22654, 22655, 22656, 22657, 22658, 22659, 22660, 22661, 22662,
22663, 22664, 22665, 23724, 23725
23726, 23727, 23728, 23729, 23730, 23731, 23732, 23733, 23734, 23735, 23736,
23737, 23738, 23739, 23740, 23741
24631, 24632, 24633, 24634, 24635, 24636, 24637, 24638, 24639, 24640, 24641,
24642, 24643, 24644, 25703, 25704
25705, 25706, 25707, 25708, 25709, 25710, 25711, 25712, 25713, 25714, 25715,
25716, 25717, 25718, 25719, 25720
26610, 26611, 26612, 26613, 26614, 26615, 26616, 26617, 26618, 26619, 26620,
26621, 26622, 26623, 27682, 27683
27684, 27685, 27686, 27687, 27688, 27689, 27690, 27691, 27692, 27693, 27694,
27695, 27696, 27697, 27698, 27699
28589, 28590, 28591, 28592, 28593, 28594, 28595, 28596, 28597, 28598, 28599,
28600, 28601, 28602, 29661, 29662
29663, 29664, 29665, 29666, 29667, 29668, 29669, 29670, 29671, 29672, 29673,
29674, 29675, 29676, 29677, 29678
30568, 30569, 30570, 30571, 30572, 30573, 30574, 30575, 30576, 30577, 30578,
30579, 30580, 30581, 31640, 31641
31642, 31643, 31644, 31645, 31646, 31647, 31648, 31649, 31650, 31651, 31652,
31653, 31654, 31655, 31656, 31657
32547, 32548, 32549, 32550, 32551, 32552, 32553, 32554, 32555, 32556, 32557,
32558, 32559, 32560, 33619, 33620
33621, 33622, 33623, 33624, 33625, 33626, 33627, 33628, 33629, 33630, 33631,
33632, 33633, 33634, 33635, 33636
*Nset, nset=NSET-control_point, instance=Clot-1
4,
*Nset, nset=Outline, instance=Clot-1
35191, 35193, 35194, 35195, 35196, 35197, 35198, 35199, 35200, 35201, 35239,
35240, 35241, 35242, 35243, 35244
35245, 35246, 35247, 35248, 35249, 35250, 35251, 35252, 35253, 35254, 35255,
35256, 35257, 35258, 35259, 35260
35261, 35262, 35263, 35264, 35265, 35266, 35267, 35268, 35269, 35270, 35271,
35272, 35273, 35274, 35275, 35300
35301, 35302, 35303, 35304, 35305, 35306, 35307, 35308, 35309, 35310, 35311,
35312, 35313, 35314, 35315, 35316
35317, 35318, 35319, 35320, 35321, 35322, 35323, 35324, 35325, 35326, 35327,
35328, 35329, 35330, 35331, 35332
35333, 35334, 35335, 35336, 35337, 35338, 35339, 35340, 35341, 35342, 35343,
35344, 35369, 35370, 35371, 35372

3537, 35374, 35375, 35376, 35377, 35378, 35379, 35380, 35381, 35382, 35383,
35384, 35385, 35386, 35387, 35388
3538, 35390, 35391, 35392, 35393, 35394, 35395, 35396, 35397, 35398, 35399,
35400, 35401, 35402, 35403, 35404
3540, 35406, 35407, 35408, 35409, 35410, 35411, 35412, 35413, 35414, 35415,
35416, 35417, 35418, 35419, 35420
3542, 35422, 35423, 35424, 35425, 35426, 35427, 35428, 35429, 35430, 35431,
35432, 35433, 35434, 35435, 35436
3543, 35438, 35439, 35440, 35441, 35442, 35443, 35444, 35445, 35446, 35447,
35448, 35449, 35450, 35451, 35452
3545, 35454, 35455, 35456
*Elset, elset=Outline, instance=Clot-1
3166, 31686, 31707, 31728, 31749, 31770, 31791, 31812, 31833, 31854, 31875,
31896, 31917, 31938, 31959, 31980
3200, 32022, 32023, 32024, 32025, 32026, 32027, 32028, 32029, 32030, 32031,
32032, 32033, 32034, 32035, 32036
3203, 32038, 32039, 32040, 32041, 32042, 32247, 32260, 32273, 32286, 32299,
32312, 32325, 32338, 32351, 32364
3237, 32390, 32403, 32416, 32429, 32442, 32455, 32468, 32481, 32494, 32507,
32520, 32533, 32546, 32547, 32548
3254, 32550, 32551, 32552, 32553, 32554, 32555, 32556, 32557, 32558, 32559,
32560, 32561, 32562, 32563, 32564
3256, 32566, 32567, 32568, 32593, 32618, 32643, 32668, 32693, 32718, 32743,
32768, 32793, 32818, 32843, 32868
3289, 32918, 32943, 32968, 32993, 32994, 32995, 32996, 32997, 32998, 32999,
33000, 33001, 33002, 33003, 33004
3300, 33006, 33007, 33008, 33009, 33010, 33011, 33012, 33013, 33014, 33015,
33016, 33017, 33018, 33019, 33044
3306, 33094, 33119, 33144, 33169, 33194, 33219, 33244, 33269, 33294, 33319,
33344, 33369, 33394, 33419, 33444
3346, 33494, 33519, 33544, 33569, 33594, 33619, 33620, 33621, 33622, 33623,
33624, 33625, 33626, 33627, 33628
3362, 33630, 33631, 33632, 33633, 33634, 33635, 33636, 33637, 33638, 33639,
33640, 33641, 33642, 33643
*Nset, nset=Top, instance=Clot-1
1, 4, 5, 69, 70, 71, 72, 73, 74, 75, 76,
77, 78, 79, 80, 81
82, 83, 84, 85, 110, 111, 112, 113, 114, 115, 116,
117, 118, 119, 120, 121
122, 123, 124, 125, 126, 127, 128, 129, 130, 131, 132,
133, 2071, 2074, 2075, 2139
2140, 2141, 2142, 2143, 2144, 2145, 2146, 2147, 2148, 2149, 2150,
2151, 2152, 2153, 2154, 2155
2180, 2181, 2182, 2183, 2184, 2185, 2186, 2187, 2188, 2189, 2190,
2191, 2192, 2193, 2194, 2195
2196, 2197, 2198, 2199, 2200, 2201, 2202, 2203, 4141, 4144, 4145,
4209, 4210, 4211, 4212, 4213
4214, 4215, 4216, 4217, 4218, 4219, 4220, 4221, 4222, 4223, 4224,
4225, 4250, 4251, 4252, 4253
4254, 4255, 4256, 4257, 4258, 4259, 4260, 4261, 4262, 4263, 4264,
4265, 4266, 4267, 4268, 4269
4270, 4271, 4272, 4273, 6211, 6214, 6215, 6279, 6280, 6281, 6282,
6283, 6284, 6285, 6286, 6287
6288, 6289, 6290, 6291, 6292, 6293, 6294, 6295, 6320, 6321, 6322,
6323, 6324, 6325, 6326, 6327
6328, 6329, 6330, 6331, 6332, 6333, 6334, 6335, 6336, 6337, 6338,
6339, 6340, 6341, 6342, 6343

8281, 8284, 8285, 8349, 8350, 8351, 8352, 8353, 8354, 8355, 8356,
8357, 8358, 8359, 8360, 8361
8362, 8363, 8364, 8365, 8390, 8391, 8392, 8393, 8394, 8395, 8396,
8397, 8398, 8399, 8400, 8401
8402, 8403, 8404, 8405, 8406, 8407, 8408, 8409, 8410, 8411, 8412,
8413, 10351, 10354, 10355, 10419
10420, 10421, 10422, 10423, 10424, 10425, 10426, 10427, 10428, 10429, 10430,
10431, 10432, 10433, 10434, 10435
10460, 10461, 10462, 10463, 10464, 10465, 10466, 10467, 10468, 10469, 10470,
10471, 10472, 10473, 10474, 10475
10476, 10477, 10478, 10479, 10480, 10481, 10482, 10483, 12421, 12424, 12425,
12489, 12490, 12491, 12492, 12493
12494, 12495, 12496, 12497, 12498, 12499, 12500, 12501, 12502, 12503, 12504,
12505, 12530, 12531, 12532, 12533
12534, 12535, 12536, 12537, 12538, 12539, 12540, 12541, 12542, 12543, 12544,
12545, 12546, 12547, 12548, 12549
12550, 12551, 12552, 12553, 14491, 14494, 14495, 14559, 14560, 14561, 14562,
14563, 14564, 14565, 14566, 14567
14568, 14569, 14570, 14571, 14572, 14573, 14574, 14575, 14600, 14601, 14602,
14603, 14604, 14605, 14606, 14607
14608, 14609, 14610, 14611, 14612, 14613, 14614, 14615, 14616, 14617, 14618,
14619, 14620, 14621, 14622, 14623
16561, 16564, 16565, 16629, 16630, 16631, 16632, 16633, 16634, 16635, 16636,
16637, 16638, 16639, 16640, 16641
16642, 16643, 16644, 16645, 16670, 16671, 16672, 16673, 16674, 16675, 16676,
16677, 16678, 16679, 16680, 16681
16682, 16683, 16684, 16685, 16686, 16687, 16688, 16689, 16690, 16691, 16692,
16693, 18631, 18634, 18635, 18699
18700, 18701, 18702, 18703, 18704, 18705, 18706, 18707, 18708, 18709, 18710,
18711, 18712, 18713, 18714, 18715
18740, 18741, 18742, 18743, 18744, 18745, 18746, 18747, 18748, 18749, 18750,
18751, 18752, 18753, 18754, 18755
18756, 18757, 18758, 18759, 18760, 18761, 18762, 18763, 20701, 20704, 20705,
20769, 20770, 20771, 20772, 20773
20774, 20775, 20776, 20777, 20778, 20779, 20780, 20781, 20782, 20783, 20784,
20785, 20810, 20811, 20812, 20813
20814, 20815, 20816, 20817, 20818, 20819, 20820, 20821, 20822, 20823, 20824,
20825, 20826, 20827, 20828, 20829
20830, 20831, 20832, 20833, 22771, 22774, 22775, 22839, 22840, 22841, 22842,
22843, 22844, 22845, 22846, 22847
22848, 22849, 22850, 22851, 22852, 22853, 22854, 22855, 22880, 22881, 22882,
22883, 22884, 22885, 22886, 22887
22888, 22889, 22890, 22891, 22892, 22893, 22894, 22895, 22896, 22897, 22898,
22899, 22900, 22901, 22902, 22903
24841, 24844, 24845, 24909, 24910, 24911, 24912, 24913, 24914, 24915, 24916,
24917, 24918, 24919, 24920, 24921
24922, 24923, 24924, 24925, 24950, 24951, 24952, 24953, 24954, 24955, 24956,
24957, 24958, 24959, 24960, 24961
24962, 24963, 24964, 24965, 24966, 24967, 24968, 24969, 24970, 24971, 24972,
24973, 26911, 26914, 26915, 26979
26980, 26981, 26982, 26983, 26984, 26985, 26986, 26987, 26988, 26989, 26990,
26991, 26992, 26993, 26994, 26995
27020, 27021, 27022, 27023, 27024, 27025, 27026, 27027, 27028, 27029, 27030,
27031, 27032, 27033, 27034, 27035
27036, 27037, 27038, 27039, 27040, 27041, 27042, 27043, 28981, 28984, 28985,
29049, 29050, 29051, 29052, 29053

29054, 29055, 29056, 29057, 29058, 29059, 29060, 29061, 29062, 29063, 29064,
29065, 29090, 29091, 29092, 29093
29094, 29095, 29096, 29097, 29098, 29099, 29100, 29101, 29102, 29103, 29104,
29105, 29106, 29107, 29108, 29109
29110, 29111, 29112, 29113, 31051, 31054, 31055, 31119, 31120, 31121, 31122,
31123, 31124, 31125, 31126, 31127
31128, 31129, 31130, 31131, 31132, 31133, 31134, 31135, 31160, 31161, 31162,
31163, 31164, 31165, 31166, 31167
31168, 31169, 31170, 31171, 31172, 31173, 31174, 31175, 31176, 31177, 31178,
31179, 31180, 31181, 31182, 31183
33121, 33124, 33125, 33189, 33190, 33191, 33192, 33193, 33194, 33195, 33196,
33197, 33198, 33199, 33200, 33201
33202, 33203, 33204, 33205, 33230, 33231, 33232, 33233, 33234, 33235, 33236,
33237, 33238, 33239, 33240, 33241
33242, 33243, 33244, 33245, 33246, 33247, 33248, 33249, 33250, 33251, 33252,
33253, 35191, 35194, 35195, 35259
35260, 35261, 35262, 35263, 35264, 35265, 35266, 35267, 35268, 35269, 35270,
35271, 35272, 35273, 35274, 35275
35300, 35301, 35302, 35303, 35304, 35305, 35306, 35307, 35308, 35309, 35310,
35311, 35312, 35313, 35314, 35315
35316, 35317, 35318, 35319, 35320, 35321, 35322, 35323
*Elset, elset=Top, instance=Clot-1
     1,   22,   43,   64,   85,   106,   127,   148,   169,   190,   211,
232,   253,   274,   295,   316
   337,   358,   583,   596,   609,   622,   635,   648,   661,   674,   687,
700,   713,   726,   739,   752
   765,   778,   791,   804,   817,   830,   843,   856,   869,   882,   883,
1980, 2001, 2022, 2043, 2064
  2085, 2106, 2127, 2148, 2169, 2190, 2211, 2232, 2253, 2274, 2295,
2316, 2337, 2562, 2575, 2588
  2601, 2614, 2627, 2640, 2653, 2666, 2679, 2692, 2705, 2718, 2731,
2744, 2757, 2770, 2783, 2796
  2809, 2822, 2835, 2848, 2861, 2862, 3959, 3980, 4001, 4022, 4043,
4064, 4085, 4106, 4127, 4148
  4169, 4190, 4211, 4232, 4253, 4274, 4295, 4316, 4541, 4554, 4567,
4580, 4593, 4606, 4619, 4632
  4645, 4658, 4671, 4684, 4697, 4710, 4723, 4736, 4749, 4762, 4775,
4788, 4801, 4814, 4827, 4840
  4841, 5938, 5959, 5980, 6001, 6022, 6043, 6064, 6085, 6106, 6127,
6148, 6169, 6190, 6211, 6232
  6253, 6274, 6295, 6520, 6533, 6546, 6559, 6572, 6585, 6598, 6611,
6624, 6637, 6650, 6663, 6676
  6689, 6702, 6715, 6728, 6741, 6754, 6767, 6780, 6793, 6806, 6819,
6820, 7917, 7938, 7959, 7980
  8001, 8022, 8043, 8064, 8085, 8106, 8127, 8148, 8169, 8190, 8211,
8232, 8253, 8274, 8499, 8512
  8525, 8538, 8551, 8564, 8577, 8590, 8603, 8616, 8629, 8642, 8655,
8668, 8681, 8694, 8707, 8720
  8733, 8746, 8759, 8772, 8785, 8798, 8799, 9896, 9917, 9938, 9959,
9980, 10001, 10022, 10043, 10064
 10085, 10106, 10127, 10148, 10169, 10190, 10211, 10232, 10253, 10478, 10491,
10504, 10517, 10530, 10543, 10556
 10569, 10582, 10595, 10608, 10621, 10634, 10647, 10660, 10673, 10686, 10699,
10712, 10725, 10738, 10751, 10764
 10777, 10778, 11875, 11896, 11917, 11938, 11959, 11980, 12001, 12022, 12043,
12064, 12085, 12106, 12127, 12148

12169, 12190, 12211, 12232, 12457, 12470, 12483, 12496, 12509, 12522, 12535, 12548, 12561, 12574, 12587, 12600
12613, 12626, 12639, 12652, 12665, 12678, 12691, 12704, 12717, 12730, 12743, 12756, 12757, 13854, 13875, 13896
13917, 13938, 13959, 13980, 14001, 14022, 14043, 14064, 14085, 14106, 14127, 14148, 14169, 14190, 14211, 14436
14449, 14462, 14475, 14488, 14501, 14514, 14527, 14540, 14553, 14566, 14579, 14592, 14605, 14618, 14631, 14644
14657, 14670, 14683, 14696, 14709, 14722, 14735, 14736, 15833, 15854, 15875, 15896, 15917, 15938, 15959, 15980
16001, 16022, 16043, 16064, 16085, 16106, 16127, 16148, 16169, 16190, 16415, 16428, 16441, 16454, 16467, 16480
16493, 16506, 16519, 16532, 16545, 16558, 16571, 16584, 16597, 16610, 16623, 16636, 16649, 16662, 16675, 16688
16701, 16714, 16715, 17812, 17833, 17854, 17875, 17896, 17917, 17938, 17959, 17980, 18001, 18022, 18043, 18064
18085, 18106, 18127, 18148, 18169, 18394, 18407, 18420, 18433, 18446, 18459, 18472, 18485, 18498, 18511, 18524
18537, 18550, 18563, 18576, 18589, 18602, 18615, 18628, 18641, 18654, 18667, 18680, 18693, 18694, 19791, 19812
19833, 19854, 19875, 19896, 19917, 19938, 19959, 19980, 20001, 20022, 20043, 20064, 20085, 20106, 20127, 20148
20373, 20386, 20399, 20412, 20425, 20438, 20451, 20464, 20477, 20490, 20503, 20516, 20529, 20542, 20555, 20568
20581, 20594, 20607, 20620, 20633, 20646, 20659, 20672, 20673, 21770, 21791, 21812, 21833, 21854, 21875, 21896
21917, 21938, 21959, 21980, 22001, 22022, 22043, 22064, 22085, 22106, 22127, 22352, 22365, 22378, 22391, 22404
22417, 22430, 22443, 22456, 22469, 22482, 22495, 22508, 22521, 22534, 22547, 22560, 22573, 22586, 22599, 22612
22625, 22638, 22651, 22652, 23749, 23770, 23791, 23812, 23833, 23854, 23875, 23896, 23917, 23938, 23959, 23980
24001, 24022, 24043, 24064, 24085, 24106, 24331, 24344, 24357, 24370, 24383, 24396, 24409, 24422, 24435, 24448
24461, 24474, 24487, 24500, 24513, 24526, 24539, 24552, 24565, 24578, 24591, 24604, 24617, 24630, 24631, 25728
25749, 25770, 25791, 25812, 25833, 25854, 25875, 25896, 25917, 25938, 25959, 25980, 26001, 26022, 26043, 26064
26085, 26310, 26323, 26336, 26349, 26362, 26375, 26388, 26401, 26414, 26427, 26440, 26453, 26466, 26479, 26492
26505, 26518, 26531, 26544, 26557, 26570, 26583, 26596, 26609, 26610, 27707, 27728, 27749, 27770, 27791, 27812
27833, 27854, 27875, 27896, 27917, 27938, 27959, 27980, 28001, 28022, 28043, 28064, 28289, 28302, 28315, 28328
28341, 28354, 28367, 28380, 28393, 28406, 28419, 28432, 28445, 28458, 28471, 28484, 28497, 28510, 28523, 28536
28549, 28562, 28575, 28588, 28589, 29686, 29707, 29728, 29749, 29770, 29791, 29812, 29833, 29854, 29875, 29896
29917, 29938, 29959, 29980, 30001, 30022, 30043, 30268, 30281, 30294, 30307, 30320, 30333, 30346, 30359, 30372
30385, 30398, 30411, 30424, 30437, 30450, 30463, 30476, 30489, 30502, 30515, 30528, 30541, 30554, 30567, 30568
31665, 31686, 31707, 31728, 31749, 31770, 31791, 31812, 31833, 31854, 31875, 31896, 31917, 31938, 31959, 31980
32001, 32022, 32247, 32260, 32273, 32286, 32299, 32312, 32325, 32338, 32351, 32364, 32377, 32390, 32403, 32416
32429, 32442, 32455, 32468, 32481, 32494, 32507, 32520, 32533, 32546, 32547

```
*Surface, type=NODE, name=Top_CNS_, internal
Top, 1.
** Constraint: Constraint-1
*Coupling, constraint name=Constraint-1, ref node=NSET-control_point,
surface=Top_CNS_
*Kinematic
*End Assembly
**
** MATERIALS
**
*Material, name=Material-1
*Depvar
      7,
*User Material, constants=20
 0.1,     0.4,  5e-05,  0.003,      5.,   0.27,    0.8, 0.0015
   0.06,   0.08,  0.016,    0.2,    0.4,     2.,     2.,    90.
    45.,    90.,   -45.,   0.01
**
** BOUNDARY CONDITIONS
**
** Name: Bottom Type: Symmetry/Antisymmetry/Encastre
*Boundary
Bottom, ENCASTRE
** Name: Mirror Type: Displacement/Rotation
*Boundary
MiddlePlane, 1, 1
MiddlePlane, 4, 4
MiddlePlane, 5, 5
MiddlePlane, 6, 6
** Name: Top Type: Displacement/Rotation
*Boundary
Top, 1, 1
Top, 3, 3
Top, 4, 4
Top, 5, 5
Top, 6, 6
** ----------------------------------------------------------------
**
** STEP: Step-1
**
*Step, name=Step-1, nlgeom=YES, inc=1000000
*Static, stabilize=0.0002, allsdtol=0.05, continue=NO
0.001, 1., 1e-12, 0.01
**
** BOUNDARY CONDITIONS
**
** Name: Tension Type: Displacement/Rotation
*Boundary
NSET-control_point, 2, 2, 3.1
**
** OUTPUT REQUESTS
**
*Restart, write, frequency=0
**
** FIELD OUTPUT: Coordinate
**
*Output, field, time interval=0.01
```

```
*Node Output, nset=Outline
COORD,
**
** FIELD OUTPUT: F-Output-1
**
*Output, field, variable=PRESELECT, time interval=0.01
**
** HISTORY OUTPUT: H-Output-1
**
*Output, history, time interval=0.01
*Node Output, nset=Top
RF1, RF2, RF3, RM1, RM2, RM3, RT
*Energy Output, elset=Top
ALLAE, ALLCD, ALLDMD, ALLEE, ALLFD, ALLIE, ALLJD, ALLKE, ALLKL, ALLPD, ALLQB,
ALLSD, ALLSE, ALLVD, ALLWK, ETOTAL
*End Step
```

D. The MATLAB script utilized to conduct the shape comparison

```
%Enter the coordinate data of the experiment
x_e=[…];
y_e=[…];

%Enter the coordinate data of the simulation
x_s=[…];
y_s=[…];

%Plot the outlines in the same figure and add legend, label, and title
plot(XE, YE, 'LineWidth', 1.5)
hold on
grid on
plot(XS, YS, 'LineWidth', 1.5)
title('title text')
xlabel('displacement (mm)')
ylabel('displacement (mm)')
legend('EXP', 'FEA','Location','eastoutside')
```

E. The input file for the CZ study using rigid clots

a) Applying displacement in the normal direction

```
*Heading
** Job name: CZ_n Model name: CZ_n
** Generated by: Abaqus/CAE 2020
*Preprint, echo=NO, model=NO, history=NO, contact=NO
**
** PARTS
**
*Part, name=clot
*Node
      1,           1.,           0.5
      2,           0.,           0.5
      3,           1.,          -0.5
      4,           0.,          -0.5
*Element, type=CPS4
1, 1, 2, 4, 3
*Nset, nset=clot, generate
 1,  4,  1
*Elset, elset=clot
 1,
** Section: Section-1
*Solid Section, elset=clot, material=Material-1
1.,
*End Part
**
*Part, name=vessel
*End Part
**
**
** ASSEMBLY
**
*Assembly, name=Assembly
**
*Instance, name=vessel-1, part=vessel
*Surface, type=SEGMENTS, name=Surf-vessel
START,           1.,          -2.5
 LINE,           1.,           2.5
*End Instance
**
*Instance, name=clot-1, part=clot
*End Instance
**
*Node
      1,           1.,           2.5,           0.
*Nset, nset=coupledpoint, instance=clot-1
 2,
*Nset, nset=rp
 1,
*Nset, nset=_PickedSet10, internal
 1,
*Elset, elset=_Surf-clot_S4, internal, instance=clot-1
 1,
*Surface, type=ELEMENT, name=Surf-clot
_Surf-clot_S4, S4
*Elset, elset=_clot_nor_S2, internal, instance=clot-1
```

```
 1,
*Surface, type=ELEMENT, name=clot_nor
_clot_nor_S2, S2
** Constraint: coupledpoint
*Coupling, constraint name=coupledpoint, ref node=coupledpoint,
surface=clot_nor
*Kinematic
** Constraint: rigid
*Rigid Body, ref node=_PickedSet10, analytical surface=vessel-1.Surf-vessel
*End Assembly
**
** MATERIALS
**
*Material, name=Material-1
*Elastic
 1e+12, 0.5
**
** INTERACTION PROPERTIES
**
*Surface Interaction, name=coh
1.,
*Cohesive Behavior, eligibility=CURRENT CONTACTS
4000.,4000.,4000.
*Damage Initiation, criterion=MAXS
 1, 1, 1
*Damage Evolution, type=ENERGY, softening=EXPONENTIAL
 0.00035,
*Damage Stabilization
0.
**
** BOUNDARY CONDITIONS
**
** Name: fix Type: Symmetry/Antisymmetry/Encastre
*Boundary
rp, ENCASTRE
**
** INTERACTIONS
**
** Interaction: CZ
*Contact Pair, interaction=coh
Surf-clot, vessel-1.Surf-vessel
** ----------------------------------------------------------------
**
** STEP: Step-1
**
*Step, name=Step-1, nlgeom=YES, inc=1000000
*Static
0.0001, 1., 1e-15, 0.001
**
** BOUNDARY CONDITIONS
**
** Name: disp Type: Displacement/Rotation
*Boundary
coupledpoint, 1, 1, -0.0025
coupledpoint, 2, 2
coupledpoint, 6, 6
**
```

```
** CONTROLS
**
*Controls, reset
*Controls, parameters=time incrementation
, , , , , , , 30, , ,
**
** OUTPUT REQUESTS
**
*Restart, write, frequency=0
**
** FIELD OUTPUT: F-Output-2
**
*Output, field
*Contact Output
CSDMG,
**
** FIELD OUTPUT: F-Output-1
**
*Output, field, variable=PRESELECT
**
** HISTORY OUTPUT: H-Output-2
**
*Output, history
*Contact Output
ENRRT11, ENRRT12, ENRRT13
**
** HISTORY OUTPUT: H-Output-1
**
*Output, history, variable=PRESELECT
*End Step
```

b) Applying displacement in the shear direction

```
*Heading
** Job name: CZ_cyc_s Model name: CZ_cyclic_s
** Generated by: Abaqus/CAE 2020
*Preprint, echo=NO, model=NO, history=NO, contact=NO
**
** PARTS
**
*Part, name=clot
*Node
      1,           1.,           0.5
      2,           0.,           0.5
      3,           1.,          -0.5
      4,           0.,          -0.5
*Element, type=CPS4
1, 1, 2, 4, 3
*Nset, nset=clot, generate
 1,  4,  1
*Elset, elset=clot
 1,
** Section: Section-1
*Solid Section, elset=clot, material=Material-1
1.,
*End Part
**
```

```
*Part, name=vessel
*End Part
**
**
** ASSEMBLY
**
*Assembly, name=Assembly
**
*Instance, name=vessel-1, part=vessel
*Surface, type=SEGMENTS, name=Surf-vessel
START,            1.,         -2.5
 LINE,            1.,          2.5
*End Instance
**
*Instance, name=clot-1, part=clot
*End Instance
**
*Node
      1,           1.,          2.5,           0.
*Nset, nset=coupledpoint, instance=clot-1
 4,
*Nset, nset=rp
 1,
*Nset, nset=_PickedSet10, internal
 1,
*Elset, elset=_Surf-clot_S4, internal, instance=clot-1
 1,
*Surface, type=ELEMENT, name=Surf-clot
_Surf-clot_S4, S4
*Elset, elset=_clot_bottom_S3, internal, instance=clot-1
 1,
*Surface, type=ELEMENT, name=clot_bottom
_clot_bottom_S3, S3
** Constraint: coupledpoint
*Coupling, constraint name=coupledpoint, ref node=coupledpoint,
surface=clot_bottom
*Kinematic
** Constraint: rigid
*Rigid Body, ref node=_PickedSet10, analytical surface=vessel-1.Surf-vessel
*End Assembly
**
** MATERIALS
**
*Material, name=Material-1
*Elastic
 1e+12, 0.5
**
** INTERACTION PROPERTIES
**
*Surface Interaction, name=coh
1.,
*Cohesive Behavior, eligibility=CURRENT CONTACTS
4000.,4000.,4000.
*Damage Initiation, criterion=MAXS
1.,1.,1.
*Damage Evolution, type=ENERGY, softening=EXPONENTIAL
 0.00035,
```

```
*Damage Stabilization
0.
**
** BOUNDARY CONDITIONS
**
** Name: fix Type: Symmetry/Antisymmetry/Encastre
*Boundary
rp, ENCASTRE
**
** INTERACTIONS
**
** Interaction: CZ
*Contact Pair, interaction=coh
Surf-clot, vessel-1.Surf-vessel
** ----------------------------------------------------------------
**
** STEP: Step-1
**
*Step, name=Step-1, nlgeom=YES, inc=1000000
*Static
0.0001, 1., 1e-15, 0.001
**
** BOUNDARY CONDITIONS
**
** Name: disp Type: Displacement/Rotation
*Boundary
coupledpoint, 1, 1
coupledpoint, 2, 2, -0.0025
coupledpoint, 6, 6
**
** CONTROLS
**
*Controls, reset
*Controls, parameters=time incrementation
, , , , , , , 30, , ,
**
** OUTPUT REQUESTS
**
*Restart, write, frequency=0
**
** FIELD OUTPUT: F-Output-2
**
*Output, field
*Contact Output
CSDMG,
**
** FIELD OUTPUT: F-Output-1
**
*Output, field, variable=PRESELECT
**
** HISTORY OUTPUT: H-Output-2
**
*Output, history
*Contact Output
ENRRT11, ENRRT12, ENRRT13
**
** HISTORY OUTPUT: H-Output-1
```

```
**
*Output, history, variable=PRESELECT
*End Step
```

F. The input file for the CZ study using hyper foam clots

a) Applying displacement in the normal direction

```
*Heading
** Job name: CZn_HF Model name: CZn_HF
** Generated by: Abaqus/CAE 2020
*Preprint, echo=NO, model=NO, history=NO, contact=NO
**
** PARTS
**
*Part, name=clot
*Node
** For the mesh and node settings of the clot, set the approximate global
size to be 0.025 in Sizing control section in global seeds, the detail codes
will not be shown in this appendix

*Element, type=CPS4
** For the mesh and node settings of the clot, set the approximate global
size to be 0.025 in Sizing control section in global seeds, the detail codes
will not be shown in this appendix
*Nset, nset=clot, generate
    1,  1681,     1
*Elset, elset=clot, generate
    1,  1600,     1
** Section: Section-1
*Solid Section, elset=clot, material=Material-1
1.,
*End Part
**
*Part, name=vessel
*End Part
**
**
** ASSEMBLY
**
*Assembly, name=Assembly
**
*Instance, name=vessel-1, part=vessel
*Surface, type=SEGMENTS, name=Surf-vessel
START,           1.,         -2.5
 LINE,           1.,          2.5
*End Instance
**
*Instance, name=clot-1, part=clot
*End Instance
**
*Node
      1,           1.,          2.5,           0.
*Nset, nset=coupledpoint, instance=clot-1
 41,
*Nset, nset=interface, instance=clot-1, generate
    1,  1641,    41
*Elset, elset=interface, instance=clot-1, generate
    1,  1561,    40
*Nset, nset=norsurf, instance=clot-1, generate
   41,  1681,    41
*Elset, elset=norsurf, instance=clot-1, generate
```

```
   40,  1600,    40
*Nset, nset=rp
 1,
*Nset, nset=_PickedSet10, internal
 1,
*Elset, elset=_Surf-clot_S4, internal, instance=clot-1, generate
    1,  1561,    40
*Surface, type=ELEMENT, name=Surf-clot
_Surf-clot_S4, S4
*Elset, elset=_clot_nor_S2, internal, instance=clot-1, generate
   40,  1600,    40
*Surface, type=ELEMENT, name=clot_nor
_clot_nor_S2, S2
** Constraint: rigid
*Rigid Body, ref node=_PickedSet10, analytical surface=vessel-1.Surf-vessel
*End Assembly
**
** MATERIALS
**
*Material, name=Material-1
*Hyperfoam, n=2
 0.0043,  6.9409,  0.0002, -0.2094,  0.1778,    0.35
**
** INTERACTION PROPERTIES
**
*Surface Interaction, name=coh
1.,
*Cohesive Behavior, eligibility=CURRENT CONTACTS
 0.02, 0.02, 0.02
*Damage Initiation, criterion=MAXS
 0.01, 0.01, 0.01
*Damage Evolution, type=ENERGY, softening=EXPONENTIAL
 0.00744,
*Damage Stabilization
1e-07
*Time Points, name=TimePoints-1, GENERATE
0., 1., 0.001
**
** BOUNDARY CONDITIONS
**
** Name: fix Type: Symmetry/Antisymmetry/Encastre
*Boundary
rp, ENCASTRE
**
** INTERACTIONS
**
** Interaction: CZ
*Contact Pair, interaction=coh
Surf-clot, vessel-1.Surf-vessel
** ----------------------------------------------------------------
**
** STEP: Step-1
**
*Step, name=Step-1, nlgeom=YES, inc=1000000
*Static
0.001, 1., 1e-15, 0.01
**
```

```
** BOUNDARY CONDITIONS
**
** Name: disp Type: Displacement/Rotation
*Boundary
norsurf, 1, 1, -2.
**
** CONTROLS
**
*Controls, reset
*Controls, parameters=time incrementation
, , , , , , , 30, , ,
**
** OUTPUT REQUESTS
**
*Restart, write, frequency=0
**
** FIELD OUTPUT: F-Output-2
**
*Output, field
*Contact Output
CSDMG,
**
** FIELD OUTPUT: F-Output-1
**
*Output, field, variable=PRESELECT
**
** FIELD OUTPUT: Traction
**
*Output, field, time points=TimePoints-1
*Element Output, elset=interface, directions=YES
TRNOR, TRSHR
*Contact Output, nset=interface
CFORCE, CSTRESS, CSTRESSETOS
**
** HISTORY OUTPUT: H-Output-2
**
*Output, history
*Contact Output
ENRRT11, ENRRT12, ENRRT13
**
** HISTORY OUTPUT: H-Output-1
**
*Output, history, variable=PRESELECT
**
** HISTORY OUTPUT: Traction
**
*Output, history, time points=TimePoints-1
*Node Output, nset=interface
U1,
*Contact Output, nset=interface
CFN1, CFN2, CFN3, CFNM, CFS1, CFS2, CFS3, CFSM, CSTRESS
*End Step
```

b) Applying displacement in the shear direction

```
*Heading
** Job name: CZs_HF Model name: CZs_HF
```

```
** Generated by: Abaqus/CAE 2020
*Preprint, echo=NO, model=NO, history=NO, contact=NO
**
** PARTS
**
*Part, name=clot
*Node
** For the mesh and node settings of the clot, set the approximate global
size to be 0.025 in Sizing control section in global seeds, the detail codes
will not be shown in this appendix
*Element, type=CPS4
** For the mesh and node settings of the clot, set the approximate global
size to be 0.025 in Sizing control section in global seeds, the detail codes
will not be shown in this appendix
*Nset, nset=clot, generate
    1,  1681,     1
*Elset, elset=clot, generate
    1,  1600,     1
** Section: Section-1
*Solid Section, elset=clot, material=Material-1
1.,
*End Part
**
*Part, name=vessel
*End Part
**
**
** ASSEMBLY
**
*Assembly, name=Assembly
**
*Instance, name=vessel-1, part=vessel
*Surface, type=SEGMENTS, name=Surf-vessel
START,           1.,         -2.5
 LINE,           1.,          2.5
*End Instance
**
*Instance, name=clot-1, part=clot
*End Instance
**
*Node
      1,           1.,          2.5,           0.
*Nset, nset=bottom, instance=clot-1, generate
 1641,  1681,     1
*Elset, elset=bottom, instance=clot-1, generate
 1561,  1600,     1
*Nset, nset=coupledpoint, instance=clot-1
 1681,
*Nset, nset=interface, instance=clot-1, generate
    1,  1641,    41
*Elset, elset=interface, instance=clot-1, generate
    1,  1561,    40
*Nset, nset=normalsurf, instance=clot-1, generate
   41,  1681,    41
*Elset, elset=normalsurf, instance=clot-1, generate
   40,  1600,    40
*Nset, nset=rp
```

```
 1,
*Nset, nset=_PickedSet10, internal
 1,
*Elset, elset=_Surf-clot_S4, internal, instance=clot-1, generate
    1,  1561,    40
*Surface, type=ELEMENT, name=Surf-clot
_Surf-clot_S4, S4
*Elset, elset=_clot_bottom_S3, internal, instance=clot-1, generate
 1561,  1600,     1
*Surface, type=ELEMENT, name=clot_bottom
_clot_bottom_S3, S3
** Constraint: rigid
*Rigid Body, ref node=_PickedSet10, analytical surface=vessel-1.Surf-vessel
*End Assembly
**
** MATERIALS
**
*Material, name=Material-1
*Hyperfoam, n=2
 0.0043,  6.9409,  0.0002, -0.2094,  0.1778,    0.35
**
** INTERACTION PROPERTIES
**
*Surface Interaction, name=coh
1.,
*Cohesive Behavior, eligibility=CURRENT CONTACTS
 0.02, 0.02, 0.02
*Damage Initiation, criterion=MAXS
 0.01, 0.01, 0.01
*Damage Evolution, type=ENERGY, softening=EXPONENTIAL
 0.00744,
*Damage Stabilization
1e-07
**
** BOUNDARY CONDITIONS
**
** Name: fix Type: Symmetry/Antisymmetry/Encastre
*Boundary
rp, ENCASTRE
**
** INTERACTIONS
**
** Interaction: CZ
*Contact Pair, interaction=coh
Surf-clot, vessel-1.Surf-vessel
** ----------------------------------------------------------------
**
** STEP: Step-1
**
*Step, name=Step-1, nlgeom=YES, inc=1000000
*Static
0.0001, 1., 1e-15, 0.001
**
** BOUNDARY CONDITIONS
**
** Name: disp Type: Displacement/Rotation
*Boundary
```

```
bottom, 2, 2, -2.
**
** CONTROLS
**
*Controls, reset
*Controls, parameters=time incrementation
, , , , , , , 30, , ,
**
** OUTPUT REQUESTS
**
*Restart, write, frequency=0
**
** FIELD OUTPUT: F-Output-2
**
*Output, field
*Contact Output
CSDMG,
**
** FIELD OUTPUT: Traction
**
*Element Output, elset=interface, directions=YES
TRNOR, TRSHR
*Contact Output, nset=interface
CFORCE, CSTRESS, CSTRESSETOS
**
** FIELD OUTPUT: F-Output-1
**
*Output, field, variable=PRESELECT
**
** HISTORY OUTPUT: H-Output-2
**
*Output, history
*Contact Output
ENRRT11, ENRRT12, ENRRT13
**
** HISTORY OUTPUT: Traction
**
*Node Output, nset=interface
U2,
*Contact Output, nset=interface
CFS1, CFS2, CFS3, CFSM, CSTRESS
**
** HISTORY OUTPUT: H-Output-1
**
*Output, history, variable=PRESELECT
*End Step
```

G. The input file for the CZ study using anisotropic bilinear clots

```
*Heading
** Job name: CZ_UM_axis Model name: CZ_UM_axis
** Generated by: Abaqus/CAE 2020
*Preprint, echo=NO, model=NO, history=NO, contact=NO
**
** PARTS
**
*Part, name=clot
*Node
** For the mesh and node settings of the clot, set the approximate global
size to be 0.025 in Sizing control section in global seeds, the detail codes
will not be shown in this appendix
*Element, type=CAX4
** For the mesh and node settings of the clot, set the approximate global
size to be 0.025 in Sizing control section in global seeds, the detail codes
will not be shown in this appendix
*Nset, nset=clot, generate
    1,  1681,     1
*Elset, elset=clot, generate
    1,  1600,     1
** Section: Section-1
*Solid Section, elset=clot, material=Material-1
,
*End Part
**
*Part, name=vessel
*End Part
**
**
** ASSEMBLY
**
*Assembly, name=Assembly
**
*Instance, name=vessel-1, part=vessel
*Surface, type=SEGMENTS, name=vesselwall
START,           1.,        -2.95
 LINE,           1.,           2.
*End Instance
**
*Instance, name=clot-1, part=clot
*End Instance
**
*Node
      1,           1.,           2.,           0.
*Nset, nset=bottom, instance=clot-1, generate
 1641,  1681,     1
*Elset, elset=bottom, instance=clot-1, generate
 1561,  1600,     1
*Nset, nset=interface, instance=clot-1, generate
    1,  1641,    41
*Elset, elset=interface, instance=clot-1, generate
    1,  1561,    40
*Nset, nset=rp
 1,
*Nset, nset=xsymm, instance=clot-1, generate
```

```
   41,  1681,    41
*Elset, elset=xsymm, instance=clot-1, generate
   40,  1600,    40
*Nset, nset=_PickedSet9, internal
 1,
*Elset, elset=_clotsurf_S4, internal, instance=clot-1, generate
    1,  1561,    40
*Surface, type=ELEMENT, name=clotsurf
_clotsurf_S4, S4
** Constraint: rigid
*Rigid Body, ref node=_PickedSet9, analytical surface=vessel-1.vesselwall
*End Assembly
**
** MATERIALS
**
*Material, name=Material-1
*Depvar
      7,
*User Material, constants=20
 0.55,  0.65, 2e-05, 0.008,    5., 0.014, 0.022, 0.002
 0.006,  0.03, 0.032, 0.001, 0.003,    2.,    2.,   90.
   45.,   90.,  -45.,  0.01
**
** INTERACTION PROPERTIES
**
*Surface Interaction, name=coh
1.,
*Cohesive Behavior, eligibility=CURRENT CONTACTS
 0.02, 0.02, 0.02
*Damage Initiation, criterion=MAXS
 0.01, 0.01, 0.01
*Damage Evolution, type=ENERGY, softening=EXPONENTIAL
 0.00744,
*Damage Stabilization
1e-05
**
** BOUNDARY CONDITIONS
**
** Name: fixed Type: Symmetry/Antisymmetry/Encastre
*Boundary
rp, ENCASTRE
** Name: xsymm Type: Symmetry/Antisymmetry/Encastre
*Boundary
xsymm, XSYMM
**
** INTERACTIONS
**
** Interaction: CZ
*Contact Pair, interaction=coh
clotsurf, vessel-1.vesselwall
** ----------------------------------------------------------------
**
** STEP: Step-1
**
*Step, name=Step-1, nlgeom=YES, inc=1000000
*Static
0.001, 1., 1e-15, 0.001
```

```
**
** BOUNDARY CONDITIONS
**
** Name: disp Type: Displacement/Rotation
*Boundary
bottom, 2, 2, -2.
**
** OUTPUT REQUESTS
**
*Restart, write, frequency=0
**
** FIELD OUTPUT: Damage
**
*Output, field
*Contact Output
CSDMG,
**
** FIELD OUTPUT: Traction
**
*Contact Output, nset=interface
CFORCE, CSTRESS, CSTRESSETOS
**
** FIELD OUTPUT: F-Output-1
**
*Output, field, variable=PRESELECT
**
** HISTORY OUTPUT: Traction
**
*Output, history
*Node Output, nset=interface
U2,
*Contact Output, nset=interface
CFS1, CFS2, CFS3, CFSM, CSTRESS
**
** HISTORY OUTPUT: H-Output-1
**
*Output, history, variable=PRESELECT
*End Step
```

H. The input file for the parameter study of clot dimensions

An example for D/d = 2 with 40%H clot:

```
*Heading
** Job name: Dtod=2 Model name: Dtod=2
** Generated by: Abaqus/CAE 2020
*Preprint, echo=NO, model=NO, history=NO, contact=NO
**
** PARTS
**
*Part, name=Catheter
**The catheter length = 8, inner diameter = 1.37, outer diameter = 1.67, and
filet = 0.05
*End Part
**
*Part, name=Clot
**The clot diameter = 2.74 and the clot length = 1.37
*Node
** For the mesh and settings of the clot, set the approximate global size to
be 0.02 in Sizing control section in global seeds, the detail codes will not
be shown in this appendix
*Element, type=CAX4
** For the mesh and settings of the clot, set the approximate global size to
be 0.02 in Sizing control section in global seeds, the detail codes will not
be shown in this appendix
*Nset, nset=clot, generate
     1,  19182,      1
*Elset, elset=clot, generate
     1,  18906,      1
** Section: Section-1
*Solid Section, elset=clot, material=Material-1
,
*End Part
**
**
** ASSEMBLY
**
*Assembly, name=Assembly
**
*Instance, name=Catheter-1, part=Catheter
*Surface, type=SEGMENTS, name=cat_surf
START,        0.685,        -0.05
 CIRCL,        0.735,           0.,        0.735,        -0.05
 LINE,        0.775,           0.
 CIRCL,        0.825, -0.0500000000000005,        0.775, -0.0500000000000001
 LINE,        0.825,          -8.
 LINE,        0.685,          -8.
 LINE,        0.685,        -0.05
*End Instance
**
*Instance, name=Clot-1, part=Clot
*End Instance
**
*Node
      1,  0.824999988,          -8.,           0.
*Nset, nset=rp
 1,
```

```
*Nset, nset=xsymm, instance=Clot-1
   3,   4, 211, 212, 213, 214, 215, 216, 217, 218, 219, 220, 221, 222, 223,
224
 225, 226, 227, 228, 229, 230, 231, 232, 233, 234, 235, 236, 237, 238, 239,
240
 241, 242, 243, 244, 245, 246, 247, 248, 249, 250, 251, 252, 253, 254, 255,
256
 257, 258, 259, 260, 261, 262, 263, 264, 265, 266, 267, 268, 269, 270, 271,
272
 273, 274, 275, 276, 277, 278, 279, 280, 281, 282, 283, 284, 285, 286, 287,
288
 289, 290, 291, 292, 293, 294, 295, 296, 297, 298, 299, 300, 301, 302, 303,
304
 305, 306, 307, 308, 309, 310, 311, 312, 313, 314, 315, 316, 317, 318, 319,
320
 321, 322, 323, 324, 325, 326, 327, 328, 329, 330, 331, 332, 333, 334, 335,
336
 337, 338, 339, 340, 341, 342, 343, 344, 345, 346
*Elset, elset=xsymm, instance=Clot-1, generate
 9317,  9453,     1
*Nset, nset=_PickedSet8, internal
 1,
*Elset, elset=_clot_bottom_S4, internal, instance=Clot-1, generate
    1,  9317,   137
*Elset, elset=_clot_bottom_S2, internal, instance=Clot-1, generate
  9590,  18906,    137
*Surface, type=ELEMENT, name=clot_bottom
_clot_bottom_S4, S4
_clot_bottom_S2, S2
*Elset, elset=_suction_area_S4, internal, instance=Clot-1, generate
    1,  9317,   137
*Surface, type=ELEMENT, name=suction_area
_suction_area_S4, S4
** Constraint: rigid
*Rigid Body, ref node=_PickedSet8, analytical surface=Catheter-1.cat_surf
*End Assembly
**
** MATERIALS
**
**Material parameters of 40%H clot
*Material, name=Material-1
*Depvar
      7,
*User Material, constants=20
 0.55,  0.65, 2e-05, 0.008,    5., 0.014, 0.022, 0.002
 0.006,  0.03, 0.032, 0.001, 0.003,    2.,    2.,   90.
   45.,   90.,  -45.,  0.01
**
** INTERACTION PROPERTIES
**
*Surface Interaction, name=IntProp-1
1.,
*Friction
0.,
*Surface Behavior, pressure-overclosure=HARD
**
** BOUNDARY CONDITIONS
```

```
**
** Name: Fixed Type: Symmetry/Antisymmetry/Encastre
*Boundary
rp, ENCASTRE
** Name: xsymm Type: Symmetry/Antisymmetry/Encastre
*Boundary
xsymm, XSYMM
**
** INTERACTIONS
**
** Interaction: Int-1
*Contact Pair, interaction=IntProp-1
clot_bottom, Catheter-1.cat_surf
** ----------------------------------------------------------------
**
** STEP: Step-1
**
*Step, name=Step-1, nlgeom=YES, inc=1000000
*Static, stabilize=0.0002, allsdtol=0.05, continue=NO
0.001, 1., 1e-15, 0.01
**
** LOADS
**
** Name: Suction   Type: Pressure
*Dsload
suction_area, P, -0.02
**
** CONTROLS
**
*Controls, reset
*Controls, parameters=time incrementation
, , , , , , , 30, , ,
**
** OUTPUT REQUESTS
**
*Restart, write, frequency=0
**
** FIELD OUTPUT: F-Output-1
**
*Output, field, variable=PRESELECT, frequency=3
**
** HISTORY OUTPUT: H-Output-1
**
*Output, history, variable=PRESELECT, frequency=3
*End Step
```

I. The input file for the parameter study of CZ coefficients in aspiration simulations

An example for D/d = 2 with 40%H clot:

```
*Heading
** Job name: Dtod=2 Model name: Dtod=2
** Generated by: Abaqus/CAE 2020
*Preprint, echo=NO, model=NO, history=NO, contact=NO
**
** PARTS
**
*Part, name=Catheter
**The catheter length = 8, inner diameter = 1.37, outer diameter = 1.67, and
filet = 0.05
*End Part
**
*Part, name=Clot
**The clot diameter = 2.74 and the clot length = 2.74
*Node
** For the mesh and settings of the clot, set the approximate global size to
be 0.02 in Sizing control section in global seeds, the detail codes will not
be shown in this appendix
*Element, type=CAX4
** For the mesh and settings of the clot, set the approximate global size to
be 0.02 in Sizing control section in global seeds, the detail codes will not
be shown in this appendix
*Nset, nset=clot, generate
     1,  19182,      1
*Elset, elset=clot, generate
     1,  18906,      1
** Section: Section-1
*Solid Section, elset=clot, material=Material-1
,
*End Part
**
*Part, name=vessel
**The diameter of the vessel = 2.74 and the length = 5
*End Part
**
**
** ASSEMBLY
**
*Assembly, name=Assembly
**
*Instance, name=Catheter-1, part=Catheter
*Surface, type=SEGMENTS, name=cat_surf
START,         0.685,         -0.05
 CIRCL,         0.735,            0.,         0.735,         -0.05
 LINE,         0.775,            0.
 CIRCL,         0.825, -0.0500000000000005,         0.775, -0.0500000000000001
 LINE,         0.825,           -8.
 LINE,         0.685,           -8.
 LINE,         0.685,         -0.05
*End Instance
**
*Instance, name=Clot-1, part=Clot
*End Instance
**
```

```
*Instance, name=vessel-1, part=vessel
*Surface, type=SEGMENTS, name=vessel
START,         1.37, -2.00000000002328
 LINE,         1.37, 1.99999999997672
*End Instance
**
*Node
      1,  0.824999988,          -8.,           0.
*Node
      2,         1.37,           2.,           0.
*Nset, nset=interface, instance=Clot-1
   5,   6, 483, 484, 485, 486, 487, 488, 489, 490, 491, 492, 493, 494, 495,
496
 497, 498, 499, 500, 501, 502, 503, 504, 505, 506, 507, 508, 509, 510, 511,
512
 513, 514, 515, 516, 517, 518, 519, 520, 521, 522, 523, 524, 525, 526, 527,
528
 529, 530, 531, 532, 533, 534, 535, 536, 537, 538, 539, 540, 541, 542, 543,
544
 545, 546, 547, 548, 549, 550, 551, 552, 553, 554, 555, 556, 557, 558, 559,
560
 561, 562, 563, 564, 565, 566, 567, 568, 569, 570, 571, 572, 573, 574, 575,
576
 577, 578, 579, 580, 581, 582, 583, 584, 585, 586, 587, 588, 589, 590, 591,
592
 593, 594, 595, 596, 597, 598, 599, 600, 601, 602, 603, 604, 605, 606, 607,
608
 609, 610, 611, 612, 613, 614, 615, 616, 617, 618
*Elset, elset=interface, instance=Clot-1, generate
 18770,  18906,      1
*Nset, nset=rp
 1,
*Nset, nset=rp2
 2,
*Nset, nset=xsymm, instance=Clot-1
   3,   4, 211, 212, 213, 214, 215, 216, 217, 218, 219, 220, 221, 222, 223,
224
 225, 226, 227, 228, 229, 230, 231, 232, 233, 234, 235, 236, 237, 238, 239,
240
 241, 242, 243, 244, 245, 246, 247, 248, 249, 250, 251, 252, 253, 254, 255,
256
 257, 258, 259, 260, 261, 262, 263, 264, 265, 266, 267, 268, 269, 270, 271,
272
 273, 274, 275, 276, 277, 278, 279, 280, 281, 282, 283, 284, 285, 286, 287,
288
 289, 290, 291, 292, 293, 294, 295, 296, 297, 298, 299, 300, 301, 302, 303,
304
 305, 306, 307, 308, 309, 310, 311, 312, 313, 314, 315, 316, 317, 318, 319,
320
 321, 322, 323, 324, 325, 326, 327, 328, 329, 330, 331, 332, 333, 334, 335,
336
 337, 338, 339, 340, 341, 342, 343, 344, 345, 346
*Elset, elset=xsymm, instance=Clot-1, generate
 9317,  9453,     1
*Nset, nset=_PickedSet8, internal
 1,
*Nset, nset=_PickedSet20, internal
```

```
 2,
*Elset, elset=_clot_bottom_S4, internal, instance=Clot-1, generate
    1,  9317,   137
*Elset, elset=_clot_bottom_S2, internal, instance=Clot-1, generate
  9590,  18906,    137
*Surface, type=ELEMENT, name=clot_bottom
_clot_bottom_S4, S4
_clot_bottom_S2, S2
*Elset, elset=_interface_S3, internal, instance=Clot-1, generate
 18770,  18906,      1
*Surface, type=ELEMENT, name=interface
_interface_S3, S3
*Elset, elset=_suction_area_S4, internal, instance=Clot-1, generate
    1,  9317,   137
*Surface, type=ELEMENT, name=suction_area
_suction_area_S4, S4
** Constraint: rigid
*Rigid Body, ref node=_PickedSet8, analytical surface=Catheter-1.cat_surf
** Constraint: rigid2
*Rigid Body, ref node=_PickedSet20, analytical surface=vessel-1.vessel
*End Assembly
**
** MATERIALS
**
**Material parameters for 40%H clot
*Material, name=Material-1
*Depvar
      7,
*User Material, constants=20
 0.55,  0.65, 2e-05, 0.008,    5., 0.014, 0.022, 0.002
 0.006,  0.03, 0.032, 0.001, 0.003,    2.,    2.,   90.
   45.,   90.,  -45.,  0.01
**
** INTERACTION PROPERTIES
**
*Surface Interaction, name=IntProp-1
1.,
*Friction
0.,
*Surface Behavior, pressure-overclosure=HARD
*Surface Interaction, name=coh
1.,
**CZ stiffness
*Cohesive Behavior, eligibility=CURRENT CONTACTS
 0.02, 0.02, 0.02
*Damage Initiation, criterion=MAXS
 0.01, 0.01, 0.01
**Fracture energy
*Damage Evolution, type=ENERGY, softening=EXPONENTIAL
 0.00744,
*Damage Stabilization
1e-05
**
** BOUNDARY CONDITIONS
**
** Name: Fixed Type: Symmetry/Antisymmetry/Encastre
*Boundary
```

```
rp, ENCASTRE
** Name: Fixed2 Type: Symmetry/Antisymmetry/Encastre
*Boundary
rp2, ENCASTRE
** Name: xsymm Type: Symmetry/Antisymmetry/Encastre
*Boundary
xsymm, XSYMM
**
** INTERACTIONS
**
** Interaction: CZ
*Contact Pair, interaction=coh
interface, vessel-1.vessel
** Interaction: Int-1
*Contact Pair, interaction=IntProp-1
clot_bottom, Catheter-1.cat_surf
** Interaction: Int-3
*Contact Pair, interaction=IntProp-1
interface, Catheter-1.cat_surf
** Interaction: self
*Contact Pair, interaction=IntProp-1
interface,
** ----------------------------------------------------------------
**
** STEP: Step-1
**
*Step, name=Step-1, nlgeom=YES, inc=1000000
*Static, stabilize=0.0002, allsdtol=0.05, continue=NO
0.001, 1., 1e-15, 0.01
**
** LOADS
**
** Name: Suction   Type: Pressure
*Dsload
suction_area, P, -0.02
**
** CONTROLS
**
*Controls, reset
*Controls, parameters=time incrementation
, , , , , , , 30, , ,
**
** OUTPUT REQUESTS
**
*Restart, write, frequency=0
**
** FIELD OUTPUT: Damage
**
*Output, field
*Contact Output, nset=interface
CSDMG, CSMAXSCRT
**
** FIELD OUTPUT: F-Output-1
**
*Output, field, variable=PRESELECT
**
** HISTORY OUTPUT: Traction
```

```
**
*Output, history
*Contact Output, nset=interface
CFN1, CFN2, CFN3, CFNM, CFS1, CFS2, CFS3, CFSM, CSDMG, CSTRESS
**
** HISTORY OUTPUT: H-Output-1
**
*Output, history, variable=PRESELECT
*End Step
```

J. The input file for the parameter study of catheter designs in aspiration simulations with 40%H clot (L_1 = 5 mm and L_2 = 2 mm)

```
*Heading
** Job name: L5-2 Model name: L5-2
** Generated by: Abaqus/CAE 2020
*Preprint, echo=NO, model=NO, history=NO, contact=NO
**
** PARTS
**
*Part, name=Catheter
**The catheter length = 8, inner diameter = 2.62, outer diameter = 2.74,
filet = 0.05, L1 = 5, and L2 = 2
*End Part
**
*Part, name=Clot
**The clot diameter = 2.74 and the clot length = 2.74
*Node
** For the mesh and node settings of the clot, set the approximate global
size to be 0.02 in Sizing control section in global seeds, the detail codes
will not be shown in this appendix
*Element, type=CAX4
** For the mesh and node settings of the clot, set the approximate global
size to be 0.02 in Sizing control section in global seeds, the detail codes
will not be shown in this appendix
*Nset, nset=clot, generate
     1,  37950,      1
*Elset, elset=clot, generate
     1,  37538,      1
** Section: Section-1
*Solid Section, elset=clot, material=Material-1
,
*End Part
**
*Part, name=vessel
**The diameter of the vessel = 2.74 and the length = 5
*End Part
**
**
** ASSEMBLY
**
*Assembly, name=Assembly
**
*Instance, name=Catheter-1, part=Catheter
*Surface, type=SEGMENTS, name=cat_surf
START,        0.685,          -8.
 LINE,        0.685,          -5.
 CIRCL, 1.15375008635441,        -2.75, 6.3193740483744,          -5.
 CIRCL,         1.31,          -2., -0.568125951625594,          -2.
 LINE,         1.31,        -0.05
 CIRCL,         1.36,           0.,         1.36,        -0.05
 LINE,         1.37,           0.
 LINE,         1.37, -1.9628494287841
 CIRCL, 1.22875008635441,        -2.75, -0.893921949980383, -1.9628494287841
 CIRCL,        0.825,          -5., 7.29622354748459,          -5.
 LINE,        0.825,          -8.
 LINE,        0.685,          -8.
```

```
*End Instance
**
*Instance, name=Clot-1, part=Clot
*End Instance
**
*Instance, name=vessel-1, part=vessel
*Surface, type=SEGMENTS, name=vessel
START,         1.37,          -2.
 LINE,         1.37,           3.
*End Instance
**
*Node
      1,         1.37,           3.,           0.
*Node
      2,  0.824999988,          -8.,           0.
*Nset, nset=interface, instance=Clot-1
    5,    6,  818,  819,  820,  821,  822,  823,  824,  825,  826,  827,
828,  829,  830,  831
  832,  833,  834,  835,  836,  837,  838,  839,  840,  841,  842,  843,
844,  845,  846,  847
  848,  849,  850,  851,  852,  853,  854,  855,  856,  857,  858,  859,
860,  861,  862,  863
  864,  865,  866,  867,  868,  869,  870,  871,  872,  873,  874,  875,
876,  877,  878,  879
  880,  881,  882,  883,  884,  885,  886,  887,  888,  889,  890,  891,
892,  893,  894,  895
  896,  897,  898,  899,  900,  901,  902,  903,  904,  905,  906,  907,
908,  909,  910,  911
  912,  913,  914,  915,  916,  917,  918,  919,  920,  921,  922,  923,
924,  925,  926,  927
  928,  929,  930,  931,  932,  933,  934,  935,  936,  937,  938,  939,
940,  941,  942,  943
  944,  945,  946,  947,  948,  949,  950,  951,  952,  953,  954,  955,
956,  957,  958,  959
  960,  961,  962,  963,  964,  965,  966,  967,  968,  969,  970,  971,
972,  973,  974,  975
  976,  977,  978,  979,  980,  981,  982,  983,  984,  985,  986,  987,
988,  989,  990,  991
  992,  993,  994,  995,  996,  997,  998,  999, 1000, 1001, 1002, 1003,
1004, 1005, 1006, 1007
 1008, 1009, 1010, 1011, 1012, 1013, 1014, 1015, 1016, 1017, 1018, 1019,
1020, 1021, 1022, 1023
 1024, 1025, 1026, 1027, 1028, 1029, 1030, 1031, 1032, 1033, 1034, 1035,
1036, 1037, 1038, 1039
 1040, 1041, 1042, 1043, 1044, 1045, 1046, 1047, 1048, 1049, 1050, 1051,
1052, 1053, 1054, 1055
 1056, 1057, 1058, 1059, 1060, 1061, 1062, 1063, 1064, 1065, 1066, 1067,
1068, 1069, 1070, 1071
 1072, 1073, 1074, 1075, 1076, 1077, 1078, 1079, 1080, 1081, 1082, 1083,
1084, 1085, 1086, 1087
 1088, 1089, 1090
*Elset, elset=interface, instance=Clot-1, generate
 37265,  37538,      1
*Nset, nset=rp
 2,
*Nset, nset=rp2
 1,
```

```
*Nset, nset=xsymm, instance=Clot-1
   3,   4, 410, 411, 412, 413, 414, 415, 416, 417, 418, 419, 420, 421, 422,
423
 424, 425, 426, 427, 428, 429, 430, 431, 432, 433, 434, 435, 436, 437, 438,
439
 440, 441, 442, 443, 444, 445, 446, 447, 448, 449, 450, 451, 452, 453, 454,
455
 456, 457, 458, 459, 460, 461, 462, 463, 464, 465, 466, 467, 468, 469, 470,
471
 472, 473, 474, 475, 476, 477, 478, 479, 480, 481, 482, 483, 484, 485, 486,
487
 488, 489, 490, 491, 492, 493, 494, 495, 496, 497, 498, 499, 500, 501, 502,
503
 504, 505, 506, 507, 508, 509, 510, 511, 512, 513, 514, 515, 516, 517, 518,
519
 520, 521, 522, 523, 524, 525, 526, 527, 528, 529, 530, 531, 532, 533, 534,
535
 536, 537, 538, 539, 540, 541, 542, 543, 544, 545, 546, 547, 548, 549, 550,
551
 552, 553, 554, 555, 556, 557, 558, 559, 560, 561, 562, 563, 564, 565, 566,
567
 568, 569, 570, 571, 572, 573, 574, 575, 576, 577, 578, 579, 580, 581, 582,
583
 584, 585, 586, 587, 588, 589, 590, 591, 592, 593, 594, 595, 596, 597, 598,
599
 600, 601, 602, 603, 604, 605, 606, 607, 608, 609, 610, 611, 612, 613, 614,
615
 616, 617, 618, 619, 620, 621, 622, 623, 624, 625, 626, 627, 628, 629, 630,
631
 632, 633, 634, 635, 636, 637, 638, 639, 640, 641, 642, 643, 644, 645, 646,
647
 648, 649, 650, 651, 652, 653, 654, 655, 656, 657, 658, 659, 660, 661, 662,
663
 664, 665, 666, 667, 668, 669, 670, 671, 672, 673, 674, 675, 676, 677, 678,
679
 680, 681, 682
*Elset, elset=xsymm, instance=Clot-1, generate
 35621,  35894,      1
*Nset, nset=_PickedSet20, internal
 1,
*Nset, nset=_PickedSet31, internal
 2,
*Elset, elset=_clot_bottom_S4, internal, instance=Clot-1, generate
     1,  35621,    274
*Elset, elset=_clot_bottom_S2, internal, instance=Clot-1, generate
 36168,  37538,    274
*Surface, type=ELEMENT, name=clot_bottom
_clot_bottom_S4, S4
_clot_bottom_S2, S2
*Elset, elset=_interface_S3, internal, instance=Clot-1, generate
 37265,  37538,      1
*Surface, type=ELEMENT, name=interface
_interface_S3, S3
*Elset, elset=_suction_area_S4, internal, instance=Clot-1, generate
     1,  35621,    274
*Surface, type=ELEMENT, name=suction_area
_suction_area_S4, S4
```

```
** Constraint: rigid
*Rigid Body, ref node=_PickedSet31, analytical surface=Catheter-1.cat_surf
** Constraint: rigid2
*Rigid Body, ref node=_PickedSet20, analytical surface=vessel-1.vessel
*End Assembly
**
** MATERIALS
**
**Material parameters for 40%H clot
*Material, name=Material-1
*Depvar
      7,
*User Material, constants=20
 0.55,  0.65, 2e-05, 0.008,    5., 0.014, 0.022, 0.002
 0.006,  0.03, 0.032, 0.001, 0.003,    2.,    2.,   90.
   45.,   90.,  -45.,  0.01
**
** INTERACTION PROPERTIES
**
*Surface Interaction, name=IntProp-1
1.,
*Friction
0.,
*Surface Behavior, pressure-overclosure=HARD
*Surface Interaction, name=coh
1.,
**The CZ stiffness
*Cohesive Behavior, eligibility=CURRENT CONTACTS
 0.02, 0.02, 0.02
*Damage Initiation, criterion=MAXS
 0.0015, 0.0015, 0.0015
**Fracture energy
*Damage Evolution, type=ENERGY, softening=EXPONENTIAL
 6e-5,
*Damage Stabilization
1e-05
**
** BOUNDARY CONDITIONS
**
** Name: Fixed Type: Symmetry/Antisymmetry/Encastre
*Boundary
rp, ENCASTRE
** Name: Fixed2 Type: Symmetry/Antisymmetry/Encastre
*Boundary
rp2, ENCASTRE
** Name: xsymm Type: Symmetry/Antisymmetry/Encastre
*Boundary
xsymm, XSYMM
**
** INTERACTIONS
**
** Interaction: CZ
*Contact Pair, interaction=coh
interface, vessel-1.vessel
** Interaction: Int-1
*Contact Pair, interaction=IntProp-1
clot_bottom, Catheter-1.cat_surf
```

```
** Interaction: Int-3
*Contact Pair, interaction=IntProp-1
interface, Catheter-1.cat_surf
** Interaction: self
*Contact Pair, interaction=IntProp-1
interface,
** ----------------------------------------------------------------
**
** STEP: Step-1
**
*Step, name=Step-1, nlgeom=YES, inc=1000000
*Static, stabilize=0.0002, allsdtol=0.05, continue=NO
0.001, 1., 1e-15, 0.01
**
** LOADS
**
** Name: Suction   Type: Pressure
*Dsload
suction_area, P, -0.02
**
** CONTROLS
**
*Controls, reset
*Controls, parameters=time incrementation
, , , , , , , 30, , ,
**
** OUTPUT REQUESTS
**
*Restart, write, frequency=0
**
** FIELD OUTPUT: Damage
**
*Output, field
*Contact Output, nset=interface
CSDMG, CSMAXSCRT
**
** FIELD OUTPUT: F-Output-1
**
*Output, field, variable=PRESELECT
**
** HISTORY OUTPUT: Traction
**
*Output, history
*Contact Output, nset=interface
CFN1, CFN2, CFN3, CFNM, CFS1, CFS2, CFS3, CFSM, CSDMG, CSTRESS
**
** HISTORY OUTPUT: H-Output-1
**
*Output, history, variable=PRESELECT
*End Step
```

K. Rezoning method

In *section 2.4.*, the aspiration pressure of 0.02 MPa is adopted to avoid large deformation in elements and converge issues. However, an adaptivity technique, rezoning, could help optimize the mesh to control the computational cost (ABAQUS Analysis User's Manual, Dassault Systèmes Simulia Corp.). This can be accomplished by employing the geometry from a completed simulation, redefining the mesh, and applying loadings and boundary conditions. This process allows for the replacement of elements that have undergone significant deformation with new ones.

Take a model shown in *Figure 17.* for example. Firstly, one command line in the input file:

**Restart, write, frequency=0*

must be changed to:

**Restart, write, frequency=1*

Next, the simulation will be finalized, and a novel model will be established. In this updated model, the distorted clot from the previous *.odb* file's final increment must be imported. Additionally, two command lines must be input in Abaqus/CAE to extract the geometry:

deformed_clot = mdb.models['new model'].parts['deformed part']

mdb.models['new model'].Part2DGeomFrom2DMesh (name="deform_clot" ,part=deformed_clot, featureAngle=0)

Subsequently, in mesh → controls → algorithm, medial axis should be selected before assigning the new mesh. Furthermore, the constraints and boundary conditions in *Figure 17.* are applied, and a new loading is assigned. In addition, a command line, **MAP SOLUTION, UNBALANCED STRESS=STEP*, is added to the input file before ***STEP: Step-1*. The objective is to transfer the stress distribution from the previous model to the new one. Ultimately, by inputting the command:

abaqus job='new job' oldjob='old job' inp='input file of the new job' user='UMAT'

in the Abaqus command, the simulation can be executed, and the data from the previous job is inherited.

This approach enables the simulation to continue based on the outcomes of the previous job. Through the creation of multiple jobs, it is possible to achieve aspiration pressure comparable to clinical usage. Incorporating the models with D/d ratios of 2, 3, and 4, and applying a total aspiration pressure of 0.05 MPa, reveals a trend presented in *Figure 47.*, which is similar to that depicted in *Figure 37.* This shows that the discoveries presented in this thesis offer meaningful insights even under stronger suction pressures.

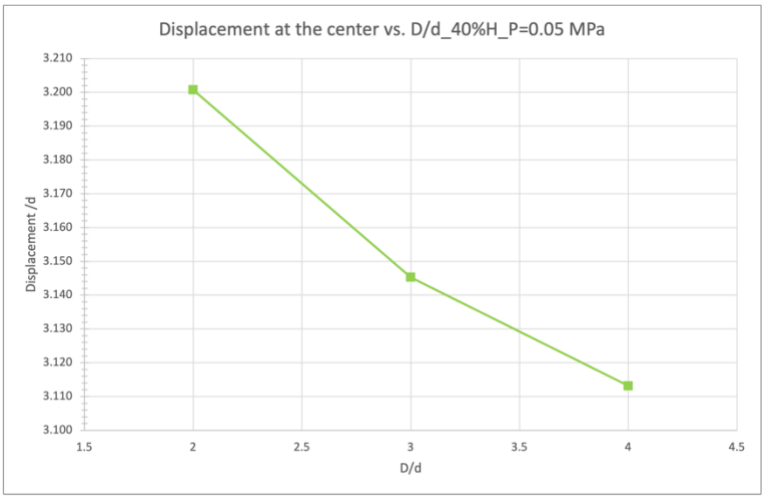

Figure 47. The relationship between the deformation at the clot bottom center and the clot diameter when a suction pressure of 0.05 MPa is applied (using rezoning method). The clot composition is 40%H (All the values are divided by the catheter diameter to make them dimensionless).

Nonetheless, it is important to note that these simulations require substantial time. Therefore, exploring further advancements could serve as an interesting subject for future research.

a) Input file for rezoning method for D/d = 2 with 40%H clot

```
*Heading
** Job name: Dtod=2_rezoning Model name: Dtod=2_rezoning
** Generated by: Abaqus/CAE 2020
*Preprint, echo=NO, model=NO, history=NO, contact=NO
**
** PARTS
**
*Part, name=Catheter
**The catheter length = 8, inner diameter = 1.37, outer diameter = 1.67, and
filet = 0.05
*End Part
**
*Part, name=declot
*Node
** For the mesh settings of the deformed clot, set the approximate global
size to be 0.02 in Sizing control section in global seeds, the detail codes
will not be shown in this appendix
*Element, type=CAX4
** For the mesh settings of the deformed clot, set the approximate global
size to be 0.02 in Sizing control section in global seeds, the detail codes
will not be shown in this appendix
*Element, type=CAX3
6420,  718,  732,  745
6421, 2309, 2312, 2311
6422, 2981, 2988, 2987
6423, 3311, 3317, 3316
6424, 3640, 3657, 3656
6425, 6158, 6160, 6159
6426, 6212, 6215, 6214
*Nset, nset=declot, generate
    1,  6607,     1
```

```
*Elset, elset=declot, generate
    1,  6426,     1
** Section: Section-1
*Solid Section, elset=declot, material=Material-1
,
*End Part
**
**
** ASSEMBLY
**
*Assembly, name=Assembly
**
*Instance, name=Catheter-1, part=Catheter
*Surface, type=SEGMENTS, name=cat_surf
START,         0.685,         -0.05
 CIRCL,         0.735,            0.,         0.735,         -0.05
 LINE,         0.775,           0.
 CIRCL,         0.825, -0.0500000000000005,         0.775, -0.0500000000000001
 LINE,         0.825,           -8.
 LINE,         0.685,           -8.
 LINE,         0.685,         -0.05
*End Instance
**
*Instance, name=declot-1, part=declot
*End Instance
**
*Node
      1,  0.824999988,           -8.,            0.
*Nset, nset=rp
 1,
*Nset, nset=xsymm, instance=declot-1
  99, 100, 131, 134, 183, 324, 325, 326, 327, 328, 329, 330, 331, 332, 333,
334
 335, 336, 337, 338, 339, 340, 341, 342, 343, 344, 440, 441, 442, 443, 444,
445
 446, 447, 448, 534, 535, 536, 537, 538, 539, 540, 541, 542, 543, 544, 545,
546
 547, 548, 549, 550, 551, 552, 553, 554, 555, 556, 557, 558, 559, 560, 561,
562
 563, 564, 565, 566, 567, 568, 569, 570, 571, 572, 573, 574, 575, 576, 577,
578
 579, 605, 606, 607, 608, 609, 610, 611, 612, 613, 614, 615, 616, 617, 618,
619
 620, 621, 622, 623
*Elset, elset=xsymm, instance=declot-1
 1848, 1871, 1894, 1917, 1940, 1963, 1964, 1965, 1966, 1967, 1968, 1969,
1970, 1971, 1972, 1973
 1974, 1975, 1976, 1977, 1978, 1979, 2952, 2956, 2960, 2964, 2968, 2972,
2976, 2980, 2984, 2988
 5440, 5446, 5452, 5458, 5464, 5470, 5476, 5482, 5488, 5494, 5500, 5506,
5512, 5518, 5524, 5530
 5536, 5542, 5548, 5554, 5560, 5566, 5572, 5578, 5584, 5590, 5596, 5602,
5608, 5614, 5620, 5626
 5632, 5638, 5644, 5650, 5656, 5662, 5668, 5674, 5680, 5686, 5692, 5698,
5704, 5710, 5716, 6134
 6149, 6164, 6179, 6194, 6209, 6224, 6239, 6254, 6255, 6256, 6257, 6258,
6259, 6260, 6261, 6262
```

```
 6263, 6264, 6265
*Nset, nset=_PickedSet8, internal
 1,
*Elset, elset=_clot_bottom_S4, internal, instance=declot-1
 5770, 5775, 5780, 5888, 5890, 5892, 5894, 5896, 6021, 6032, 6043, 6054,
6065, 6076, 6087, 6098
 6109,
*Elset, elset=_clot_bottom_S2, internal, instance=declot-1
 2342, 2353, 2364, 2375, 2386, 2397, 2408, 2419, 2430, 2441, 2452, 2463,
2474, 2485, 2496, 2507
 2536, 2543, 2551, 2559, 5807, 5812, 5817, 5822, 5827, 5832, 6265, 6276,
6287, 6298, 6309, 6320
 6331, 6342, 6353, 6364, 6375, 6386, 6397, 6408, 6419
*Elset, elset=_clot_bottom_S1, internal, instance=declot-1
 2508, 2509, 3322, 3323, 3324, 3325, 3326, 3327, 3328, 3329, 3330, 3331,
3332, 3333, 3334, 3335
 3336, 3337, 3338, 3339, 3340, 3341, 3342, 3343, 3344, 3345, 3346, 3347,
3348, 3349, 3350, 3351
 3352, 3353, 3354, 3355, 3356, 3357, 3358, 3359, 3360, 3361, 3362, 3363,
3364, 3365, 3366, 3367
 3368, 3369, 3370, 3371, 3372, 3373, 3374, 4700, 4701, 4702, 4703, 4704,
4705, 4706, 4707, 4708
 4709, 4710, 4711, 4712, 4713
*Elset, elset=_clot_bottom_S3, internal, instance=declot-1
  137,  138, 2770, 2771
*Surface, type=ELEMENT, name=clot_bottom
_clot_bottom_S4, S4
_clot_bottom_S2, S2
_clot_bottom_S1, S1
_clot_bottom_S3, S3
*Elset, elset=_suction_area_S2, internal, instance=declot-1
 2342, 2353, 2364, 2375, 2386, 2397, 2408, 2419, 2430, 2441, 2452, 2463,
2474, 2485, 2496, 2507
 6265, 6276, 6287, 6298, 6309, 6320, 6331, 6342, 6353, 6364, 6375, 6386,
6397, 6408, 6419
*Elset, elset=_suction_area_S4, internal, instance=declot-1, generate
 6021,  6109,    11
*Elset, elset=_suction_area_S1, internal, instance=declot-1
 3322, 3323, 3324, 3325, 3326, 3327, 3328, 3329, 3330, 3331, 3332, 3333,
3334, 3335, 3336, 3337
 3338, 3339, 3340, 3341, 3342, 3343, 3344, 3345, 3346, 3347, 3348, 3349,
3350, 3351, 3352, 3353
 3354, 3355, 3356, 3357, 3358, 3359, 3360, 3361, 3362, 3363, 3364, 3365,
3366, 3367, 3368, 3369
 3370, 3371, 3372, 3373, 3374, 4700, 4701, 4702, 4703, 4704, 4705, 4706,
4707, 4708, 4709, 4710
 4711, 4712, 4713
*Surface, type=ELEMENT, name=suction_area
_suction_area_S2, S2
_suction_area_S4, S4
_suction_area_S1, S1
** Constraint: rigid
*Rigid Body, ref node=_PickedSet8, analytical surface=Catheter-1.cat_surf
*End Assembly
**
** MATERIALS
**
```

```
*Material, name=Material-1
*Depvar
      7,
*User Material, constants=20
 0.55,  0.65, 2e-05, 0.008,    5., 0.014, 0.022, 0.002
 0.006,  0.03, 0.032, 0.001, 0.003,    2.,    2.,   90.
   45.,   90.,  -45.,  0.01
**
** INTERACTION PROPERTIES
**
*Surface Interaction, name=IntProp-1
1.,
*Friction
0.,
*Surface Behavior, pressure-overclosure=HARD
**
** BOUNDARY CONDITIONS
**
** Name: Fixed Type: Symmetry/Antisymmetry/Encastre
*Boundary
rp, ENCASTRE
** Name: xsymm Type: Symmetry/Antisymmetry/Encastre
*Boundary
xsymm, XSYMM
**
** INTERACTIONS
**
** Interaction: Int-1
*Contact Pair, interaction=IntProp-1
clot_bottom, Catheter-1.cat_surf
** ----------------------------------------------------------------
*MAP SOLUTION, UNBALANCED STRESS=STEP
**
**
** STEP: Step-1
**
*Step, name=Step-1, nlgeom=YES, inc=1000000
*Static, stabilize=0.0002, allsdtol=0.05, continue=NO
0.001, 1., 1e-15, 0.01
**
** LOADS
**
** Name: Suction   Type: Pressure
*Dsload
suction_area, P, -0.03
**
** CONTROLS
**
*Controls, reset
*Controls, parameters=time incrementation
, , , , , , , 30, , ,
**
** OUTPUT REQUESTS
**
*Restart, write, frequency=1
**
** FIELD OUTPUT: F-Output-1
```

```
**
*Output, field, variable=PRESELECT, frequency=3
**
** HISTORY OUTPUT: H-Output-1
**
*Output, history, variable=PRESELECT, frequency=3
*End Step
```